
Doctoral Dissertations


Student Theses and Dissertations

Spring 2018

High temperature polymer composites using out-of-autoclave processing

Sudharshan Anandan

Follow this and additional works at: https://scholarsmine.mst.edu/doctoral_dissertations

 Part of the [Materials Science and Engineering Commons](#), and the [Mechanical Engineering Commons](#)
Department: **Mechanical and Aerospace Engineering**

Recommended Citation

Anandan, Sudharshan, "High temperature polymer composites using out-of-autoclave processing" (2018).
Doctoral Dissertations. 2758.
https://scholarsmine.mst.edu/doctoral_dissertations/2758

This thesis is brought to you by Scholars' Mine, a service of the Missouri S&T Library and Learning Resources. This work is protected by U. S. Copyright Law. Unauthorized use including reproduction for redistribution requires the permission of the copyright holder. For more information, please contact scholarsmine@mst.edu.

HIGH TEMPERATURE POLYMER COMPOSITES USING OUT-OF-AUTOCLAVE
PROCESSING

by

SUDHARSHAN ANANDAN

A DISSERTATION

Presented to the Faculty of the Graduate School of the
MISSOURI UNIVERSITY OF SCIENCE AND TECHNOLOGY

In Partial Fulfillment of the Requirements for the Degree

DOCTOR OF PHILOSOPHY
in
MECHANICAL ENGINEERING

2018

Approved

K. Chandrashekhara, Advisor

A.C. Okafor

V. Birman

X. Yang

V.A. Samaranayake

© 2018

Sudharshan Anandan

All Rights Reserved

PUBLICATION DISSERTATION OPTION

This dissertation has been prepared in the form of four papers for publication as follows:

Paper I: Influence of Cure Conditions on Out-of-Autoclave Bismaleimide Composite Laminates (Pages 12-37). This paper has been published in Journal of Applied Polymer Science in 2016.

Paper II: Processing and Performance of Out-of-Autoclave Bismaleimide Composite Sandwich Structures (Pages 38-60). The paper is published in SAMPE Journal, 2016.

Paper III - Curing of Thick Thermoset Composite Laminates: Multiphysics Modeling and Experiments (Pages 61-86). The paper was published in Applied Composite Materials, 2017.

Paper IV - Investigation of Sandwich Composite Failure under Three-point Bending: Simulation and Experimental Validation (Pages 87-118). This paper is intended for publication in Journal of Sandwich Structures and Materials.

ABSTRACT

High performance polymer composites possess high strength-to-weight ratio, corrosion resistance, and have design flexibility. Carbon/epoxy composites are commonly used aerospace materials. Bismaleimide based composites are used as a replacement for epoxy systems at higher service temperatures. Aerospace composites are usually manufactured, under high pressure, in an autoclave which requires high capital investments and operating costs. In contrast, out-of-autoclave manufacturing, specifically vacuum-bag-only prepreg process, is capable of producing low cost and high performance composites. In the current study, out-of-autoclave processing of high temperature carbon/bismaleimide composites was evaluated. The cure and process parameters were optimized. The properties of out-of-autoclave cured laminates compared well to autoclave manufactured composites. Numerical models were developed which simulate the curing process in composite laminates and used to optimize cycles and change processing parameters to obtain high-quality parts. The results were extended to enable manufacturing of high temperature composite sandwich structures. Sandwich structures were manufactured and thermo-mechanical properties were evaluated. Numerical models were built to simulate the effect of elevated temperatures on composite sandwich structures and validated using experiments. The results show that it is feasible to manufacture lab-scale high quality composites using the out-of-autoclave process. Also, numerical models are powerful tools which can be used to optimize cure cycles and simulate thermo-mechanical behavior of these composite parts.

ACKNOWLEDGMENTS

I express my heartfelt gratitude to my academic advisor Dr. K Chandrashekhara whose guidance and advice have been invaluable throughout my Master's degree as well as my Ph.D. His constructive suggestions have been invaluable during the course of my graduate research.

I thank the members of my advisory committee, Dr. A. C. Okafor, Dr. V. A. Samaranayake, Dr. X. Yang, and Dr. V. Birman for their valuable time and advice in the review of this dissertation.

I am indebted to the members of the Composite Research group, especially Mr. Gurjot Singh Dhaliwal and Rafid Hussein, who worked with me extensively during my graduate program.

Thanks must also go to Mr. Tom Berkel (Boeing), Mr. Doug Pfitzinger (GKN Aerospace) and The Center for Aerospace Manufacturing Technologies (CAMT) for their guidance and financial support. I would also like to acknowledge our industry collaborators, Dr. Nicole Apetre and Dr. Nagaraja Iyyer, for their valuable input.

Finally, I also express my gratitude to my family for all the love and encouragement.

TABLE OF CONTENTS

	Page
PUBLICATION DISSERTATION OPTION	iii
ABSTRACT	iv
ACKNOWLEDGMENTS	v
LIST OF ILLUSTRATIONS	xiii
LIST OF TABLES	xvii
 SECTION	
1. INTRODUCTION.....	1
2. LITERATURE SURVEY	4
2.1. MANUFACTURING OF AEROSPACE COMPOSITES	4
2.2. PROCESS-PROPERTY RELATIONSHIP IN COMPOSITES	6
2.3. COMPOSITE SANDWICH STRUCTURES	7
3. SCOPE AND OBJECTIVES	9
 PAPER	
I. INFLUENCE OF CURE CONDITIONS ON OUT-OF-AUTOCLAVE BISMALEIMIDE COMPOSITE LAMINATES.....	12

ABSTRACT.....	12
1. INTRODUCTION.....	13
2. MATERIALS.....	16
3. MANUFACTURING.....	17
4. METHODOLOGY.....	19
4.1. POROSITY STUDY.....	19
4.2. INFLUENCE OF BASE CURE CONDITIONS.....	20
4.3. EXPERIMENTAL DESIGN.....	20
4.4. SHORT BEAM SHEAR TEST.....	21
4.5. INFLUENCE OF POST CURE CONDITIONS.....	22
4.5.1. Glass Transition Temperature.....	22
4.5.2. Mechanical Testing.....	22
5. RESULTS AND DISCUSSION.....	23
5.1. POROSITY STUDY.....	23
5.2. INFLUENCE OF BASE CURE CONDITIONS.....	24
5.3. SHORT BEAM SHEAR TEST.....	24

5.4. VERIFICATION OF RESULTS	28
5.5. INFLUENCE OF POST CURE CONDITIONS.....	29
5.6. GLASS TRANSITION TEMPERATURE.....	29
5.7. MECHANICAL TESTING	30
5.8. COMPARISON WITH AUTOCLAVE CURED COMPOSITES	33
6. CONCLUSIONS.....	34
ACKNOWLEDGEMENTS.....	35
REFERENCES	35
II. PROCESSING AND PERFORMANCE OF OUT-OF-AUTOCLAVE BISMALEIMIDE COMPOSITE SANDWICH STRUCTURES.....	38
ABSTRACT.....	38
1. INTRODUCTION.....	39
2. MATERIALS	42
3. MANUFACTURING.....	43
4. EXPERIMENTS	45
4.1. THERMOGRAVIMETRIC ANALYSIS	45

4.2. FLATWISE TENSILE TEST	46
4.3. EDGEWISE COMPRESSION TEST	47
4.4. ADHESIVE BOND FRACTURE TOUGHNESS TEST	47
5. RESULTS AND DISCUSSION	49
5.1. THERMOGRAVIMETRIC ANALYSIS	49
5.2. FLATWISE TENSILE TEST	50
5.3. EDGEWISE COMPRESSION TEST	53
5.4. ADHESIVE BOND FRACTURE TOUGHNESS TEST	55
6. SUMMARY AND CONCLUSIONS	57
ACKNOWLEDGEMENTS	58
REFERENCES	58
III. CURING OF THICK THERMOSET COMPOSITE LAMINATES: MULTIPHYSICS MODELING AND EXPERIMENTS	61
ABSTRACT	61
1. INTRODUCTION	62
2. METHODOLOGY	65

2.1. CURE KINETICS MODELING.....	65
2.2. THERMAL MODEL	66
2.3. MULTIPHYSICS CURE MODELING.....	69
2.4. EXPERIMENTAL EVALUATION OF PART TEMPERATURE.....	72
3. RESULTS AND DISCUSSION	73
3.1. EFFECT OF POST-CURING ON DEGREE OF CURE	76
3.2. EFFECT OF CONVECTION IN THE AUTOCLAVE.....	76
3.3. EFFECT OF CURE CYCLE MODIFICATION	77
3.4. EFFECT OF MODIFIED CURE CYCLES ON INTERLAMINAR SHEAR STRENGTHS.....	80
4. CONCLUSIONS.....	82
ACKNOWLEDGEMENTS	83
REFERENCES	83
IV. INVESTIGATION OF SANDWICH COMPOSITE FAILURE UNDER THREE- POINT BENDING: SIMULATION AND EXPERIMENTAL VALIDATION.....	87
ABSTRACT.....	87
1. INTRODUCTION.....	88

1.1. BACKGROUND.....	88
1.2. FAILURE IN THREE-POINT BENDING.....	90
1.3. CURRENT WORK.....	93
2. NUMERICAL MODELING.....	94
2.1. FACESHEET FAILURE	94
2.2. HONEYCOMB CORE MODEL	98
2.3. MODELING OF THREE-POINT BENDING TEST.....	100
3. EXPERIMENTS	101
4. RESULTS AND DISCUSSION	104
4.1. FAILURE UNDER THREE-POINT BENDING.....	104
4.2. EFFECT OF ELEVATED TEMPERATURES	109
4.3. EFFECT OF PUNCHER LOCATION	113
5. CONCLUSIONS.....	114
ACKNOWLEDGEMENTS.....	115
REFERENCES	116

SECTION

4. CONCLUSIONS119

BIBLIOGRAPHY123

VITA 125

LIST OF ILLUSTRATIONS

SECTION	Page
Figure 1.1. Constituents of a composite laminate.....	1
Figure 1.2. Schematic of a honeycomb sandwich (Hexcel.com).....	2
Figure 2.1. Recommended cure cycle for carbon/BMI composite laminates.....	4
 PAPER I	
Figure 1. Manufacturer recommended cure cycle	16
Figure 2. OOA process bagging assembly.....	18
Figure 3. Face centered central composite design	21
Figure 4. Effect of cure conditions on ILSS	25
Figure 5. Response surface plot of the influence of base cure temperature and time on ILSS.....	28
Figure 6. Variation of glass transition temperature with post cure conditions	30
Figure 7. Variation of ILSS with post cure conditions	31
 PAPER II	
Figure 1. Schematic of bagging layup	43

Figure 2. Cure Cycle	44
Figure 3. Schematic of modified CSB test.....	48
Figure 4. Crack propagation in a modified CSB test	48
Figure 5. Mass loss of adhesive during TGA	49
Figure 6. Adhesive fillet formation in sandwich composites manufactured under full vacuum pressure	51
Figure 7. Representative images of fracture surfaces of samples cured under full vacuum at different locations	51
Figure 8. Representative images of fracture surfaces of samples cured under partial vacuum at different locations	52
Figure 9. Load vs Extension in edgewise compression test at 177 °C (350 °F) of sandwich samples cured under full vacuum.....	54
Figure 10 (a) and (b). Stable end crushing failure	55
Figure 11. Loading–unloading cycle in modified CSB test of a sample cured under partial vacuum.....	56

PAPER III

Figure 1. Three-dimensional model of the problem setup	69
Figure 2. Cross section of the thermo-chemical multiphysics model.....	70
Figure 3. Multiphysics modeling of composite curing	71

Figure 4. Experimental setup	72
Figure 5. Comparison of temperature at laminate center, experiment vs simulation	74
Figure 6. Degree of cure development during cure	75
Figure 7. Effect of post-cure on degree of cure of the laminate	75
Figure 8. Variation of temperature at center with varying convection coefficient (W/m ² K)	77
Figure 9. Cure cycle for modification	78
Figure 10. Effect of modified cure cycles on thermal spike. T _A (Figure 9) was varied from 233-260 °F	79
Figure 11. Degree of cure variation in the laminate with recommended and modified cure cycles	79
 PAPER IV	
Figure 1. Schematic of linear softening behavior [22]	97
Figure 2. Honeycomb cell modeling	98
Figure 3. Honeycomb core showing regions of fine and coarse mesh	99
Figure 4. Three-point bending test setup	100
Figure 5. Experimental setup for three-point bending test	102
Figure 6. Load-displacement behavior under three-point bending	103

Figure 7. Damage evolution in the facesheet during three-point bending. HSNFCCRT stands for Hashin's Fiber Compression Failure Criterion	105
Figure 8. Failure in composite sandwich structures under three-point bending. HSNFCCRT stands for Hashin's Fiber Compression Failure Criterion. Damaged regions are colored red	106
Figure 9. Progression of failure in the honeycomb core	108
Figure 10. Core failure in three-point bending. Comparison between experimental and simulation results is shown. PE stands for plastic strain	109
Figure 11. Temperature dependent variation in the properties of honeycomb and facesheet	110
Figure 12. Comparison of load displacement curves at room temperature and high temperature (100 °C). Experimental results are shown in the figure	112
Figure 13. Experimental and numerical load-displacement curves at elevated temperature of 100 °C	112
Figure 14. Effect of relative position of the puncher on results of the three-point bending tests	113
Figure 15. Variation of localized damage with a change in puncher location	114

LIST OF TABLES

	Page
PAPER I	
Table 1. Laminates manufactured in the study.	17
Table 2. Cure conditions	19
Table 3. Evaluation of bleeders	23
Table 4. ANOVA table for the effect of base cure conditions on ILSS	26
Table 5. ANOVA table for the effect of post cure conditions on ILSS	31
Table 6. Comparison of autoclave and OOA cured composite laminates.	33
PAPER II	
Table 1. Materials used	42
Table 2. FWT test results	50
Table 3. Edgewise compression test results.....	53
Table 4. Adhesive bond fracture toughness test results	57
PAPER III	
Table 1. Cure kinetic parameters for Cycom 5230-1 prepreg system [5].....	67

Table 2 Material properties of the mold and caul plate material (Aluminum 5052) 67

Table 3. Material parameters for Cycom IM7/5320-1 prepreg..... 68

Table 4. Material properties of consumables [17] 70

Table 5. Results of short beam shear tests 81

PAPER IV

Table 1. Temperature dependent properties of the facesheet material [24]..... 95

Table 2. Fracture energies of the facesheet material [22]..... 98

SECTION

1. INTRODUCTION

Composites are defined as structures made from two or more components to form a new material system with enhanced properties. The current work focuses on fiber reinforced polymer composites.

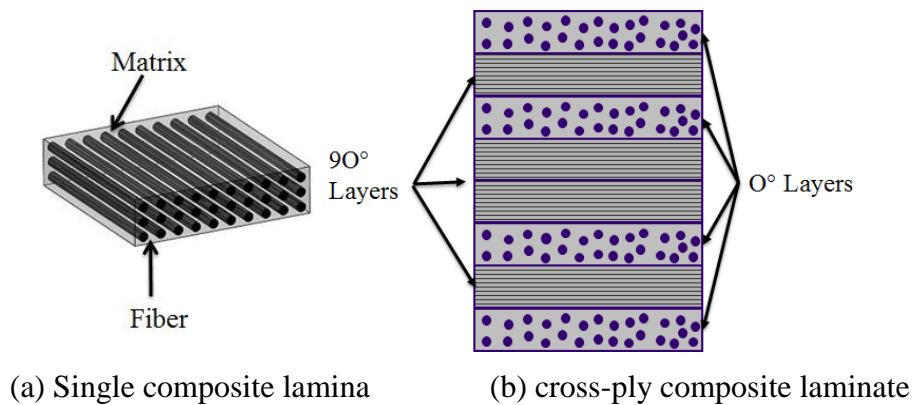


Figure 1.1. Constituents of a composite laminate

The fibers are made of carbon while the matrix material comprises of thermoset polymers such as epoxy or Bismaleimide (Figure 1.1). High temperature systems such as BMI based composites are used in the aerospace industry due to higher service temperatures compared to epoxy systems, and better processing behavior compared to polyimides. BMIs also exhibit good tack and drape, and an epoxy-like addition cure mechanism. In addition, they possess desirable properties such as high tensile strength,

corrosion and chemical resistance, and good hot-wet performance [1]. Composite structures have been widely utilized in diverse applications ranging from housing, automobile to aerospace industries due to their high strength-to-weight ratio and design flexibility.

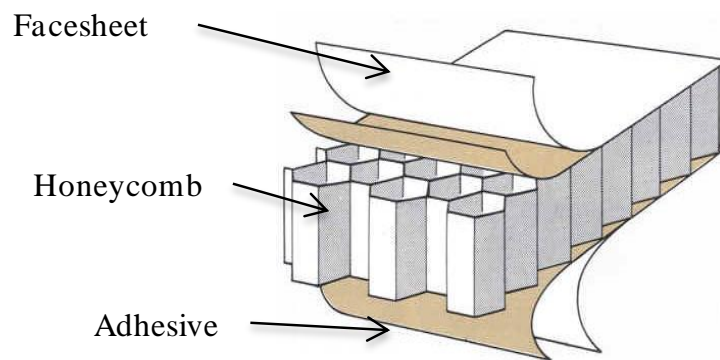


Figure 1.2. Schematic of a honeycomb sandwich (Hexcel.com)

A composite laminate consists of a stack of multiple layers or “lamina”. Figure 1.1 (b) shows a cross-ply composite laminate where subsequent layers have fibers oriented perpendicular to each other. The orientation of the plies can be tailored to obtain a specific combination of properties, according to design requirements. Composite laminates and sandwich structures are commonly used in aerospace, civil and automobile industries. Composite sandwich structures are used in because they exhibit better resistance to bending and out-of-plane loading compared to composite laminates. The sandwich structures, in this study, consist of two thin facesheets, an adhesive layer and a honeycomb core (Figure

1.2). In a composite sandwich structure, the facesheet absorbs in-plane loads while the core is resistant to shear loading. The composite facesheet is bonded to the core using a film adhesive. The current work involves manufacturing, evaluation and modeling of composite laminates as well as sandwich structures. Carbon/Bismaleimide (BMI) systems are used, which have higher service temperatures compared to commonly used carbon/epoxy systems.

2. LITERATURE SURVEY

2.1. MANUFACTURING OF AEROSPACE COMPOSITES

The raw material required for manufacturing a composite laminate is called a “prepreg”, or pre-impregnated fiber mat. The prepreg consists of a unidirectional or woven fabric, infused with the uncured resin.

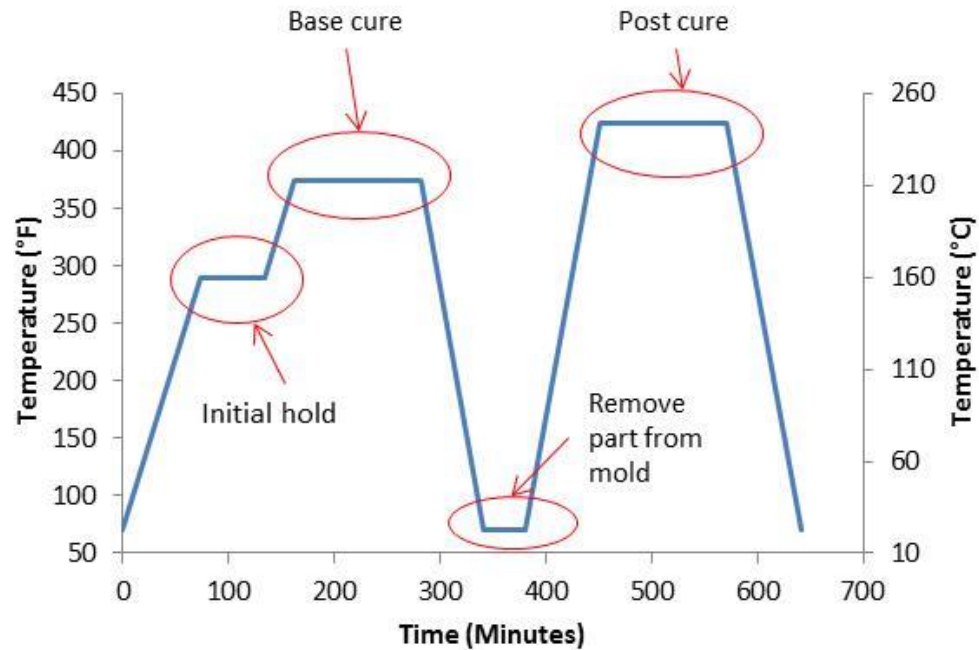


Figure 2.1. Recommended cure cycle for carbon/BMI composite laminates

The layers of prepreg are stacked according to the desired laminate orientation and cured at high temperatures. In addition, high pressures are used in order to remove

entrapped air from the layup. A 2-step cure cycle is commonly used to cure composite laminates.

Figure 2.1 shows the recommended cure cycle for carbon/BMI laminates. An initial hold is provided to improve the mobility of all reacting groups in the polymer resin. The base cure region is where the initial curing takes place; the resin cures to form a hard and brittle polymer. Post curing is performed at higher temperatures to improve part properties and to increase glass transition temperature.

Aerospace composite materials are generally manufactured in an autoclave under high temperature and high pressure. The combination of high temperature and pressure ensures low void content and good part consolidation. The Out-of-Autoclave (OOA) process, specifically a vacuum bag only OOA process, is a low cost alternative to conventional autoclave manufacturing of composite components [2,3]. The OOA process requires low capital investment and provides greater design flexibility for the production of large structural components with complex geometries. The part size is no longer limited by the size of the autoclave [4]. During OOA processing, sandwich components can be co-cured, a process where adhesive and the prepreg is cured simultaneously, resulting in further time and cost reduction. Manufacturing co-cured sandwich panels, out-of-autoclave, eliminates core crushing which can occur at autoclave pressures [5] and enables the use of lighter cores.

While autoclave pressures are high enough to suppress void formation, OOA cure processes can lead to higher void contents as the part is cured under atmospheric pressures [6]. Proper control of the prepreg breathing mechanism is required to produce void free

parts. OOA prepregs feature dry, relatively permeable areas that allow gas evacuation when vacuum is applied for consolidation of layup. These areas consist of macro-porosity between plies and around the reinforcement architecture, or micro-porosity inside the tows, between individual fibers. During the cure cycle, once the melting point of the resin is reached, these pores are filled by the matrix material to produce a void free structure [7]. The relationship between porosity and reduced mechanical properties is well established [8]. OOA processes generally use atmospheric pressure and therefore venting entrapped air from the laminate stack is a key concern. Entrapped gasses need to be removed through engineered pathways provided within the prepreg [9]. The processing parameters for OOA processing of composite laminates and sandwich structures should be carefully established, in order to reap the benefits of low manufacturing costs. Therefore, the current work involves evaluation of OOA cured composite laminates and sandwich structures and optimization of process parameters to reduce void contents.

2.2. PROCESS-PROPERTY RELATIONSHIP IN COMPOSITES

In addition to pressure, the cure cycle also has a significant influence on the final property of composite parts. The properties of a composite laminate are significantly affected by cure conditions. A high degree of cure is essential to ensure good part quality. Mechanical properties and glass transition temperature of composite laminates can be further improved by incorporating a post cure cycle. Rise in post cure temperature has been shown to increase degree of cure, glass transition temperature and mechanical strength of carbon fiber/epoxy composite systems [10]. Post curing also increases the crosslink density

in a composite. A high crosslink density leads to high glass transition temperatures because of stiffer polymer chains. On the other hand high crosslink densities also cause matrix embrittlement. At higher degrees of cure and crosslink densities, the glass transition temperature of BMI based systems can approach 300 °C. The manufacturer recommended cure cycles are not optimized, especially for thick and complex shaped parts. The effect of varying cure cycles on composite components needs to be evaluated. In the current work, the effect of varying processing conditions on carbon/ BMI composite laminates is investigated. In addition, numerical modeling is performed to simulate the progress of cure in thick composite laminates.

2.3. COMPOSITE SANDWICH STRUCTURES

The adhesive bond between core and facesheet is of great importance in the design of sandwich structures. The relation between the adhesive fillet and sandwich properties was described by Grimes et al. [11]. The mechanical performance of a sandwich composite depends on the quality of the core-to-facesheet adhesive bond. In case of honeycomb cores, the cell walls provide a relatively small area for bonding. Structural strength depends on the presence of a well-formed fillet at the interface of the core cell wall and facesheet. Larger adhesive fillets absorb a higher amount of energy upon fracture, due to which they have high fracture toughness [12]. Grove et al. [13] showed that higher debonding energy was obtained with larger, regular-shaped adhesive fillets between the honeycomb cell walls and the skin. In composite sandwich structures, internal core pressure in the cells of a honeycomb core has been shown to affect adhesive foaming and fracture toughness in

sandwich composites with carbon/epoxy facesheets [14]. Core pressure fluctuations were observed when internal core pressures equaled atmospheric pressure [15]. Increased adhesive permeability due to perforation resulted in enhanced fracture toughness of the adhesive layer. The optimal range of honeycomb core pressure during processing was estimated to be 40-70 kPa, to reduce adhesive outgassing and ensure good fillet formation. Previous studies involve manufacturing and evaluation of sandwich composites with carbon/epoxy facesheets. There is little literature concerning high temperature composite sandwich structures. Therefore, the current work involves on high temperature composite sandwich structures having carbon/BMI facesheets.

3. SCOPE AND OBJECTIVES

This dissertation comprises of four papers dealing with the following problems. The first paper is titled, “Influence of Cure Conditions on Out-of-Autoclave Bismaleimide Composite Laminates.” In this paper, the effect of varying cure cycles on the properties of out-of-autoclave cured carbon/BMI laminates is evaluated. BMI composite laminates were manufactured using OOA process. The quality of composite panels manufactured using the out-of-autoclave prepreg was evaluated using void content tests. Once the laminate quality was established, the effect of varying base cure time on mechanical properties of green composite panels was evaluated using short beam shear (SBS) tests. The influence of post cure conditions on glass transition temperature and mechanical strength of BMI composite panels was studied using Thermomechanical Analysis (TMA) and SBS tests respectively. Using these results, a composite panel was manufactured and its properties were compared with an autoclave cured specimen. OOA fabricated composites exhibited properties similar to autoclave cured parts.

The second paper is titled, “Processing and Performance of Out-of-Autoclave Bismaleimide Composite Sandwich Structures.” In this study, sandwich composites were manufactured using aluminum honeycomb, carbon/BMI facesheets and a toughened BMI adhesive system. The effect of varying vacuum pressure on thermo-mechanical properties of out-of-autoclave cured sandwich composite was evaluated. Adhesive bond quality was evaluated using flatwise tensile tests and adhesive bond fracture toughness tests. Load bearing capability structure was evaluated using edgewise compression tests. The test

results were compared with commercial BMI systems. The adhesive bond quality was found to be comparable to autoclave cured high temperature sandwich composites.

The third paper is titled, “Curing of Thick Thermoset Composite Laminates: Multiphysics Modeling and Experiments.” The study involves the investigation of the degree of cure and temperature distribution in thick composite laminates during cure. Multiphysics simulations were built to evaluate the curing behavior of thick composite laminates. A thermo-chemical model was built to simulate the degree of cure and temperature distribution in a laminate stack during cure. The numerical model was validated using experiments. The effect of including a post-cure step was investigated. The effect of varying cure conditions on the degree of cure of resultant composite laminate was also evaluated. Based on the results, a modified cure cycle was developed, which can result in reduced thermal spike in composite laminates. Composite laminates were manufactured using the recommended and modified cure cycles. The properties of the laminate manufactured using the modified cure cycle was similar to the one made using recommended cure cycle. The study shows that it is possible to design cure cycles for thick and complex parts to reduce the thermal spike while maintaining part quality.

The fourth paper is titled, “Investigation of Sandwich Composite Failure under Three-point Bending: Simulation and Experimental Validation.” This paper focused on modeling of a composite sandwich structure under three-point bending, at room temperature and elevated temperature. The sandwich structure had facesheets made of carbon/epoxy composites and the core material was aluminum honeycomb. Hashin’s failure model was used to simulate damage propagation in the facesheets. The model was

validated experimentally and simulation results showed good accuracy in predicting the load carrying capacity as well as overall damage behavior in the sandwich composite. When the temperature was increased to 100 °C, the strength of the sandwich structure decreased by 9.2%, while the stiffness did not change. This effect was also captured effectively by the numerical model. The location of the puncher axis relative to cell geometry is a parameter is difficult to determine using experiments, was evaluated using the numerical model. It was observed that the sandwich stiffness was not significantly affected by the relative location of the puncher, while the load to failure decreased slightly. The study shows that numerical simulations, after experimental validation, can be used to effectively determine parameters which affect behavior of sandwich composites.

PAPER**I. INFLUENCE OF CURE CONDITIONS ON OUT-OF-AUTOCLAVE
BISMALEIMIDE COMPOSITE LAMINATES**

S. Anandan, G. S. Dhaliwal, V.A. Samaranayake and K. Chandrashekhara
Missouri University of Science and Technology, Rolla, MO 65409

T. R. Berkel

Boeing Research & Technology, St. Louis, MO 63166

D. Pfitzinger

GKN Aerospace, St. Louis, MO 63042

ABSTRACT

Bismaleimides (BMI) are thermosetting polymers that are widely used in the aerospace industry due to their good physical properties at elevated temperatures and humid environments. BMI based composites are used as a replacement for conventional epoxy resins at higher service temperatures. Out-of-Autoclave processing of BMI composites is similar to that of epoxies but requires higher cure temperatures. Polymer properties such as degree of cure and crosslink density are dependent on the cure cycle used. These properties affect mechanical strength as well as glass transition temperature of the composite. In the current research, carbon fiber/ BMI composite laminates were manufactured by out-of-autoclave processing. The void content was measured using acid digestion techniques. The influence of cure cycle variations on glass transition temperature

and mechanical strength was investigated. Properties of manufactured specimens were compared with that of conventional autoclave cured BMI composites. Laminates fabricated via out-of-autoclave processing exhibited properties comparable to that of autoclave cured composites.

1. INTRODUCTION

The Out-of-Autoclave (OOA) process, specifically a vacuum bag only OOA process, is a low cost alternative to conventional autoclave manufacturing of composite components [1, 2]. The OOA process requires low capital investment and provides greater design flexibility for the production of large structural components with complex geometries. The part size is no longer limited by the size of the autoclave [3]. On the other hand, autoclave pressures are high enough to suppress void formation. OOA cure processes can lead to higher void contents as the part is cured under atmospheric pressures [4]. Proper control of the prepreg breathing mechanism is required to produce void free parts. OOA prepreps feature dry, relatively permeable areas that allow gas evacuation when vacuum is applied for consolidation of layup. These areas consist of macro-porosity between plies and around the reinforcement architecture, or micro-porosity inside the tows, between individual fibers. During the cure cycle, once the melting point of the resin is reached, these pores are filled by the matrix material to produce a void free structure [5].

The relationship between porosity and reduced mechanical properties is well established [6]. In autoclave processing, high working pressures combined with vacuum evacuation gives rise to a high pressure differential that enhances removal of entrapped air.

OOA processes generally use atmospheric pressure and therefore venting entrapped air from the laminate stack is a key concern. Entrapped gasses need to be removed through engineered pathways provided within the prepreg [7]. The material must also exhibit low viscosity before cure and low outgassing during cure.

OOA processes using carbon/epoxy prepregs have been used to fabricate large and complex composite structures such as the Boeing Wing Spar, Advanced Composite Cargo Aircraft, and the Ares V interstage and payload shroud [8, 9]. OOA processing of Bismaleimide (BMI) based composite systems is relatively new [10]. BMIs are used in the aerospace industry due to higher service temperatures compared to epoxy systems, and better processing behavior compared to polyimides. BMIs also exhibit good tack and drape, and an epoxy-like addition cure mechanism. In addition, they possess desirable properties such as high tensile strength, corrosion and chemical resistance, and good hot-wet performance [11]. OOA BMI laminates were manufactured as a part of the NASA CoEx (Composite for Exploration) project using prepreg from Renegade Materials Corporation, Tencate and Stratton Composite Solutions [12]. Sandwich composites made with BMI OOA prepregs were also evaluated as a part of CoEx [13]. Due to a limitation in tooling, the cure temperature in was limited to 350 °F (177 °C). The manufactured laminates had poor consolidation, high voids and also a high glass transition temperature.

Cure conditions affect mechanical properties of thermosetting resins and composites. Mechanical properties and glass transition temperature of composite laminates can be improved by incorporating a post cure cycle. Rise in post cure temperature has been shown to increase degree of cure, glass transition temperature and mechanical strength of

carbon fiber/epoxy composite systems [14]. Post curing also increases the crosslink density in a composite. A high crosslink density leads to high glass transition temperatures because of stiffer polymer chains. On the other hand high crosslink densities also cause matrix embrittlement. At higher degrees of cure and crosslink densities, the glass transition temperature of BMI based systems can approach 300 °C. He, et al investigated the effect of post cure cycles on IM7/5250-4 composites [15]. It was found that glass transition temperature increased with post-cure temperature. Flexure properties and mode II fracture toughness were also enhanced for composites post cured at 425 °F (218°C), as compared with those post cured at (375 °F) 191 °C or at 475 °F (246°C).

In the current work, BMI composite laminates are manufactured using OOA process. First, the quality of composite panels manufactured using the out-of-autoclave prepreg was evaluated using void content tests. Edge bleeding was used to evacuate entrapped air within the laminate stack. The void content of manufactured laminates was evaluated using acid digestion. Once the laminate quality was established, the effect of varying base cure time on mechanical properties of green composite panels was evaluated using short beam shear (SBS) tests. The influence of post cure conditions on glass transition temperature and mechanical strength of BMI composite panels was studied using Thermomechanical Analysis (TMA) and SBS tests respectively. Using these results, a composite panel was manufactured and its properties were compared with an autoclave cured specimen. OOA fabricated composites exhibited properties similar to autoclave cured parts.

2. MATERIALS

Composite laminates were manufactured using IM7G/AR4550 BMI unidirectional prepreg system (Aldila Composite Materials). AR4550 is a toughened BMI resin system, ideal for OOA curing. The unidirectional prepreg contains 35% resin by weight with a prepreg areal weight of 304.8 g/m². It has low tack compared to epoxy prepregs and has a shelf life of two weeks. To bleed entrapped air from the edge of a laminate stack, a light weight 54 gsm leno glass cloth and Vac-Pak EB1590 edge bleeder were used. EB1590 is an open weave, 600 °F (315 °C), high tensile strength Teflon-coated lightweight fiberglass material suitable for edge breathing.

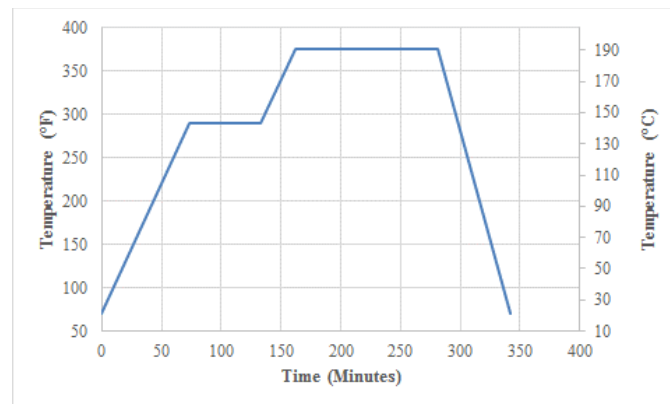


Figure 1. Manufacturer recommended cure cycle

The Teflon coating ensures easy release from the composite laminate. The manufacturer recommended cure cycle is shown in Figure 1. The temperature is first raised

to 290 °F (143.3 °C) for one hour, in order to enhance the mobility of reacting groups and then raised to the required base cure temperature.

3. MANUFACTURING

Laminates were manufactured using an Out-of-Autoclave (OOA) prepreg process. The details of configuration and dimensions of the laminates manufactured are shown in Table 1.

Table 1. Laminates manufactured in the study.

Number of laminates	Layup	Dimensions	Test
4	$[0^\circ/90^\circ/+45^\circ/-45^\circ]_{2s}$	6 in. x 6 in. x 0.076 in. (152.4 mm x 152.4 mm x 1.9 mm)	Porosity analysis
11	$[0^\circ/90^\circ/+45^\circ/-45^\circ]_{3s}$	12 in. x 12 in. x 0.12 in. (304.8 mm x 304.8 mm x 3.02 mm)	Base cure study
1	$[0^\circ/90^\circ/+45^\circ/-45^\circ]_{3s}$	12 in. x 12 in. x 0.12 in. (304.8 mm x 304.8 mm x 3.02 mm)	Post cure study
1	$[0^\circ]_8$	12 in. x 12 in. x 0.039 in. (304.8 mm x 304.8 mm x 1 mm)	Comparison with autoclave cured laminates

An aluminum mold was cleaned and covered with an Ethylene Tetrafluoroethylene (ETFE) release film. Prepreg layers were cut to size and placed on the mold until the

laminates had the required number of layers. EB1590, a Teflon coated glass fabric, was used as an edge bleeder to remove entrapped air from the laminate stack. A layer of N10 breather (Airtech) was used for even distribution of vacuum. The entire setup was sealed using a vacuum bag. The vacuum pressure was 28 in. Hg. Debulking was performed every four layers, for a duration of thirty minutes, to remove the entrapped air from the laminate stack and ensure good prepreg compaction. The bagging scheme is shown in Figure 2. A final warm debulk was performed at 121 °F (50 °C) for one hour. The laminate was then sealed using a double bagging scheme and cured in an oven. The base cure options used in this study are shown in Table 2. Test specimens were cut from the manufactured laminate for mechanical testing.

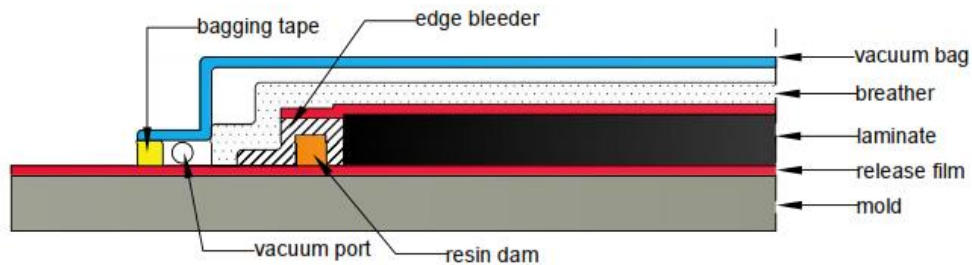


Figure 2. OOA process bagging assembly

For the study on the effect of post-cure conditions, a single 24 ply laminate with orientation, $[0^\circ/90^\circ/+45^\circ/-45^\circ]_{3s}$, was manufactured using the base cure cycle, 375 °F

(191 °C) /2 hours. Test samples were extracted and post cured according to the post cure options in Table 2.

Table 2. Cure conditions

Base cure options		Post cure options	
Temperature (°F / °C)	Time (hours)	Temperature (°F / °C)	Time (hours)
325 (162)	2	425 (218)	2
325 (162)	4	425 (218)	4
325 (162)	6	450 (232)	2
350 (177)	2	450 (232)	4
350 (177)	4	475 (246)	2
350 (177)	6	475 (246)	4
375 (191)	2	500 (260)	2
375 (191)	4	500 (260)	4
375 (191)	6		

4. METHODOLOGY

4.1. POROSITY STUDY

Efficient air bleeding is required in order to obtain a relatively void free composite panel. Removal of entrapped air is an important part of the OOA process as working pressure differential is not high enough, compared to autoclave processing. Two bleeding techniques were evaluated- fiber glass cloth edge bleeder and Vac-Pak EB1590. 16 ply, Quasi-isotropic laminates with layup, $[0^{\circ}/90^{\circ}/+45^{\circ}/-45^{\circ}]_{2s}$, were used. The manufacturer recommended base cure cycle (Figure 1) was used for all bleeder evaluation panels. Each

panel was tested for void content by acid digestion according to ASTM D3171. Five samples (25.4 mm x 25.4 mm) were cut from the composite panels and density measured by water displacement according to ASTM D792. The samples were dissolved in concentrated sulfuric acid and the resin was oxidized using hydrogen peroxide. The fibers were separated and weighed.

4.2. INFLUENCE OF BASE CURE CONDITIONS

Properties such as chain length and degree of cure are influenced by the cure history of a polymer [16]. These properties have a direct impact on its mechanical properties. Low green strength (strength before post cure) can also result in droop during free-standing post cure.

4.3. EXPERIMENTAL DESIGN

The influence of base cure cycles on mechanical properties of the composite laminate was evaluated utilizing experimental data via the design of experiments (DOE) approach. Interlaminar shear strength (ILSS) was the response variable. The effect of two factors were investigated, namely cure temperature and curing time. The experimental factors referred in DOE nomenclature are input variables, set at predetermined levels. A central composite design, rather than a full-factorial experiment was used (Figure 2). The Central composite design chosen for this study can be used to fit a second order model. The end points (-1 and +1 values in coded form) of the central composite design were

temperatures of 325 °F (162 °C) and 375 °F (191 °C) and cure times of 2 hours and 6 hours. A face centered central composite (CCF) design was selected with axial points corresponding to 350 °F (177 °C)/4 hours, 375 °F (191 °C)/4 hours, 350 °F (177 °C)/2 hours, and 375 °F (191 °C)/6 hours. The center point (0 in coded form), 350 °F (177 °C)/4 hours was replicated thrice.

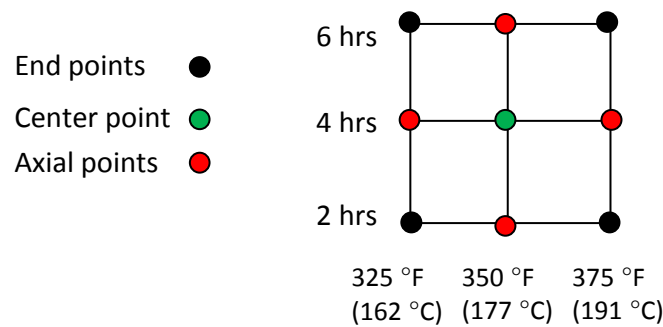


Figure 3. Face centered central composite design

4.4. SHORT BEAM SHEAR TEST

Green strength (strength before post cure) of the composite panels was evaluated using SBS test. Eleven composite panels, according to the central composite design, were manufactured. Each laminate had 24 plies arranged in quasi isotropic stacking sequence $[0^\circ/90^\circ/+45^\circ/-45^\circ]_{3s}$. Five samples, measuring 38.1 mm x 7.62 mm x 3.02 mm, were extracted from each panel. The test was performed on an Instron 5985 machine at room

temperature. Span to thickness ratio was 3:1. Samples were loaded under three point bending at a machine crosshead speed of 0.05 in. per minute (1.27 mm/min.).

4.5. INFLUENCE OF POST CURE CONDITIONS

4.5.1. Glass Transition Temperature. The glass transition temperature was evaluated using Thermomechanical Analysis (TMA). A sample of size 3 mm x 3 mm was cut from the laminate and placed in the thermomechanical analyzer (Perkins-Elmer). A sample of size 3 mm x 3 mm x 3.02 mm was cut from the laminate and heated to 572 °F (300 °C) at a rate of 9 °F (5 °C) per minute. The glass transition temperature is the temperature at which a second order transition in the rate of expansion of the sample was observed.

4.5.2. Mechanical Testing. The delamination resistance of the composite samples was evaluated using SBS, using the same experimental conditions as mentioned earlier. Three samples were tested for each post cure option. The results of mechanical testing at room temperature were evaluated using the design of experiments approach. A full factorial design was used. Post cure temperature and duration were the input factors. The factor, "post-cure temperature" had four levels i.e. 425, 450, 475 and 500 °F (218, 232, 246 and 260 °C). The other factor, "post cure time" (duration) had two levels, 2 hours and 4 hours.

5. RESULTS AND DISCUSSION

5.1. POROSITY STUDY

Both bleeder materials, fiberglass cloth and EB1590, were capable of producing low void contents in the manufactured laminate (Table 3). Debulking every 4 layers resulted in a decrease in void contents.

Table 3. Evaluation of bleeders

Panels	Bleeder	Debulking	Mean void content (%)
1	fiberglass cloth	Yes	0.78±0.28
2	fiberglass cloth	No	3.85±1.19
3	EB1590	Yes	0.31±0.13
4	EB1590	No	1.44±0.65

Both the fiberglass cloth as well as the EB1590 were capable of ensuring <1% void contents which is a requirement for aerospace composites. The Teflon coating in EB1590 offers easy release from the cured laminate compared to the 54 gsm fiberglass cloth. To ensure ease of processing as well as high laminate quality, EB1590 was selected. Therefore, laminates used to evaluate variations in the base cure and post cure cycles, were manufactured using the Vak-Pak EB1590 bleeder and a debulk cycle.

5.2. INFLUENCE OF BASE CURE CONDITIONS

A change in cure cycles results has a significant effect on matrix dominated behavior such as interlaminar shear strength. Previous studies on cure kinetics of BMI based thermoset systems have demonstrated that the dependence of reaction rate on cure conditions can be described by an nth order reaction model [17]:

$$\frac{d\alpha}{dt} = A \exp\left(\frac{-E}{RT}\right) (1 - \alpha)^n \quad (1)$$

Where α is the degree of cure, $d\alpha/dt$ is the reaction rate, E is energy of activation, T is the temperature, R is the universal gas constant, n is the reaction order and A is a constant. The rate of reaction increases with an increase in temperature. The degree of cure of the composite system is expected to increase with an increase in the cure temperature as well as the cure duration. This behavior should be reflected in macroscopic properties such as ILSS, which are resin dominated.

5.3. SHORT BEAM SHEAR TEST

Results of short beam shear tests are shown in Figure 4. Failure was due to ply cracking in the central layers of the specimen, which is an acceptable mode of failure according to ASTM D2344. On continued application of load, delamination of other layers was observed. Low ILSS of samples cured at 325 °F (162 °C) can be a result of low degree of cure at the central layers of the laminate. In general, a rise in base cure temperature and

time resulted in an increase in short beam shear strength (Figure 4), which agrees with the hypothesis mentioned earlier.

In order to quantify the effect of cure temperature and time on ILSS, test results were evaluated using Analysis of Variance (ANOVA). In the current study, the null hypothesis is, “A change in factor levels, cure temperature and time, does not produce a significant change in the response variable”.

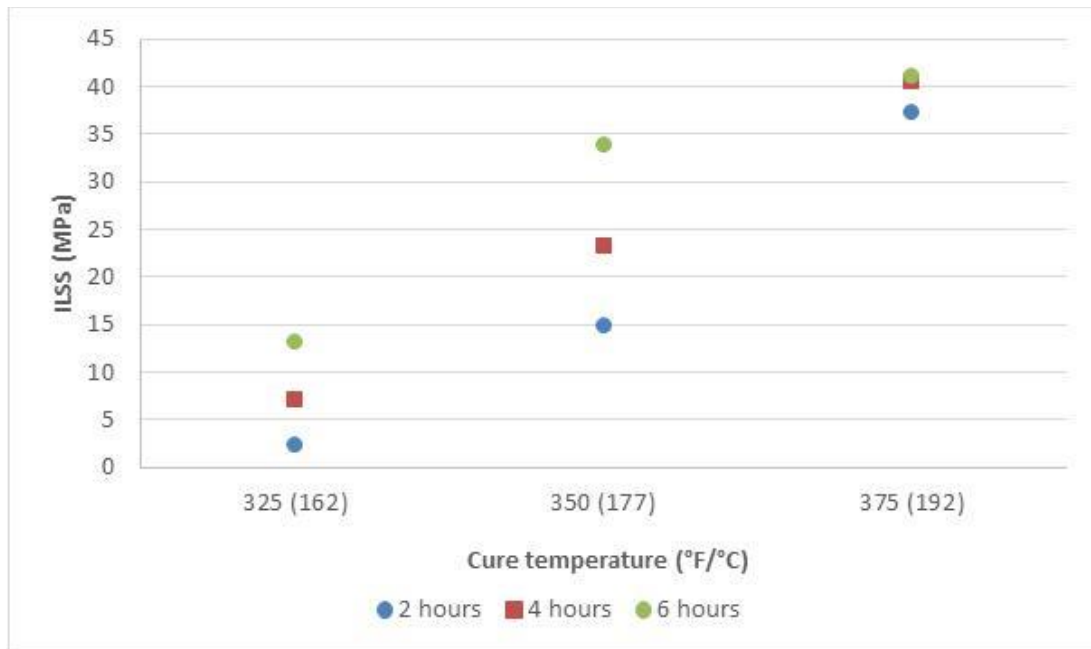


Figure 4. Effect of cure conditions on ILSS

If the *p-value*, calculated using analysis of variance (ANOVA), is less than a pre-determined significance level, the null hypothesis can be rejected, concluding that: a change in base cure temperature and time results in a statistically significant change in

laminate mechanical properties. In the current study, a significance level of 0.05 was selected. The *p-value* for model is 0.001 which indicates that the model is significant and the null hypothesis can be rejected (Table 4). In addition to testing model significance, the statistical significance of the two factors, cure temperature and curing time, were tested, specifically looking at the linear and quadratic effects of those variables on ILSS.

Table 4. ANOVA table for the effect of base cure conditions on ILSS

Term	Deg. of freedom	Adj. sum of Sq.	Adj. mean sq.	F	<i>p</i>
Model	5	1748.58	349.71	34.75	0.001
Linear	2	1735.08	867.54	86.19	0.000
Temperature (°F)	1	1547.00	1547.00	153.70	0.000
Time (Hours)	1	188.08	188.08	18.69	0.008
Square	2	0.42	0.21	0.02	0.979
Temperature(°F)*Temperature(°F)	1	0.10	0.01	0.01	0.979
Time (Hours)*Time (Hours)	1	0.40	0.04	0.04	0.924
Interaction	1	13.08	13.08	1.30	0.306
Temperature (°F)*Time (Hours)	1	13.08	1.30	1.30	0.306
Error	5	50.33	10.07		
Lack-of-Fit	3	49.83	16.61	67.39	0.015
Pure Error	2	0.49	0.24		
Total	10	1798.90			

The *p-values* of the square terms as well as the interaction terms are greater than 0.05. Therefore, they do not have a significant effect on the response, ILSS, and can be rejected. Since the *p-values* of the linear terms (of both temperature and time) are less than

0.05, their effects are statically significant. Sample ILSS is affected by both base cure time and temperature.

A regression model was fit, in order to study how the ILSS changes in response to a change in base cure temperature and time. A regression model is an empirical relation which relates the factors to the responses considered in the experiment. The response, ILSS can be related to the factors as a second order quadratic equation,

$$\begin{aligned} \text{ILSS} = & \beta_0 + \beta_1(\text{Time}) + \beta_2(\text{Temperature}) + \beta_3(\text{Time}^2) + \beta_4(\text{Temperature}^2) \\ & + \beta_5(\text{Time} * \text{Temperature}) + \varepsilon \end{aligned} \quad (2)$$

Where the terms labeled “ β ” represents coefficients to be determined and ε is the error. Since the effects of square and interaction terms are negligible, their coefficients were set to zero.

$$\text{ILSS} = -212.3 + 0.6423(\text{Temperature}) + 2.799(\text{Time}) \quad (3)$$

where ILSS is interlaminar shear strength, Temperature is expressed in °F and Time is expressed in hours. The variation of ILSS with time and temperature is shown in Equation 2. The response surface plot corresponding to the regression equation is shown in Figure 5. As seen in Figure 5, the delamination resistance increases with a rise in curing temperature as well as time. A rise in cure temperature and time can result in an improvement in the degree of cure, resulting in a better bond between the fiber and matrix.

Accordingly, the laminate fabricated using a cure condition of 375 °F (191 °C) /6 hours exhibited the greatest ILSS of 41.06 MPa. A 4.67 °F (2.59 °C) change in cure temperature is capable of producing a similar effect on delamination resistance, compared to a 1 hour change in cure time.

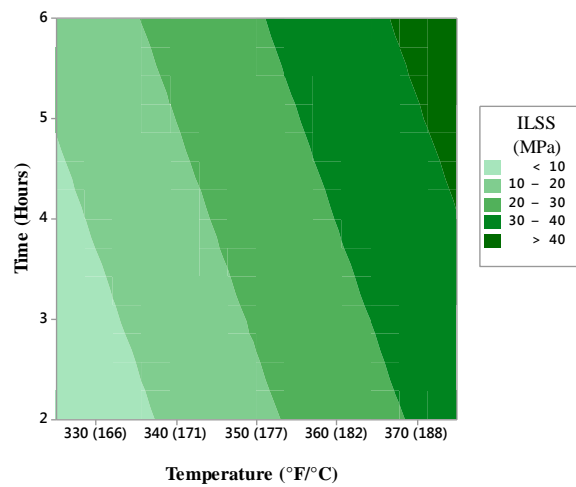


Figure 5. Response surface plot of the influence of base cure temperature and time on ILSS

5.4. VERIFICATION OF RESULTS

Lowering base cure temperatures can reduce tooling costs. The results of the response surface design show that using a base cure cycle of 360 °F (182.2 °C) /6 hours can result in a laminate of high quality compared to the manufacturer recommended cure cycle of 375 °F (191 °C) /2 hours. For the purpose of verification, a composite panel was manufactured using a cure cycle of 360 °F (182.2 °C) /6 hours. The sample thickness was

2.99 mm, void content was 0.83% and the density was 1.56 g/cm³. Five samples were removed and their ILSS was measured by short beam shear. The average ILSS was calculated to be 38.1 MPa. This compares well with the observed value of ILSS (37.43 MPa) at the manufacturer recommended cure cycle.

5.5. INFLUENCE OF POST CURE CONDITIONS

The purpose of post curing a composite is twofold: to improve the degree of cure and to increase the crosslink density. Results from prior Fourier transform infrared spectroscopy of BMI systems have indicated the presence of multiple reactions during cure [18, 19, 20]. In early stages of cure, the chain extension reactions dominate [21]. During later stages of cure, the reaction mechanism is dominated by crosslinking. The crosslinking reaction occurs mainly above 180 °C.

5.6. GLASS TRANSITION TEMPERATURE

All post cure cycles were found to be capable of producing a composite that has a T_g higher than conventional epoxies. Glass transition temperatures of post cured samples increased with increase in post cure temperature in a linear fashion (Figure 6). Increase in the post cure time also lead to a rise in T_g . This is a direct result of an increase in the crosslink density between polymer chains. Maximum T_g was exhibited by samples post cured at 500 °F (260 °C) for 4 hours.

5.7. MECHANICAL TESTING

Using short beam shear tests, ILSS of green composite specimens was found to be 38.1 MPa. All post cure options resulted in an increase in ILSS of the composite specimens, which is due to the increase in degree of cure and crosslink density (Figure 7). Samples failed by the means of matrix cracking in the central layers of the specimens.

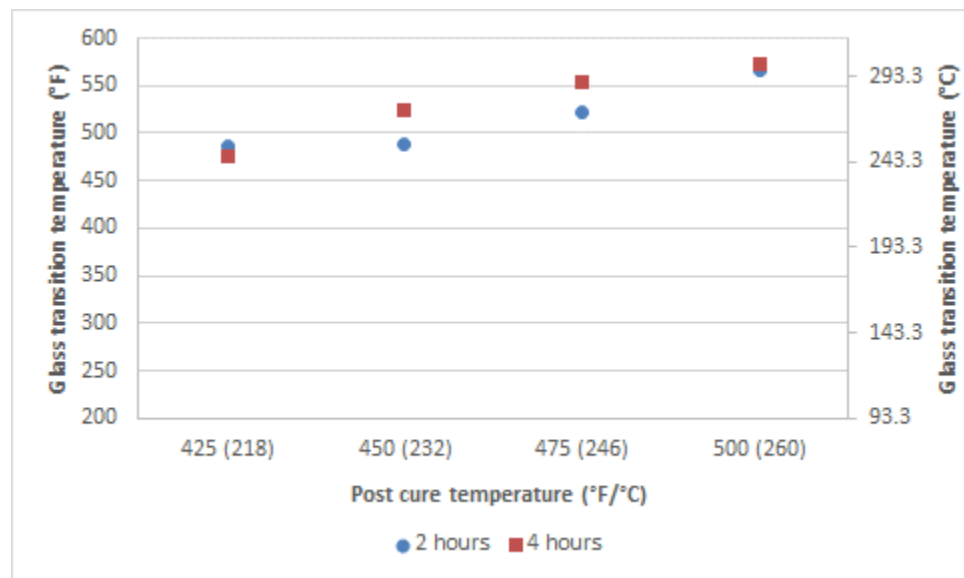


Figure 6. Variation of glass transition temperature with post cure conditions

The results of mechanical testing, evaluated using two-way ANOVA, are shown in Table 5. A significance level of 0.05 was used for the analysis. The *p-value* for model significance was 0.004. Since this is less than 0.05, a change in post cure temperature and time has a significant effect on the properties of the manufactured laminate.

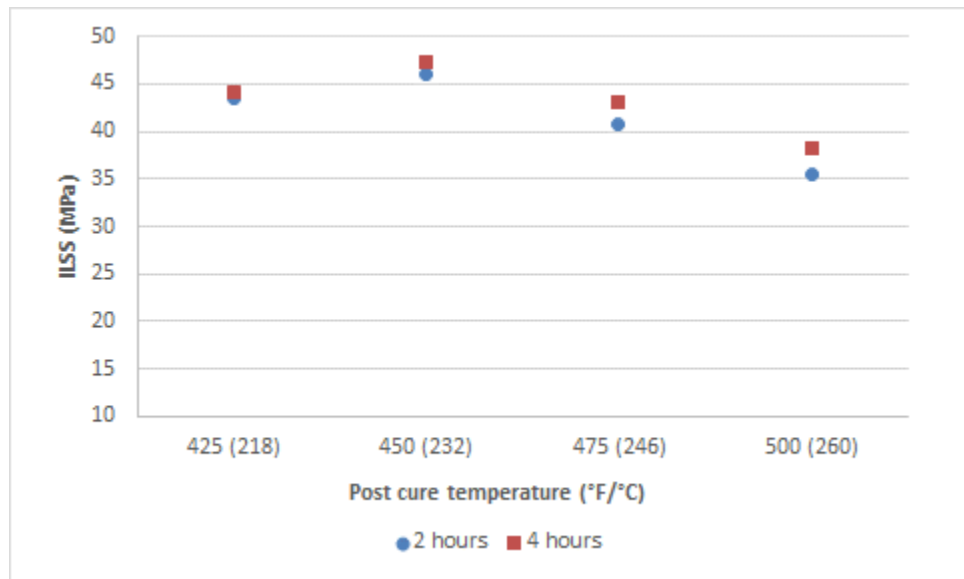


Figure 7. Variation of ILSS with post cure conditions

Table 5. ANOVA table for the effect of post cure conditions on ILSS

Term	Degrees of freedom	Adjusted Sum of Squares	Adjusted Mean Squares	F	<i>p</i>
Model	7	291.42	41.63	4.97	0.004
Temperature (°F)	3	252.93	84.30	10.07	0.001
Time (Hours)	1	31.82	31.82	3.80	0.069
Interaction	3	6.67	2.22	0.27	0.849
Error	16	133.9	188.08		
Total	23	425.32			

The effect of interaction between the factors is considered statistically insignificant, because the *p-value* is 0.849 (>0.05). The *p-value* of the temperature of the effect of temperature was 0.001 which indicates that this factor has a significant effect on the response. The effect of post cure time is less significant (*p-value* = 0.069) than the post

cure temperature. The factor, post cure time, was retained in the regression model (Equation 3) because of its proximity to the cutoff value of 0.05. The factor ILSS, shows a dependence of the form,

$$\text{ILSS} = -497 + 1.151(\text{Time}) + 2.421(\text{Temperature}) - 0.002723(\text{Temperature})^2 \quad (4)$$

Where ILSS is interlaminar shear strength, Temperature is expressed in °F and Time is expressed in hours.

According to the regression equation, obtained by least squares fitting, maximum ILSS is obtained after post cure conditions of 444.5 °F (229 °C)/ 4 hours. The increase in ILSS is due to improved degree of cure and increased crosslinking in the polymer chains. When samples are post cured at temperatures higher than 444.5 °F (229 °C), the mechanical properties begin to degrade.

Results for literature indicate that the degree of crosslinking increases with an increase in post cure temperature [15]. The initial increase in ILSS can be explained because of an increase in matrix rigidity due to increased crosslink density. On the other hand, excessive crosslink densities can lead to matrix embrittlement which is associated with a reduction in resin dominated mechanical properties. The mechanical properties of the BMI composite can be improved by post curing but they will drop if the temperature is too high. Similar reduction in resin dominated properties such as mode II fracture toughness and flexure strength was reported by He et al. for autoclave cured Cycom IM7/5250-4 composites [15].

5.8. COMPARISON WITH AUTOCLAVE CURED COMPOSITES

Unidirectional (8 ply) composite laminates were manufactured via OOA process. The laminates were cured at 375 °F (192 °C) / 2 hours followed by a free standing post cure at 450 °F (232 °C) for 4 hours.

Table 6. Comparison of autoclave and OOA cured composite laminates.

	OOA cured	Autoclave cured* (85 psi)
Cure cycle	290 °F (143 °C) for 2 hours; 375 °F (191 °C) for 2 hours;	290 °F (143 °C) for 1 hour; 310 °F (154 °C) for 1 hour; 375 °F (191 °C) for 2 hours
Post cure	450 °F (191 °C) for 4 hours	410 °F (210 °C) for 2 hours
Layup	[0°] ₈	[0°] ₈
ILSS	143.54 MPa	139.96 MPa

*source- manufacturer data sheet

The samples showed no warping on post cure. Test samples were cut and the ILSS was measured according to ASTM D2344. A span to thickness ratio of 4:1 was used. The loading rate was 1.27 mm per minute. The ILSS of the manufactured laminates was 143.54 MPa. The mechanical properties of the fabricated laminate were compared with those of autoclave cured composites (data provided by manufacturer), using the same prepreg. The properties of OOA cured laminate are comparable with the properties of the specimens fabricated in an autoclave under 85 psi (Table 6).

6. CONCLUSIONS

Laboratory scale Carbon/Bismaleimide composite laminates were manufactured successfully using the OOA process. Edge bleeding with debulking every 4 layers was found to be successful in producing parts with low void contents (<1%). The effect of cure cycle variations on mechanical and thermal properties of the OOA cured BMI composite laminates was evaluated. Low base cure temperatures produced parts with relatively low mechanical strengths. Maximum interlaminar shear strengths were obtained when parts were cured at 375 °F (191 °C) for 6 hours. Base cure cycles involving lower temperatures and cure times resulted in a drop in ILSS. A base cure cycle of 360 °F (182 °C) / 6 hours can result in a laminate having ILSS comparable to one manufactured using the recommended cure cycle of 375 °F (191 °C) / 2 hours.

The variation of T_g and ILSS with post-cure conditions was evaluated. Samples were post cured at temperatures between 425 °F (218 °C) and 500 °F (260 °C). Post cure times of 2 hours and 4 hours were evaluated. An increase in post cure temperature as well as post cure time led to a rise in T_g . The measured T_g was sufficient to replace conventional epoxy resins in high temperature applications. The interlaminar shear strength was affected by post cure temperature. Post curing up to a temperature of 444.5 °F (229.1 °C) results in an increase in ILSS. The mechanical properties degrade at higher post cure temperatures, possibly due to thermal degradation and excessive crosslinking. The effect of post cure time is less significant compared to the effect of post cure temperature. Based on the results of experimental testing it was found that maximum ILSS can be obtained in samples post cured at 444.5 °F (229.1 °C) for four hours. Test samples were manufactured at 375 °F

(191 °C) / 2 hours and post cured at 450 °F (232 °C) / 4 hours. Their properties compared well with those of an autoclave cured composite.

ACKNOWLEDGEMENTS

This work was supported by the Center for Aerospace Manufacturing Technologies (CAMT) and the Intelligent Systems Center (ISC) at Missouri S&T.

REFERENCES

1. C. Ridgard, "Next Generation Out-of-Autoclave Systems," *Proceedings of the International SAMPE Symposium and Exhibition*, pp. 1-18, Seattle, Wa, May 17-20, 2010.
2. Z. Sakota, H. Thomas Hahn, L. Lackman and G. Bullen, "Out of Autoclave Curing of Composites," *Proceedings of the International SAMPE Symposium and Exhibition*, pp. 1-13, Long Beach, CA, April 30 - May 4, 2006.
3. T. Centea, L. Gunenfelder and S. Nutt, "A Review of Out-of-Autoclave Prepregs – Material Properties, Process Phenomena, and Manufacturing Considerations," *Composites Part A: Applied Science and Manufacturing*, vol. 70, pp. 132-154, 2015.
4. L. Grunenfelder and S. Nutt, "Void Formation in Composite Prepregs- Effect of Dissolved Moisture," *Composites Science and Technology*, vol. 70, pp. 2304-2309, 2010.
5. T. Centea and P. Hubert, "Measuring the Impregnation of an Out-of-Autoclave Prepreg by Micro-CT," *Composites Science and Technology*, vol. 71, pp. 593-599, 2011.
6. M. L. Costa, S. F. Almeida and M. C. Rezende, "The Influence of Porosity on the Interlaminar Shear Strength of Carbon/ Epoxy and Carbon/Bismaleimide Fabric Laminates," *Composites Science and Technology*, vol. 61, pp. 2101-2108, 2001.

- A. Levy, J. Kratz and P. Hubert, "Air Evacuation during Vacuum Bag Only Prepreg Honeycomb Sandwich Structures: In-plane Air Evacuation Prior to Cure," *Composites Applied Science and Manufacturing*, vol. 68, pp. 365-376, 2015.
7. G. Marsh, "De-autoclaving Prepreg Processing," *Reinforced Plastics*, vol. 56, pp. 20-25, 2012.
8. J. Sutter, W. Kenner, L. Pelham, S. Miller, D. Polis, C. Nailadi, T. Hou, D. Quade, B. Lerch, R. Lort, T. Zimmerman, J. Walker and J. Fikes, "Comparison of autoclave and Out-of-Autoclave Composites," *Proceedings of the SAMPE Fall Technical Conference*, pp. 1-15, Salt Lake City UT, October 11-14, 2010.
9. R. Stratton and L. Repecka, "Demonstration of Next Generation BMI Prepregs for Out-of-Autoclave Processing," *Proceedings of the International SAMPE Technical Conference*, pp. 1-10, Long Beach, CA, May 24-26, 2011.
10. H. Stenzenberger, M. Herzog, P. Koenig, W. Roemer and W. Breitigam, "Bismaleimide Resins: Past, Present, Future," *Proceedings of the International SAMPE Symposium and Exhibition*, pp. 1877-1888, Reno NV, May 8-11, 1989.
11. W. Hastings, L. Pelham, S. Miller, J. Sutter, R. Martin, L. McCorkle and D. Scheiman, "Fabrication and Characterization of Out-of-Autoclave (OOA) Bismaleimide (BMI) Laminates for Large Composite Structures," *Proceedings of the International SAMPE Technical Conference*, pp. 1347-1360, Long Beach CA, May 6-9, 2013.
12. T. Hou, S. Miller, T. Williams and J. Sutter, "Out-of-Autoclave Processing and Properties of Bismaleimide Composites," *Journal of Reinforced Plastics and Composites*, vol. 33, pp. 137-149, 2014.
13. T. Vo, K. Vora and B. Minaie, "Effects of Postcure Temperature Variation on Hygrothermal-Mechanical Properties of an Out-of-Autoclave Polymer Composite," *Journal of Applied Polymer Science*, vol. 130, pp. 3090-3097, 2013.
14. Y. He, Y. Zhong and J. Zhou, "Post-curing Effects on Physical and Mechanical Properties of IM7/5250-4 Composites," *Proceedings of the International SAMPE Technical Conference*, pp. 226-233, San Antonio TX, October 20-24, 1998.
15. P. Painter and M. Colemon, *Fundamentals of Polymer Science: an Introductory Text*, New York (1998): CRC Press, 1998.

16. Z. Guo, S. Du, B. Zhang and Z. Wu, "Cure Kinetics of T700/BMI Prepreg used for Advanced Thermoset Composite," *Journal of Applied Polymer Science*, vol. 97, pp. 2238-2241, 2005.
17. A. Tungare and G. Martin, "Analysis of the curing behavior of bismaleimide resins," *Journal of Applied Polymer Science*, vol. 46, no. 7, pp. 1125-1135, 1992.
18. J. Mijovic´ and S. Andjelic´, "Study of the Mechanism and Rate of Bismaleimide Cure by Remote in-Situ Real Time Fiber Optic Near-Infrared Spectroscopy," *Macromolecules*, vol. 29, pp. 239-246, 1996.
19. R. Morgan, E. Shin, B. Rosenberg and A. Jurek, "Characterization of the Cure Reactions of Bismaleimide Composite Matrices," *Polymer*, vol. 38, no. 3, pp. 639-646, 1997.
20. F. Boey, X. Song, C. Yue and Q. Zhao, "Modeling the Curing Kinetics for a Modified Bismaleimide Resin," *Journal of Polymer Science: Part A: Polymer Chemistry*, vol. 38, no. 5, pp. 907-913, 2000.

II. PROCESSING AND PERFORMANCE OF OUT-OF-AUTOCLAVE BISMALEIMIDE COMPOSITE SANDWICH STRUCTURES

S. Anandan, G. S. Dhaliwal and K. Chandrashekhara
Department of Mechanical and Aerospace Engineering
Missouri University of Science and Technology, Rolla, MO 65409

T. R. Berkel
Boeing Research & Technology, St. Louis, MO 63166

D. Pfitzinger
GKN Aerospace, St. Louis, MO 63042

ABSTRACT

Composite sandwich structures offer several advantages over conventional structural materials such as lightweight, high bending and torsional stiffness, superior thermal insulation and excellent acoustic damping. In the aerospace industry, sandwich composites are commonly manufactured using the autoclave process which is associated with high operating cost. Out-of-autoclave (OOA) manufacturing has been shown to be capable of producing low cost and high performance composites. Unlike the autoclave process, OOA processing avoids the issue of core-crushing due to high pressure. However, Bismaleimide (BMI) prepregs require high cure and post-cure temperatures which can lead to high internal core pressures, core-to-facesheet disbonding and voids. In the current work, OOA sandwich composite panels are manufactured using aluminum honeycomb core, BMI

adhesive film and carbon/BMI preregs. Two vacuum levels were used during OOA processing, full vacuum (100 kPa) and partial vacuum (80 kPa). Adhesive bond quality was evaluated using flatwise tensile and fracture toughness tests. Mechanical performance was evaluated using edgewise compression. It was observed that vacuum level variation during processing had no significant effect on mechanical properties of manufactured laminates. Tests are performed at room temperature and 177 °C (350 °F). All manufactured laminates exhibited room temperature flatwise tensile strengths comparable to those of aerospace grade epoxy adhesives. Sandwich mechanical properties reduced when test temperature was increased.

1. INTRODUCTION

High performance composite materials are conventionally processed in autoclaves which are associated with high capital requirements and operating costs. Part size is also limited by the autoclave chamber volume. Out-of-autoclave (OOA) processing has emerged as an alternative to autoclave processing [1, 2]. OOA involves curing at atmospheric pressures which obviates the need for an autoclave and provides greater design flexibility for production of large and complex shaped composite components. It also reduces capital and operating costs. In an OOA prepreg process, removal of entrapped air from the prepreg layup is critical which can otherwise lead to voids which degrade mechanical properties of the composite. Sandwich components can be co-cured, a process where adhesive and the prepreg are cured simultaneously, resulting in time and cost

reduction. Manufacturing co-cured sandwich panels out-of-autoclave, eliminates core crushing which can occur at autoclave pressures [3] and enables the use of lighter cores.

In a composite sandwich structure, the facesheet absorbs in-plane loads while the core is resistant to shear loading. The composite facesheet is bonded to the core using a film adhesive. The adhesive bond between core and facesheet is of great importance in the design of sandwich structures. The relation between the adhesive fillet and sandwich properties was described by Grimes [4]. The mechanical performance of a sandwich composite depends on the quality of the core-to-facesheet adhesive bond. In the case of honeycomb cores, the cell walls provide a relatively small area for bonding. Structural strength depends on the presence of a well-formed fillet at the interface of the core cell wall and facesheet. Larger adhesive fillets absorb a higher amount of energy upon fracture, due to which they have high fracture toughness [5]. Grove et al. [6] showed that the higher debonding energy was obtained with larger, regular-shaped adhesive fillets between the honeycomb cell walls and the skin. Rion et al. [7] showed the failure occurs in the adhesive meniscus when low weight adhesive is used. Butukuri et al. [8] evaluated the effect of the reticulation technique on properties of sandwich constructions. Core reticulation resulted in improved fillet geometry and flatwise tensile strength. Hou et al. [9] reported that thermal pre-treatments can reduce adhesive foaming in OOA cured composite sandwich structures. Nagarajan et al. [10] studied the effect of processing variables on OOA sandwich panels with carbon/epoxy facesheets. Presence of dissolved moisture in the adhesive layer was found to increase adhesive foaming.

Internal core pressure in the cells of a honeycomb core has been shown to affect adhesive foaming and fracture toughness in sandwich composites with carbon/epoxy facesheets [11]. Core pressure fluctuations were observed when internal core pressures during cure equaled atmospheric pressure. Increased adhesive permeability due to perforation resulted in enhanced fracture toughness of the adhesive layer. The optimal range of honeycomb core pressure during processing was estimated to be 40-70 kPa, to reduce adhesive outgassing and ensure good fillet formation [12].

OOA epoxy prepreg systems have previously been used in the Boeing wing spar, Advanced Composite Cargo Aircraft (ACCA) and the Ares V interstage and payload shroud [13, 14]. OOA Bismaleimide (BMI) systems were evaluated as a part of NASA CoEx (Composites for Exploration) project [15]. Due to tooling limitations, the cure temperature was fixed at 177 °C (350 °F) followed by a freestanding post-cure at elevated temperatures. BMI prepreg systems from Renegade, Stratton Composites and Tencate were evaluated. Two adhesive systems namely Cytec FM 2550 and Renegade RM 3011 were evaluated. Sandwich structures exhibited no warping on post-cure, and flatwise tensile strength obtained was comparable to aerospace grade epoxy adhesives.

In the current work, sandwich composites were manufactured using aluminum honeycomb, carbon/BMI facesheets and a toughened BMI adhesive system. The sandwich composite was cured via the OOA prepreg process. One set of panels was fabricated under full vacuum pressure (100 kPa). Remaining panels were manufactured using a reduced vacuum pressure of 80 kPa. This level was chosen to ensure that the internal core pressure does not exceed atmospheric pressure during the high temperature cure. The effect of

varying vacuum pressure on mechanical properties of the sandwich composite was evaluated. Adhesive bond quality was evaluated using flatwise tensile tests and adhesive bond fracture toughness tests. Load bearing capability structure was evaluated using edgewise compression tests.

2. MATERIALS

The sandwich facesheets were fabricated using unidirectional IM7/AR4550 prepreg, a toughened carbon/BMI system suitable for OOA curing. It has a resin content of 35% and a prepreg areal weight of 304.8 gsm.

Table 1. Materials used

Name	Supplier	Specifications
Carbon/BMI prepreg (IM7/AR4550)	Aldila Composite Materials	Recommended cure cycle: 143.33 °C (290 °F) for 1 hour, 190.5 °C (375 °F) for two hours. Post cure at 232 °C (450 °F).
BMI film adhesive (Metlbond 2550)	Cytec Engineered Materials	Recommended cure cycle: 177 °C (350 °F) for 4 hours. Post cure at 226.6 °C (440 °F).
Aluminum honeycomb	Hexcel	Density: 8.1 pcf (129.7 kg/m ³) Thickness: 1 in. (25.4 mm) Cell size: 1/8 in. (3.175 mm)

Cytec Metlbond 2550 film adhesive was used to bond the facesheet to the honeycomb core. Metlbond 2550 is a modified BMI film adhesive with good high

temperature properties. The core material was aluminum honeycomb. Materials are listed in Table 1.

3. MANUFACTURING

Honeycomb sandwich composite panels were manufactured using an Out-of-Autoclave (OOA) manufacturing process. One set of panels of size 304.8 mm. x 304.8 mm (12 in. x 12 in.) and facesheet configuration $[0^\circ/90^\circ]_s$ were manufactured, which yielded samples for flatwise tensile and edgewise compression tests. A second set of sandwich panels 304.8 mm. x 152.4 mm (12 in. x 6 in.) and facesheet configuration $[0^\circ/90^\circ]_{2s}$ was manufactured for adhesive bond fracture toughness evaluation.

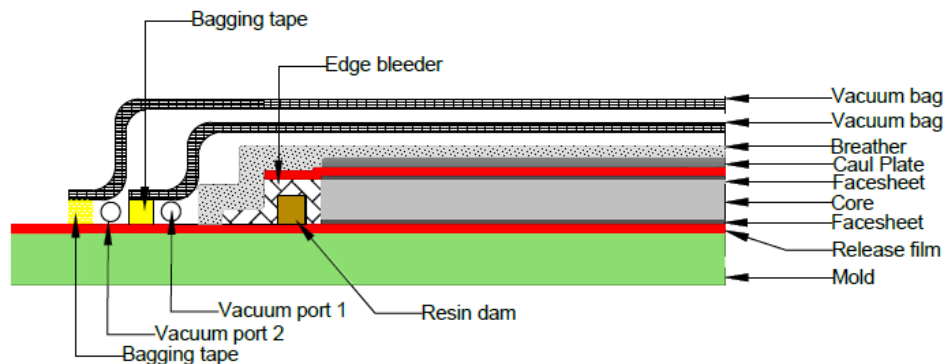


Figure 1. Schematic of bagging layup

An aluminum mold was cleaned of surface defects using sand paper, and a non-porous Ethylene tetrafluoro ethylene (ETFE) release film was placed. The prepreg layers

were cut into required dimensions and laid up according to the required facesheet configuration. Rollers along with hand pressure were used to press the prepregs, starting from the center of the layup and moving progressively towards the edges. This process was repeated for all the prepreg layers to remove entrapped air as well as folds or wrinkles. The tool-side and bag-side facesheet layups were debulked at room temperature under full vacuum for 60 minutes to ensure good compaction.

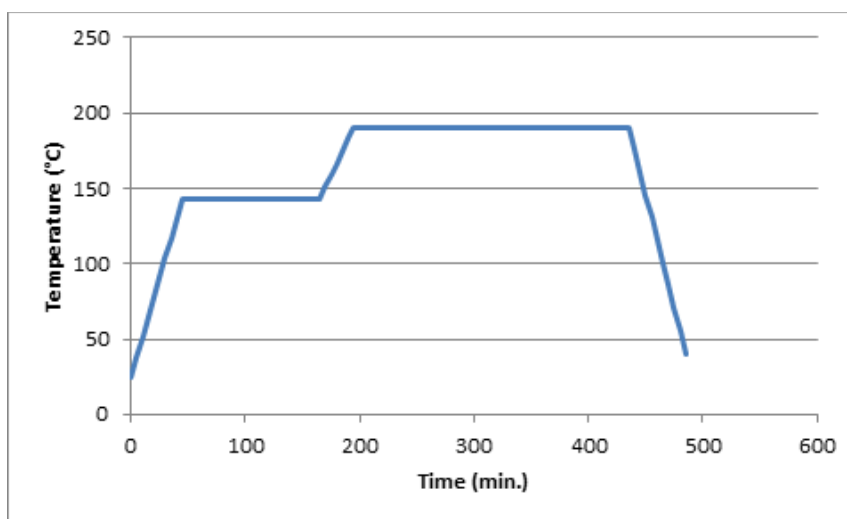


Figure 2. Cure Cycle

The schematic of the bagging procedure employed for the OOA process is shown in Figure 1. The compacted tool side facesheet layup was laid on the aluminum mold which was covered with the ETFE release film. A layer of film adhesive was placed on the prepreg layup. The honeycomb core was placed on the adhesive layer followed by the bag-side

adhesive layer and facesheet stack. Edge breathing using EB1590 edge bleeder was used to evacuate entrapped air from the sandwich layup. A layer of ETFE release film was placed on the sandwich layup followed by an aluminum caul plate. Airweave N10 breather was used to distribute the vacuum pressure evenly. The entire layup was sealed using a double vacuum bagging scheme.

The layup was debulked at 49 °C (120 °F) for two hours. The sample was cured according to the cure cycle shown in Figure 2, and allowed to cool down to room temperature. This was followed by a free-standing post-cure at 232 °C (450 °F) for two hours. The prepreg cure cycle was used to manufacture the sandwich panel. The samples did not exhibit warping following post cure.

4. EXPERIMENTS

4.1. THERMOGRAVIMETRIC ANALYSIS

Outgassing of prepreg and adhesive during cure can lead to voids in facesheets and adhesive fillets. These volatiles need to be removed during cure. The evolution of volatiles from the prepreg and adhesive was studied using Thermogravimetric analysis (TGA). The adhesive was removed from storage and allowed to warm up to room temperature. A small sample was removed and the prepreg cure cycle was simulated in a TGA. Air at a flow rate of 40 mL/min. was used as the sample purge gas and the weight loss was recorded.

4.2. FLATWISE TENSILE TEST

Flatwise tensile (FWT) strength primarily serves as a quality control parameter for bonded sandwich panels. This test produces information on the quality and strength of the core-to-facing adhesive bond. The flatwise tensile test for sandwich samples was done according to ASTM C297. Sandwich samples had a facesheet configuration of $[0^{\circ}/90^{\circ}]_s$. This test method consists of subjecting a honeycomb sandwich samples to a uniaxial tensile force normal to the plane of the sample. Honeycomb sandwich samples of 50.4 mm x 50.4 mm (2 in. x 2 in.) were cut from the manufactured panel. The sample edges were polished progressively using 80-220 grit sandpaper. The facings of the samples were lightly roughened using 80 grit sand paper. For RT testing, aluminum blocks of 50.4 mm x 50.4 mm x 50.4 mm (2 in. x 2 in. x 2 in.) were bonded to the sample facings using a high strength epoxy, 3M Scotch-Weld DP-460NS. The adhesive was allowed to cure at room temperature for 24 hrs and was post cured at 121 °C (250 °F) for two hours. Samples for elevated temperature testing at 177 °C (350 °F) were bonded to aluminum blocks using Metlbond 2550 film adhesive. Test samples were conditioned at 177°C (350°F) in the thermal testing chamber for 2 hours prior to testing. Average relative humidity was maintained at 50%. Sample loading rate was 0.5 mm/minute. Each test was replicated four times.

4.3. EDGEWISE COMPRESSION TEST

Edgewise compression test is used to measure the compressive properties of a sandwich specimen in a direction parallel to the facing plane. This test is a measure of the load bearing capacity of the sandwich structure. The edgewise compression test for sandwich samples was performed according to the ASTM C364. Sandwich samples had a facesheet configuration of $[0^\circ 90^\circ]_s$. Sandwich specimens were cut into 50.4 mm x 127 mm (2 in. x 5 in.) sizes. Tests were conducted at room temperature as well as 177 °C (350 °F). Test samples were conditioned at 177 °C (350 °F) in the environmental testing chamber for 2 hours prior to testing. Average relative humidity was maintained at 50%. A loading rate of 3 mm/min. was used. Mechanical load was applied along the core ribbon direction. Each test was replicated three times.

4.4. ADHESIVE BOND FRACTURE TOUGHNESS TEST

The interfacial fracture toughness was measured using a modified cracked sandwich beam (CSB) specimen [16]. Sandwich composites were manufactured with $[0^\circ 90^\circ]_{2s}$ facesheet orientation, using the manufacturing procedure mentioned in section 3. Specimens of size 25.4 mm x 254 mm (1 in. x 10 in.) were extracted from the manufactured panel. An initial crack of 25.4 mm (1 in.) was cut as shown in Figure 3. Aluminum blocks, with hinges, were bonded onto the sample as shown in Figure 4.

A roller support was added at the free end to prevent large rotations. Predetermined crack lengths were marked on the specimen and mechanical load was applied using an

Instron 5985 universal testing machine. This procedure was repeated for multiple loading/unloading cycles. Crack growth was along the core ribbon direction.

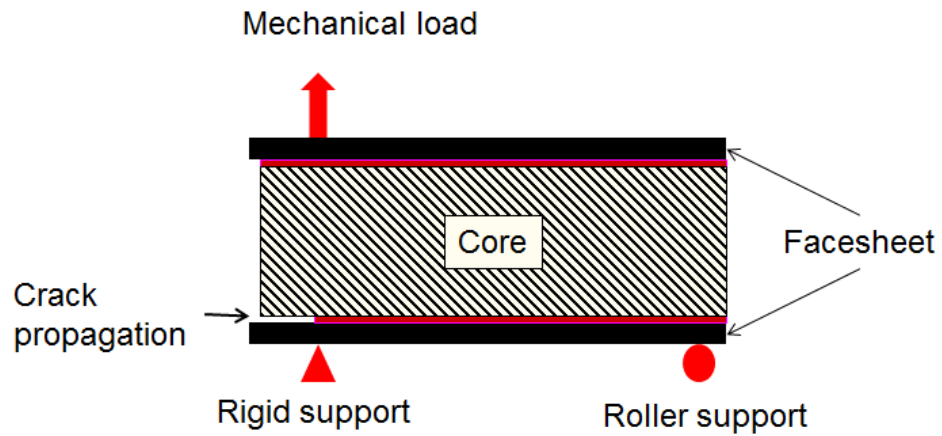
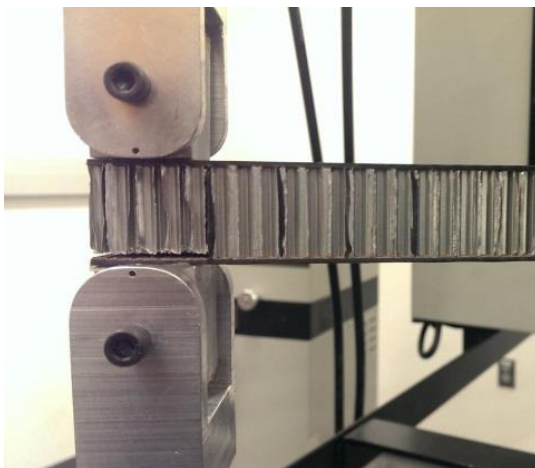
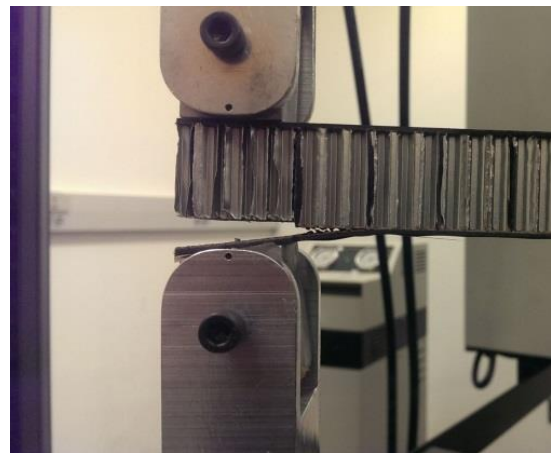


Figure 3. Schematic of modified CSB test



(a) Test setup



(b) Crack propagation on mechanical loading

Figure 4. Crack propagation in a modified CSB test

5. RESULTS AND DISCUSSION

5.1. THERMOGRAVIMETRIC ANALYSIS

Results of TGA are shown in Figure 5. The temperature was increased to 143.3 °C (290 °F) and held for 60 minutes. This isothermal hold is required to maximize the mobility of reacting groups. An initial mass loss of 1.8 % was seen during the first isothermal hold. The temperature was then increased to the cure temperature of 190.5 °C (375 °F) at 10 °C/min. An adhesive mass loss of 1.7 % was observed during this period. Mass loss during cure is due to adhesive outgassing which can lead to foaming defects in the adhesive layer.

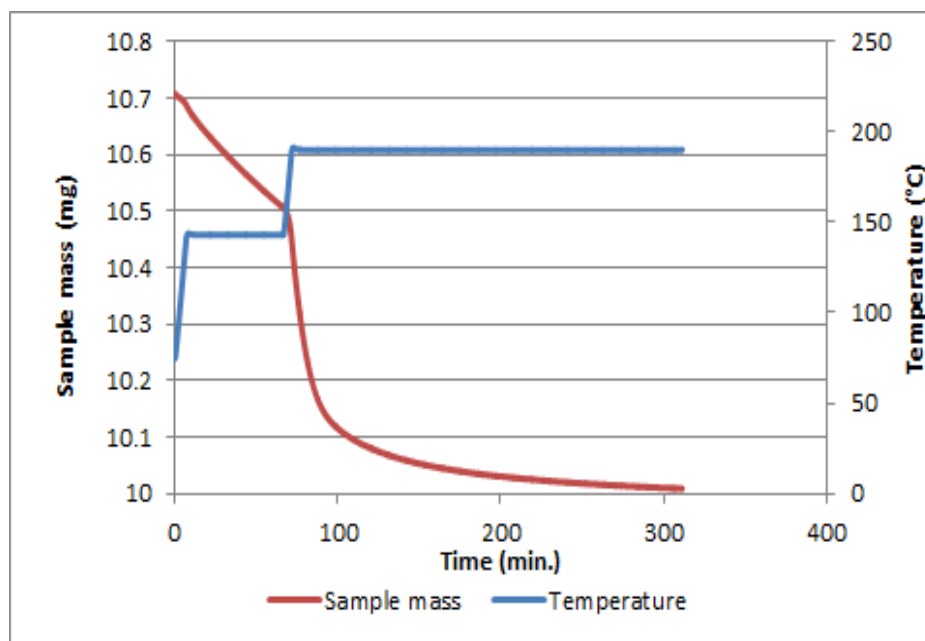


Figure 5. Mass loss of adhesive during TGA

5.2. FLATWISE TENSILE TEST

Results of the FWT tests are shown in Table 2. All samples failed in a combination of cohesive and adhesive failure mode. Values depicted in Table 2 are comparable to previously reported FWT properties of BMI sandwich structures [15].

They compare well with the FWT strength of 6167.7 kPa reported by Butukuri et al. [8] for OOA cured epoxy sandwich systems using Cycom 5320 facesheets (Cytac), Cycom FM 300-2U epoxy adhesive (Cytac) and aluminum honeycomb core (1/8 in. cell size, 12 pcf). Adhesive fillets are distributed on either side of the cell wall (Figure 6).

Table 2. FWT test results

Vacuum pressure (kPa)	Temperature °C/°F	Flatwise tensile strength	
		Average (kPa)	S.D. (%)
Full vacuum (100)	24/75	6848.77	11.8
Full vacuum (100)	177/350	5270.99	15.3
Partial vacuum (80)	24/75	6311.39	7.6
Partial vacuum (80)	177/350	4968.23	7.3

Samples cured at full vacuum pressure and at partial vacuum exhibited slightly higher FWT strengths. The adhesive bond strength reduced by 23% (full vacuum) and 21% (partial vacuum) when samples were tested at 177 °C (350 °F). The room temperature FWT strength values

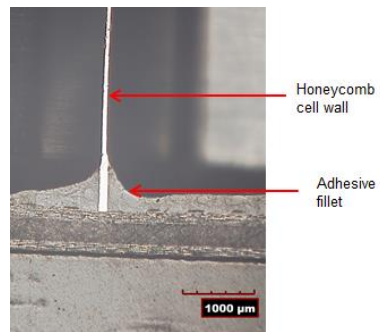
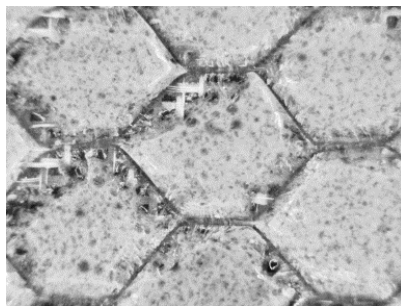
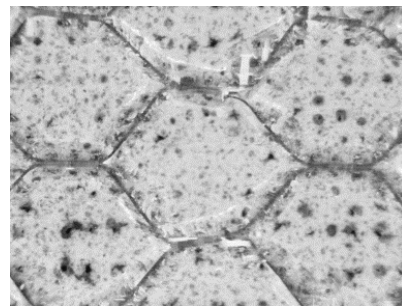


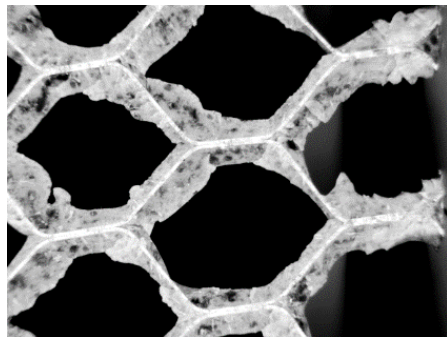
Figure 6. Adhesive fillet formation in sandwich composites manufactured under full vacuum pressure



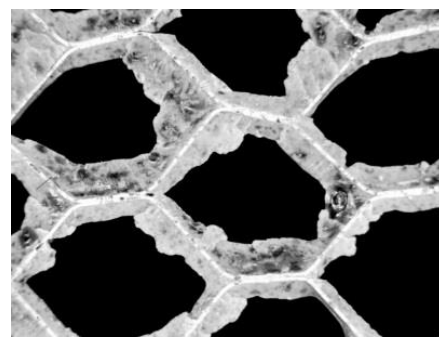
(a) Facesheet side



(b) Facesheet side



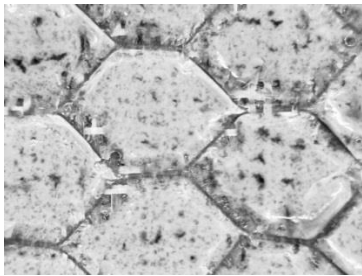
(c) Core side



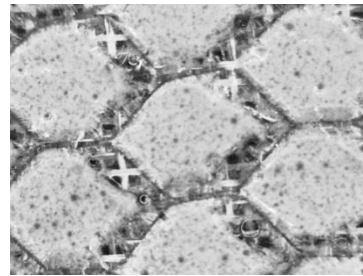
(d) Core side

Figure 7. Representative images of fracture surfaces of samples cured under full vacuum at different locations

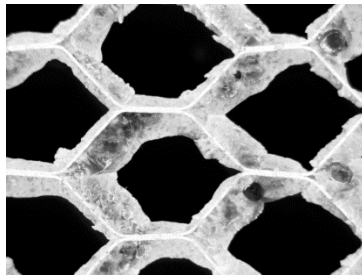
Voids and air packets are seen along the fillet regions (Figures 7(c), 7 (d),8 (c) and 8 (d)). These defects may be a result of low internal core pressures which have been linked with adhesive foaming in previous studies [11].



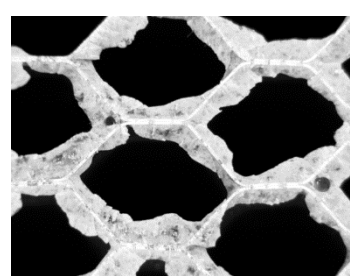
(a) Facesheet side



(b) Facesheet side



(c) Core side



(d) Core side

Figure 8. Representative images of fracture surfaces of samples cured under partial vacuum at different locations

The presence of these defects did not have a significant effect on the FWT strength. While cohesive mode of failure dominates in all specimens, regions of adhesive failure are also seen (Figure 8 (b)).

5.3. EDGEWISE COMPRESSION TEST

In the present study, edgewise compression test was conducted under room temperature and 177 °C (350 °F). Results of edgewise compressive test are shown in Table 3. Similar compressive strengths were observed in samples cured under full vacuum and partial vacuum. When test temperature was raised to 177 °C, the edgewise compression strengths dropped by 20.8 % and 32.2 % respectively. This can be an effect of reduced core stiffness under elevated temperatures.

Table 3. Edgewise compression test results

Vacuum pressure (kPa)	Temperature °C/°F	Edgewise compressive strength	
		Average (MPa)	S.D. (%)
Full vacuum (100)	24/75	12343.78	5.6
Full vacuum (100)	177/350	9781.33	4.5
Partial vacuum (80)	24/75	12825.73	2.2
Partial vacuum (80)	177/350	8689.49	5.9

A representative load-displacement plot of edgewise compression test is shown in Figure 9. The load increases gradually until it reaches a peak value. Progressive failure initiates at this point. The exact location of facesheet failure was unknown. Continued loading resulted in stable end crushing of the sandwich specimen (Figure 10).

Damage initiation in the sandwich composites was in the form of facesheet failure, because the failure strain of the core is much higher than that of the facesheets. The

composite facesheets can exhibit various failure modes such as elastic microbuckling, plastic microbuckling, fiber crushing, splitting, buckle delamination and shear band formation. On continued loading after failure initiation, sandwich structures can exhibit various failure modes such as (1) Unstable buckling of the sandwich column; (2) Facesheet delamination followed by unstable buckling in opposite directions; and (3) Stable end crushing of sandwich panels [17, 18].

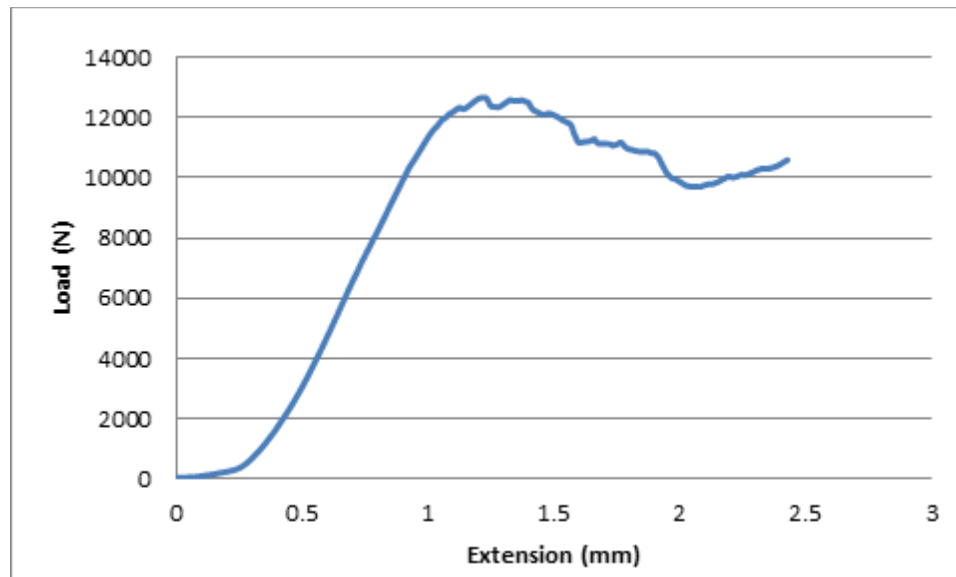


Figure 9. Load vs Extension in edgewise compression test at 177 °C (350 °F) of sandwich samples cured under full vacuum

The unstable failure modes are seen when the bending strength of the facesheets is high, compared to the strength of the fracture interface. The sandwich falls apart rapidly as the crack in the interface propagates along the length of the sandwich specimen. When the

interface strength is high compared to the bending strength of the facesheets, crack propagation is more stable. The crack arrests after a short propagation distance and other failure modes such as facesheet bending, delamination and core crushing begins to dominate.



(a) Front view



(b) Isometric view

Figure 10 (a) and (b). Stable end crushing failure

5.4. ADHESIVE BOND FRACTURE TOUGHNESS TEST

A sample load/displacement curve is shown in Figure 11. All tests were conducted at room temperature. The load increases until it reaches a critical value and crack begins to propagate. As the crack propagates, load reduces. Critical strain energy release rate was calculated from three loading/unloading cycles for each specimen. The critical strain energy release rate, G_C , can be expressed as,

$$G_C = \frac{\int P d\delta}{B\Delta a} \quad (1)$$

where, P is the external load; $d\delta$ is the displacement; B is the width of specimen and Δa is the incremental crack length during the process of test. The energy required for crack growth, $\int P d\delta$, can be calculated by calculating the area enclosed by the loading-unloading path.

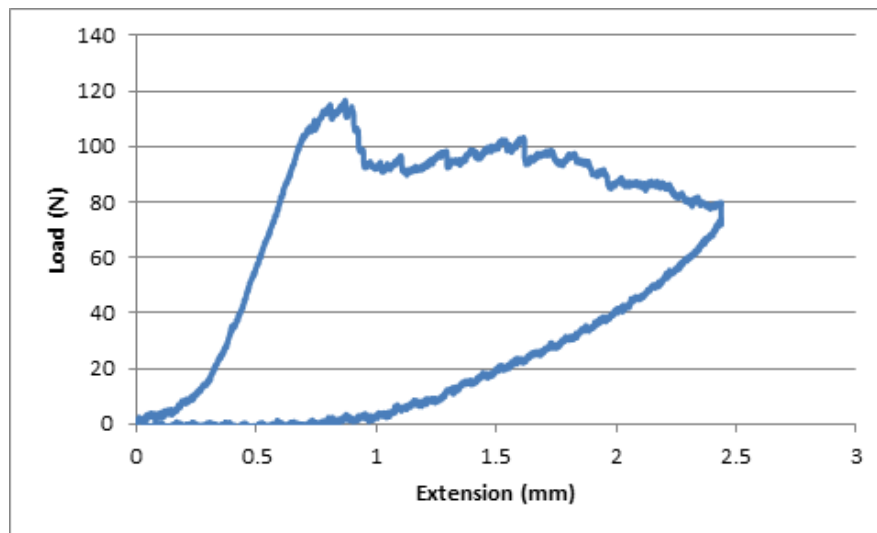


Figure 11. Loading–unloading cycle in modified CSB test of a sample cured under partial vacuum

The area under the loading/unloading path is obtained by integration using the trapezoid rule. The average interface fracture energy release rate for samples fabricated

under full vacuum and partial vacuum is shown in Table 4. About 10% variation was noticed in samples fabricated under full vacuum and partial vacuum.

Table 4. Adhesive bond fracture toughness test results

Vacuum pressure (kPa)	Strain energy release rate	
	Average (J/m ²)	S.D. (%)
Full vacuum (100)	335.19	17.3
Partial vacuum (80)	301.80	11.6

6. SUMMARY AND CONCLUSIONS

High temperature sandwich composite panels were manufactured using the OOA prepreg process. Two levels of vacuum pressure were studied, full vacuum (100 kPa) and partial vacuum (80 kPa). The prepreg cure temperature were used to manufacture the panels. No warping was visible after post cure at 232 °C (450 °F), which implies that the panels had sufficient green strength to enable a free-standing post-cure. Outgassing of adhesive during the cure cycle was studied using TGA. A mass drop of 1.7 % was observed during the ramp and cure isotherm. These volatiles need to be removed during cure to avoid foaming issues. Adhesive bond strength was evaluated using FWT tests and adhesive bond fracture toughness tests. The samples manufactured using full vacuum pressure during cure exhibited in a 6-8.5 % increase in FWT strength compared to those manufactured at a partial vacuum pressure. FWT strength reduced when samples were tested at 177 °C (350

°F). Cohesive failure dominated in all samples while some regions of adhesive failure were also present. Sandwich samples with $[0^\circ/90^\circ]_{2s}$ facesheet orientation were fabricated and a modified CSB test was conducted at room temperature. Samples exhibited a strain energy release rate of 335.19 J/m^2 (full vacuum) and 301.80 J/m^2 (partial vacuum). Edgewise compression tests were conducted on samples with facesheet orientation $[0^\circ/90^\circ]_s$. Vacuum pressure levels used in this study, did not have a significant effect on edgewise compressive strength. Increase in test temperature to $177 \text{ }^\circ\text{C}$ ($350 \text{ }^\circ\text{F}$) resulted in a reduction in edgewise compressive strength. This can be a result of reduced core stiffness at increased temperatures. Measured FWT strengths at room temperature were comparable to those mentioned in previous studies involving aerospace grade epoxy adhesives.

ACKNOWLEDGEMENTS

This research is sponsored by the Industrial Consortium of the Center for Aerospace Manufacturing Technologies (CAMT) at Missouri University of Science and Technology. The authors would like to thank Stratton Composite Solutions and Cytec Engineered Materials for the materials supplied.

REFERENCES

1. T. Centea, L. Gunenfelder and S. Nutt, "A Review of Out-of-Autoclave Prepregs – Material Properties, Process Phenomena, and Manufacturing Considerations," *Composites Part A: Applied Science and Manufacturing*, vol. 70, pp. 132-154, 2015.

2. C. Ridgard, "Next Generation Out-of-Autoclave Systems," *Proceedings of the International SAMPE Symposium and Exhibition*, pp. 1-18, Seattle, WA, May 17-20, 2010.
3. H. Hsiao, S. Lee and R. Buyby, "Core Crush Problem in Manufacturing of Composite Sandwich Structures: Mechanisms and Solutions," *AIAA Journal*, vol. 44, no. 4, pp. 901-907, 2006.
4. G. Grimes, "The Adhesive-Honeycomb Relationship," *Applied Polymer Symposium*, vol. 3, pp. 157-190, 1996.
5. R. Okada and M. Kortschot, "The Role of Resin Fillet in the Delamination of the Honeycomb Sandwich Structures," *Composites Science and Technology*, vol. 62, pp. 1811-1819, 2002.
6. S. Grove, E. Popham and M. Miles, "An Investigation of the Skin/Core Bond in Honeycomb Sandwich Structures using Statistical Experimentation Techniques," *Composites Part A: Applied Science and Manufacturing*, vol. 37, no. 5, pp. 804-812, 2006.
7. J. Rion, Y. Letterrier and J.E. Manson, "Prediction of the Adhesive Fillet Size for Skin to Honeycomb Core Bonding in Ultra-Light Sandwich Structures," *Composites: Part A*, vol. 39, pp. 1547-1555, 2008.
8. R. Butukuri, V. Bheemreddy, K. Chandrashekhara, T. Berkel and K. Rupel, "Evaluation of Skin-Core Adhesion Bond of Out-of-Autoclave Honeycomb Sandwich Structures," *Journal of Reinforced Plastics and Composites*, vol. 31, no. 5, pp. 331-339, 2012.
9. T. Hou, J. Baughman, T. Zimmerman, J. Sutter and J. Gardner, "Evaluation of Sandwich Structure Bonding in Out-of-Autoclave Processing," *Proceedings of the International SAMPE Technical Conference*, pp. 1-12, Salt Lake City, UT, October 11-14, 2010.
10. S. Nagarajan, V. Menta, K. Chandrashekhara, T. Berkel, J. Sha, P. Wu and D. Pfitzinger, "Out-of-Autoclave Sandwich Structure: Processing Study," *SAMPE Journal*, vol. 48, no. 4, pp. 24-31, 2012.
11. S. Tavares, N. Callet-Bois, V. Michaud and J.-A. Manson, "Vacuum-bag Processing of Sandwich Structures: Role of Honeycomb Pressure," *Composites Science and Technology*, vol. 70, pp. 797-803, 2010.

12. J. Kratz and P. Hubert, "Processing Out-of-Autoclave Honeycomb Structures: Internal Core Pressure Measurements," *Composites Part A: Applied Science and Manufacturing*, vol. 42, no. 8, pp. 1060-1065, 2011.
13. G. Marsh, "De-autoclaving Prepreg Processing," *Reinforced Plastics*, vol. 56, pp. 20-25, 2012.
14. J. Sutter, W. Kenner, L. Pelham, S. Miller, D. Polis, C. Nailadi, T. Hou, D. Quade, B. Lerch, R. Lort, T. Zimmerman, J. Walker and J. Fikes, "Comparison of autoclave and Out-of-Autoclave Composites," *Proceedings of the SAMPE Fall Technical Conference*, pp. 1-15, Salt Lake City, UT, October 11-14, 2010.
15. T. Hou, S. Miller, T. Williams and J. Sutter, "Out-of-Autoclave Processing and Properties of Bismaleimide Composites," *Journal of Reinforced Plastics and Composites*, vol. 33, no. 2, pp. 137-149, 2014.
16. S. Smith and K. Shivakumar, "Modified Mode-I Cracked Sandwich Beam (CSB) Fracture Test," *Proceedings of the 19th AIAA Applied Aerodynamics Conference*, pp. 1-18, Anaheim, CA, 11-14 June, 2001.
17. Mamalis, D. Manolakos, M. Loannidis and D. Papapostolou, "On the Crushing Response of Composite Sandwich Panels Subjected to Edgewise Compression: Experimental," *Composite Structures*, vol. 71, no. 2, pp. 246-257, 2005.
18. Lindström, In-Plane Compressive Response of Sandwich Panels, Doctoral Dissertation: KTH Engineering Sciences, Stockholm, Sweden, 2009.

III. CURING OF THICK THERMOSET COMPOSITE LAMINATES: MULTIPHYSICS MODELING AND EXPERIMENTS

S. Anandan, G.S. Dhaliwal, Z. Huo and K. Chandrashekhara
Department of Mechanical and Aerospace Engineering
Missouri University of Science and Technology, Rolla, MO-65401

N. Apetre and N. Iyyer
Technical Data Analysis, Inc.
Falls Church, VA 22042

ABSTRACT

Fiber reinforced polymer composites are used in high-performance aerospace applications as they are resistant to fatigue, corrosion free and possess high specific strength. The mechanical properties of these composite components depend on the degree of cure and residual stresses developed during the curing process. While these parameters are difficult to determine experimentally in large and complex parts, they can be simulated using numerical models in a cost-effective manner. These simulations can be used to develop cure cycles and change processing parameters to obtain high-quality parts. In the current work, a numerical model was built in Comsol MultiPhysics to simulate the cure behavior of a carbon/epoxy prepreg system (IM7/Cycom 5320-1). A thermal spike was observed in thick laminates when the recommended cure cycle was used. The cure cycle was modified to reduce the thermal spike and maintain the degree of cure at the laminate center. A parametric study was performed to evaluate the effect of air flow in the oven,

post cure cycles and cure temperatures on the thermal spike and the resultant degree of cure in the laminate.

1. INTRODUCTION

Thick composite laminates have found several applications in aerospace, military, marine and civil structures. Quality and repeatability of composite laminates are dependent on the conditions during manufacture. The manufacturer's recommended cycle is sometimes unsuited for thick composites because of the existence of a thermal spike and an out-of-plane temperature gradient in the laminate, during manufacture. Cure cycle should also conform to other limitations of maximum allowable cooling and heating rate. The maximum temperature in the center of a thick composite part may sometimes be sufficient to degrade the resin.

The curing of thermosetting polymer systems can be expressed mathematically through cure kinetic equations. Several researchers have worked on the mathematical modeling and simulation of composite curing kinetics [1-3]. The kinetics of common Out-of-Autoclave (OOA) systems, Cycom 5320 and MTM 45-1 were characterized by Kratz et al [4]. The cure kinetics equation which accounts for the effects of prepreg out-time was developed for Cycom 5320-1 OOA prepreg system [5].

The cure kinetics equations can be used to evaluate temperature distribution during cure of thermoset resin systems. Initial research on cure simulation of composites used one or two-dimensional finite difference analysis and was applicable for simple geometries. Loos and Springer developed a one-dimensional model the cure-process of a carbon-epoxy

laminates, called the “CURE” model [6]. The temperature, ionic conductivity, and compaction during autoclave curing of thick composite laminates made of T300/976 and Hercules AS/3501-6 systems were measured by Ciriscioli et al [7]. The experimental data was compared to the Loos-Springer CURE model. The temperature variation in thick composites has also been studied by Twardowski et al using one-dimensional simulations [8]. The effect of initial degree of cure and prepreg consolidation were investigated. Kim and Lee predicted the temperature distribution in a thick thermosetting composite during cure using a one-dimensional equation solved using finite difference method and used the model to minimize the thermal overshoot [9]. One-dimensional equations were also used for modeling continuous curing of glass fiber/polyester composites [10]. Blest et al. modeled the resin flow, heat transfer, and the cure progression of thick thermoset composite laminates during autoclave processing [11]. A finite difference numerical scheme was used to simulate the temperature and cure distribution. Results were validated using the observations of Springer and Loos. A two-dimensional cure simulation model was used by Bogetti and Gillespie to analyze temperature and degree of cure variation in thick thermoset composites with arbitrary cross section geometries [12].

Improvements in computing power and processing speeds over the past decade enabled three-dimensional modeling of the composite cure process. Oh and Lee studied the temperature variation during cure for a glass/epoxy composite laminate by three-dimensional finite element analysis [13]. An optimized cure cycle was also developed to minimize a temperature overshoot at the part center. The finite element method may be a better approach for handling complex geometries. Joshi et al. developed a finite element

package to perform cure modeling [14]. The package was used to model curing of a composite laminate, sandwich structure, and an I-beam. Park and Lee developed a two-dimensional and three-dimensional cure simulations of composite components using the finite element method [15, 16].

Commercial finite element packages can also be used to model cure in thick composite laminates if the relevant material behavior is added by the user. Guo et al studied cure of thick carbon/epoxy composite components using Ansys software package [17]. One dimensional analysis was performed and compared with experimental values. The temperature field in complex shaped composite components manufactured using resin infusion was also evaluated using Abaqus software package. The HETVAL subroutine was used to define heat generated during cure [18]. Exotherm and temperature distribution in thick-walled composites were evaluated. The developed model was used to optimize the temperature distribution in a composite spar of a helicopter blade [19]. Bheemreddy et al developed cure models for composite cure during the cavity molding process [20]. Artificial intelligence algorithms have been previously used to optimize the cure cycles in composite laminates [20-22]. Numerical modeling and simulations are cost effective alternatives to empirical trials for initial studies of such processes.

The current study involves the investigation of the degree of cure and temperature distribution in thick composite laminates during cure. While the experimental investigation of processing of the composites can be effective for understanding the effect of manufacturing parameters on part quality, an empirical approach can be complex and time-

consuming. The current work involves numerical simulation of composite cure which can be useful in selecting process parameters during the cure of complex parts.

2. METHODOLOGY

The matrix in a composite laminate consists of a thermosetting resin which is polymerized by application of heat. The cure reaction is exothermic. The extent and rate of reaction are strongly dependent on the temperature of the system. Thick composite laminates were manufactured and the temperature of the layup was monitored using an embedded thermocouple. Multiphysics models were built, corresponding to the manufacturing layup and the results of the simulation were compared with experiments. The multiphysics model contains cure kinetics and heat transfer modules.

2.1. CURE KINETICS MODELING

Differential Scanning Calorimetry (DSC) is a popular technique, used to obtain cure kinetic parameters of exothermic reactions [23, 24]. DSC is used to monitor the heat flow out of a sample during the curing process. For an exothermic reaction, the degree of cure, α , is defined as the ratio of heat evolved until a time, t , to the total heat of reaction (Equation 1).

$$\alpha = \frac{\Delta H_t}{\Delta H_U} \quad (1)$$

where, ΔH_U is the total heat of reaction and ΔH_t is the heat of reaction at time, t . Using multiple isothermal DSC experiments, the cure kinetic equation can be derived. For the carbon/epoxy prepreg system used in the current study, the cure kinetic equation is defined in Equation 2. This equation accounts for the interplay between kinetics-controlled and diffusion-controlled reaction mechanisms [5].

$$\frac{d\alpha}{dt} = \sum_{i=1,3} K_i \alpha^{m_i} (1 - \alpha)^{n_i} + \sum_{j=2,4} \frac{K_j \alpha^{m_j} (1 - \alpha)^{n_j}}{1 + e^{D_j \{\alpha - (\alpha_{c0,j} + \alpha_{cT,j} T)\}}} \quad (2)$$

$$K_l = A_l e^{(-E_{A,l}/RT)}, \quad l = i, j$$

where A_n is the Arrhenius constant, $E_{A,n}$ is the activation energy, R is the universal gas constant, m_i and n_i are reaction order-based fitting constants, D_j is the diffusion constant, T is the temperature, α_{c0} is the critical degree of cure at absolute zero, and α_{cT} accounts for the increase in critical degree of cure with temperature. Values of the parameters are given in Table 1. The out time effects were not considered in this study.

2.2. THERMAL MODEL

In the thermal portion of the model, the thermal equilibrium equation (Equation 3) was used to solve for energy balance in the laminate portion. The heat generation is both position and time dependent. There are two sources of thermal energy into the system: heat supplied by the autoclave and heat generated by the exothermic chemical reaction.

Table 1. Cure kinetic parameters for Cycom 5230-1 prepreg system [5]

A_1 (s^{-1})	1.48×10^7	A_3 (s^{-1})	6.39×10^7	A_2 (s^{-1})	8.3×10^4	A_4 (s^{-1})	9.8×10^4
$\frac{E_{A,1}}{R}$ (K)	1.02×10^4	$\frac{E_{A,3}}{R}$ (K)	8.94×10^3	$\frac{E_{A,2}}{R}$ (K)	8.54×10^3	$\frac{E_{A,4}}{R}$ (K)	7.1×10^3
m_1	0.17	m_3	1.65	m_2	0.7	m_4	1.66
n_1	19.3	n_3	16.6	n_2	0.87	n_4	3.9
D_2	97.4	D_4	63.3	$a_{c0,2}$	-1.6	$a_{c0,4}$	-0.6

$$\rho_c C_c \frac{\partial T}{\partial t} = \nabla \cdot k_c \nabla T + v_m \rho_m H_u \frac{\partial \alpha}{\partial t} \quad (3)$$

where ρ_c is the density of composite, C_c is the specific heat capacity of composite, T is temperature, t is time, k_c is the thermal conductivity of composite, v_m is the resin volume fraction, ρ_m is the resin density, H_u is ultimate heat of reaction of the system and α is the degree of cure.

Table 2 Material properties of the mold and caul plate material (Aluminum 5052)

Density (kg/m^3)	Conductivity (W/m·K)	Specific heat (J/g·K)
2700	42	8.1

The ambient air temperature was varied according to the cure cycle shown in Section 3. The material properties of the tool and prepreg materials are shown in Tables 2 and 3. They were extracted from [4] and Cycom 5320-1 datasheet. Thermal conductivities

for fiber reinforcement and matrix are obtained from [25] and [4], respectively. Thermal conductivity along fiber direction k_{xx} is calculated using Equation 4.

Table 3. Material parameters for Cycom IM7/5320-1 prepreg

ρ_c (kg/m ³)	ρ_r (kg/m ³)	ρ_f (kg/m ³)	v_r	v_f
1591.6	1310	1780	40.09%	59.91%
k_r (W/m·K)	k_f (W/m·K)	k_{xx} (W/m·K)	$k_{yy} = k_{zz}$ (W/m·K)	C_c
0.167	5.4	3.3021	0.5067	1260

$$k_{xx} = v_r k_r + v_f k_f \quad (4)$$

where k_r and k_f are thermal conductivities for matrix and fiber reinforcement, respectively. v_r and v_f are the resin and fiber volume fractions. Thermal conductivity along thickness direction k_{zz} is calculated using Springer-Tsai model [26]:

$$\frac{k_{zz}}{k_r} = \left(1 - 2\sqrt{\frac{v_f}{\pi}}\right) + \frac{1}{B} \left[\pi - \frac{4}{\sqrt{1 - (B^2 v_f / \pi)}} \right] \tan^{-1} \frac{\sqrt{1 - (B^2 v_f / \pi)}}{1 + B\sqrt{v_f / \pi}} \quad (5)$$

$$B = 2 \left(\frac{k_r}{k_f} - 1 \right)$$

It was assumed that the specific heat capacity and thermal conductivity during cure were constant during the curing process, and their dependence on degree of cure was not

incorporated into the Multiphysics model. Previous research has shown that variation in thermal conductivity and specific heat capacity for epoxy polymers during cure is no more than 5-15% [18]. This assumption is not expected to have a significant impact on the degree of cure or temperature distributions. The heat convection due to resin flow during cure is also assumed to be negligible.

2.3. MULTIPHYSICS CURE MODELING

A thermo-chemical model was built in Comsol Multiphysics software, to simulate the curing of composite parts (Figure 1).

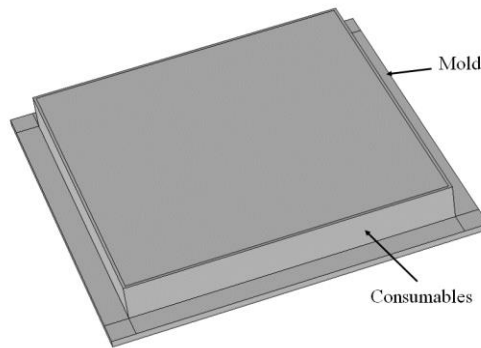


Figure 1. Three-dimensional model of the problem setup

The cure kinetics process was incorporated using the partial differential equations module. The thermal model was incorporated using the heat transfer module. The cross

section of the multiphysics model used, is shown in Figure 2. The model corresponds to the actual manufacturing layup used to cure composite components.

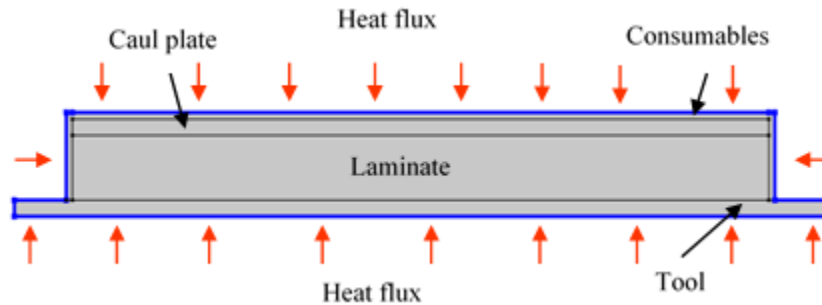


Figure 2. Cross section of the thermo-chemical multiphysics model

Table 4. Material properties of consumables [17]

Material	Thickness (mm)	Thermal Conductivity (W/m.K)	Specific heat capacity (J/gK)	Density (kg/m ³)
Release film	0.0508	0.4	1.05	2200
Vacuum bag	0.0505	0.24	1.67	1140
Breather	2.54	0.07	1.35	260
Combined layer	2.64	0.079	0.119	314.2

The tool required to make composite samples were made of Aluminum 5052, hence its material properties were used for modeling the tool and caul plate. Other consumable materials such as vacuum bag, breather, and release film were modeled as pure conductors with properties listed in Table 4.

The consumables namely release film, breather and vacuum bag were modeled as a single layer with equivalent properties derived using the rule of mixtures. A heat flux boundary condition was applied on all outer surfaces according to Equation 6. This corresponds to the cure cycle for composite manufacturing.

$$Q = h(T_{ext} - T_{boundary}) \quad (6)$$

where Q is the heat generated, h is the convection heat transfer coefficient, T_{ext} is the temperature of the autoclave and $T_{boundary}$ is the temperature at the external surface of the layup.

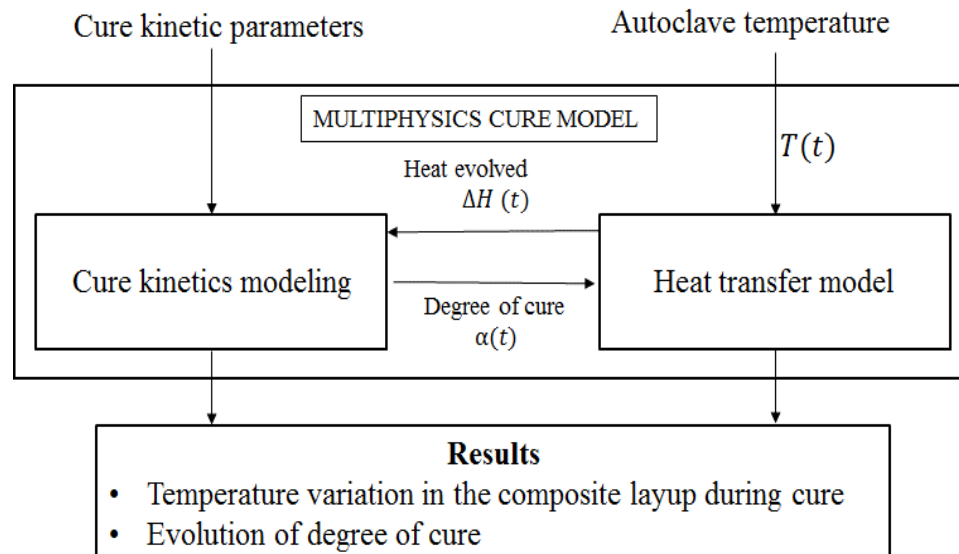


Figure 3. Multiphysics modeling of composite curing

The convective heat transfer coefficient was set to $150 \text{ W/m}^2\text{K}$. The actual heat transfer coefficient was not calculated for the autoclave used in this study. The effect of varying heat transfer coefficients will be evaluated in a parametric study in Section 3.2. The numerical model setup is shown in Figure 3.

2.4. EXPERIMENTAL EVALUATION OF PART TEMPERATURE

To manufacture thick composite laminates, IM7/Cycom 5320-1 unidirectional prepreg system (Cytac-Solvay Group, NJ) was used. The unidirectional prepreg contains 35% resin by weight with a fiber areal weight of 145 g/m^2 . Laminates measuring 12 in. x 12 in. (304.8 mm x 304.8 mm) were manufactured in an autoclave. A flat aluminum plate was used as the mold. It was covered with a release agent and a layer of ethylene tetrafluoro ethylene (ETFE) release film to ensure easy release of the laminate after curing. Prepreg layers were cut to size and laid on the mold.

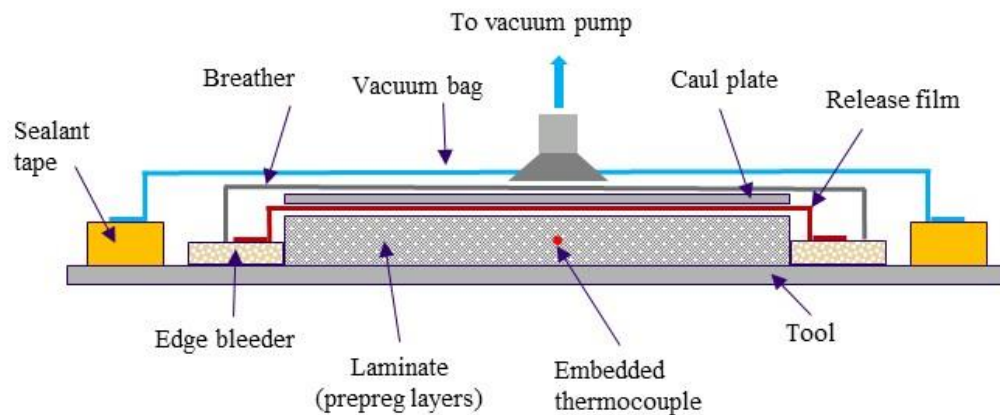


Figure 4. Experimental setup

The laminate orientation was $[0^\circ]_{100}$ and the thickness was ~ 25 mm. A thermocouple was placed in the middle of the laminate to monitor the temperature variation during cure (Figure 4). The prepreg layup was then covered with release film and an Aluminum caul plate was placed on top. The layup was sealed using a vacuum bag and debulked under full vacuum pressure (28 in. Hg) for 4 hours to ensure good prepreg compaction. Airweave N10 breather was used to distribute vacuum pressure evenly. The laminate was cured at a temperature of 130°C (265°F) for two hours, under an autoclave pressure of 85 psi. The embedded thermocouple was used to monitor temperature at the center of the laminate during cure.

3. RESULTS AND DISCUSSION

Temperature variation during composite cure was extracted from the thermochemical model. In addition, the temperatures of the autoclave and center of the part were obtained experimentally (Figure 5). A thermal spike is observed in the temperature profile, which is due to heat build-up caused by the exothermic nature of the curing reaction.

The temperature at the part center is lower than the autoclave temperature before the initiation of curing, in both experiments and simulation. This is due to the low thermal conductivity of the prepreg system. As the reaction progresses, a thermal spike is observed because of the excessive heat build-up. The temperature profile lags behind the autoclave during cool-down. The maximum temperature in the part center is 289.7°F (143.1°C), which occurs during the observed thermal spike. According to the Multiphysics model, the maximum temperature at the laminate center is predicted to be 295.9°F (146.6°C) which

is very close to the actual part temperature during cure. The difference in maximum temperature during cure can be a result of assumptions in the model such as convection coefficient and prepreg out time. Figure 6 shows the degree of cure variation through the laminate thickness. It is clear that no significant curing happens in the initial isotherm and in the heat up phase.

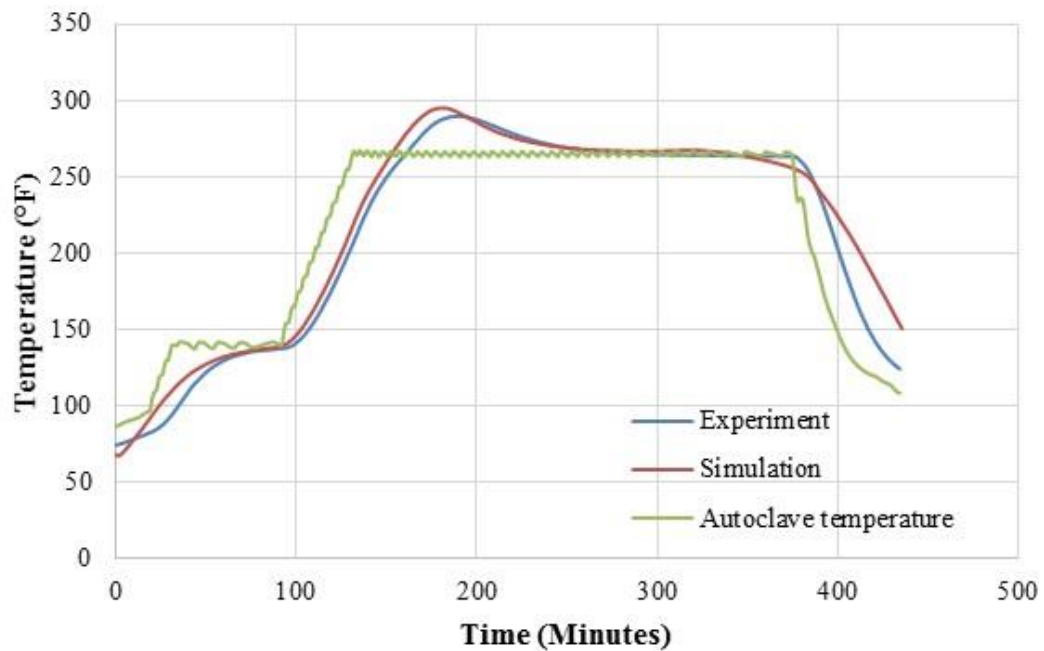


Figure 5. Comparison of temperature at laminate center, experiment vs simulation

The degree of cure at the center increases faster than the degree of cure at the laminate surface, due to the effect of the thermal spike. At the end of the curing phase, they tend towards the same value. The multiphysics model was used to perform parametric

studies in order to evaluate the effect of some process variables on the quality of the manufactured part.

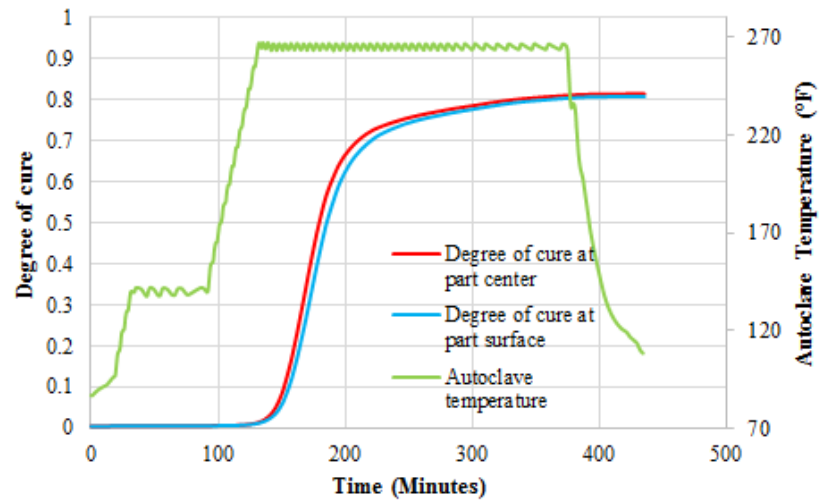


Figure 6. Degree of cure development during cure

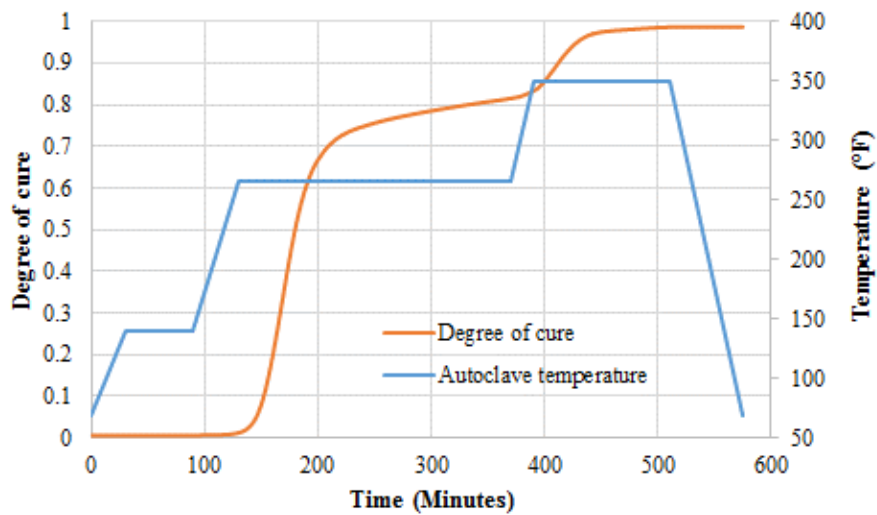


Figure 7. Effect of post-cure on degree of cure of the laminate

3.1. EFFECT OF POST-CURING ON DEGREE OF CURE

The thermo-chemical model was used to evaluate the effect of including a post-cure phase. Composite components are subjected to a freestanding post-cure after the initial curing phase in the autoclave. Post-curing is done to increase the degree of cure and crosslinking in the composite laminate. This results in improvements in mechanical properties and glass transition temperature. The recommended post-cure temperature for Cycom 5320-1 is 350 °F (177 °C). It can be observed that after the post-cure phase, the ultimate degree of cure of the laminate can increase up to 0.98 from 0.81 (Figure 7).

3.2. EFFECT OF CONVECTION IN THE AUTOCLAVE

Air flow around the part in the autoclave can also affect the quality of the manufactured composite. Researchers have studied the effect of convection in the autoclave and heat distribution, using experimental and numerical methods [27]. In the current study, the heat distribution around the composite layup is assumed to be uniform. A parametric study is used to evaluate the sensitivity of the results to a change in the convection coefficient in the autoclave. A change in air flow around the layup was simulated by varying the convection coefficient from 40 to 200 W/m².K.

The results show that an increase in convection results in quicker heating of the part. The thermal spike shifts to a later time and increases in magnitude as the convection coefficient is decreased (Figure 8). The effect of convection coefficient on the temperature profile is negligible for values greater than 120 W/m².K. At low convection coefficients

the effect on the thermal spike is significant, due to decreased heat transfer and reduced heat exchange with the environment. The thermal spike shifts to a later time. The magnitude of the thermal spike is also higher due to increased build-up of heat within the layup.

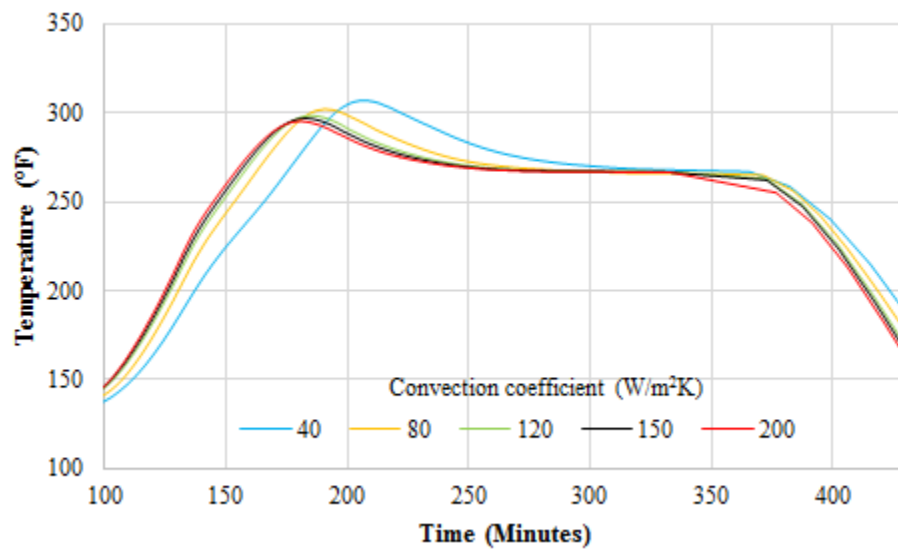


Figure 8. Variation of temperature at center with varying convection coefficient ($\text{W/m}^2\text{K}$)

3.3. EFFECT OF CURE CYCLE MODIFICATION

The effect of replacing the isothermal cure region in the cure cycle with a gradual ramp was investigated using the thermo-chemical model. The objective was to decrease the thermal spike observed during cure. The initial temperature (T_A) in Figure 9, was decreased. T_A was varied from $111\text{ }^\circ\text{C}$ ($233\text{ }^\circ\text{F}$) to $126\text{ }^\circ\text{C}$ ($260\text{ }^\circ\text{F}$). The cure time was kept

constant at 240 minutes. The effect of varying cure cycles on the temperature during cure is shown in Figure 10. Using a gradual ramp in place of an isothermal cure region can result in a decrease in the thermal spike. However, it may also result in decreased degree of cure at the center of the laminate. For further study, a modified cure cycle with T_A equal to 237 °F (114 °C) was selected.

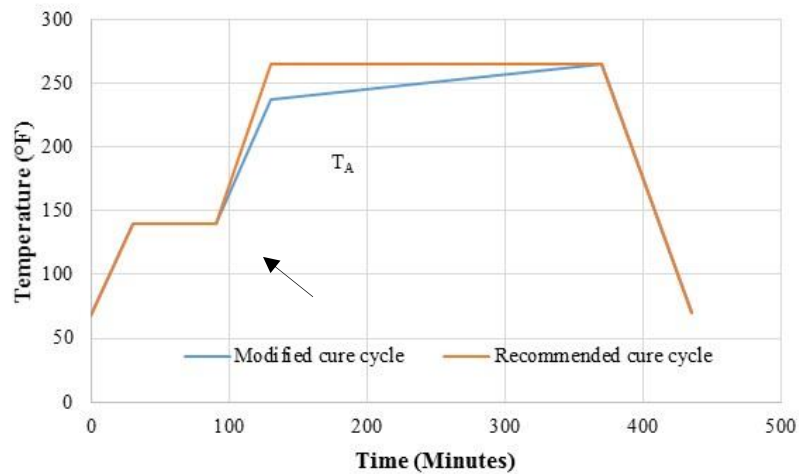


Figure 9. Cure cycle for modification

It is expected that using the modified cure cycle can reduce thermal spike during composite manufacturing while maintaining a similar degree of cure compared to composites manufactured using the recommended cure cycle. However, reducing the initial cure temperature can also result in reduced degree of cure.

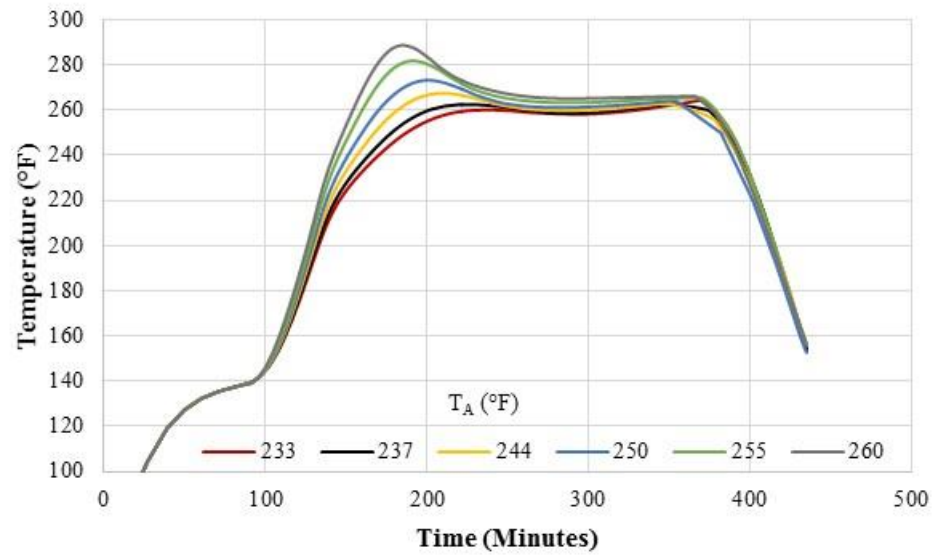
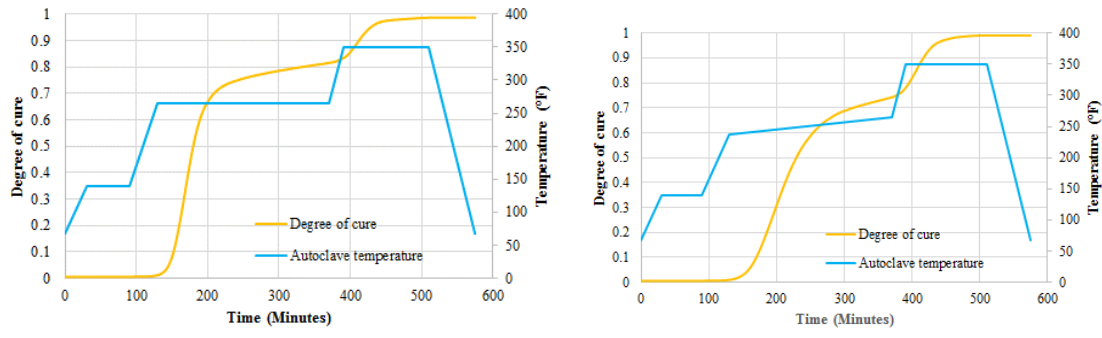


Figure 10. Effect of modified cure cycles on thermal spike. T_A (Figure 9) was varied from 233-260 °F



a) Recommended cure cycle b) modified cure cycle

Figure 11. Degree of cure variation in the laminate with recommended and modified cure cycles

The effect of using the modified cure cycle (T_A = 237 °F or 114 °C) on the degree of cure in the center of the laminate is shown in Figure 11 b. It can be seen that the degree

of cure after the initial curing phase is less than that of the recommended cure cycle (Figure 11 a). However, the final degree of cure after post-cure is equivalent to that of the recommended cure cycle.

3.4. EFFECT OF MODIFIED CURE CYCLES ON INTERLAMINAR SHEAR STRENGTHS

The effect of using a modified cure cycle was evaluated experimentally. Composite laminates were manufactured using the recommended and modified cure cycles. The composite layup was selected as $[0^\circ / 90^\circ]_{3s}$ in order to obtain interlaminar failure in the composite. They were also subjected to a post-cure at 350 °F (177 °C). No droop was observed in either laminate following the free-standing post-cure.

Interlaminar shear strength (ILSS) of samples was evaluated according to ASTM D2344. Failure in ILSS is due to interlaminar failure which is a resin dominated property. It is significantly influenced by the degree of cure at the center of the laminate and therefore was selected as the response to evaluate the effect of varying cure cycles.

For ILSS testing, five samples were taken from each laminate. The test was performed on an Instron 5985 machine. A short span equal to four times the specimen thickness was used to cause failure dominated by interlaminar shear. The specimen width was two times the thickness. Samples were loaded at a machine crosshead speed of 1 mm/min. The interlaminar shear strength was calculated as:

$$ILSS = 0.75 \times \frac{P}{b \times h} \quad (7)$$

where P is load at failure, b is sample width and h is the sample thickness.

Results of experimental testing are shown in Table 5. The laminates manufactured using the modified cure cycle had strengths in the same range as that of the samples manufactured using the recommended cure cycle.

Table 5. Results of short beam shear tests

Cure cycle	Number of layers in sample	ILSS (MPa)
Recommended cure cycle	12	79.7±7.2
Modified cure cycle	12	81.3±7.9

The results indicate that using the recommended cure cycle for composite laminates can be modified based on thermo-chemical models. Thermal spike in thick laminates can be reduced. By careful selection of cure parameters, it is possible to high quality composite laminates using a modified cure cycle. For the laminates, selected in the experiments, the modified cure cycle was capable of producing interlaminar shear strengths similar to the strengths of laminates manufactured using the recommended cure cycle.

4. CONCLUSIONS

Curing of Cycom 5320-1 was modeled using a thermo-chemical model built using the software, Comsol. Thick composite laminates were manufactured at Missouri S&T and the temperature at the center of the parts was measured using thermocouples. The magnitude of the thermal peak, predicted by the simulation, was in good agreement with the measured values. There was a time lag in the location of the peak. A parametric study was conducted in order to study a change in the process variables on the curing of composite laminates.

It was found that post-curing has a significant effect on the degree of cure in thick laminates. Variation in the convection coefficient had a significant effect on the location of the thermal spike in the temperature profile. Low air flow in the autoclave can result in reduced heat transfer in the system. The cure cycle was modified by incorporating a gradual ramp in the curing phase. It was observed that using a ramp can reduce the thermal spike but it also reduces the degree of cure in the laminate. However, the degree of cure can approach similar values after a post-cure phase, for laminates manufactured using a modified cure cycle and the recommended cure cycle. Twelve layer cross-ply laminates were manufactured. Composite laminates were manufactured using the modified cure cycle and recommended cure cycle. It was observed that the final mechanical properties, after post-curing, of both laminates were similar.

ACKNOWLEDGEMENTS

This work was supported by Technical Data Analysis, Inc. through the STTR N15A-T003 Phase I contract number N68335-15-C-0223.

REFERENCES

1. L. Khoun, T. Centea and P. Humert, "Characterization methodology of thermoset resins for the processing of composite materials - case study: CYCOM 890RTM epoxy resin," *Journal of Composite Materials*, vol. 44, no. 11, pp. 1397-1415, 2010.
2. J. Balvers, H. Bersee, A. Beukers and K. Jansen, "Determination of cure dependent properties for curing simulation of thick-walled composites," *Proceedings of 49th AIAA/ASME/ASCE/AHS/ASC Structures*, pp. 1-12, Schaumburg, IL, April 7-10, 2008.
3. P. Karkanas, I. Partridge and D. Attwood, "Modeling the cure of a commercial epoxy system for applications in resin transfer molding," *Polymer International*, vol. 41, pp. 183-191, 1996.
4. J. Kratz, K. Hisao, G. Fernlund and P. Hubert, "Thermal models for MTM45-1 and Cycom 5320 out-of-autoclave prepreg resins," *Journal of Composite Materials*, vol. 47, no. 3, pp. 341-352, 2013.
5. D. Kim, T. Centea and S. Nutt, "Out-time effects on cure kinetics and viscosity for an out-of-autoclave (OOA) prepreg: modeling and monitoring," *Composites Science and Technology*, vol. 100, pp. 63-69, 2014.
6. A. Loos and G. Springer, "Curing of epoxy matrix composites," *Journal of Composite Materials*, vol. 17, no. 2, pp. 135-139, 1983.
7. P. Ciriscioli, Q. Wang and G. Springer, "Autoclave curing – comparison of model and test results," *Journal of Composite Materials*, vol. 26, pp. 90-102, 1992.

8. T. Twardowski, S. Lin and P. Geil , "Curing in thick composite laminates: experiment and simulation," *Journal of Composite Materials*, vol. 27, no. 3, pp. 216-250, 1993 .
9. J. Kim and D. Lee, "Development of an autoclave cure cycle with cooling and reheating steps for thick thermoset composite laminates," *Journal of Composite Materials*, vol. 31, no. 22, pp. 2264-2281, 1997.
10. C. Kim, H. Teng, C. Tucker and S. White, "The continuous curing process for thermoset polymer composites. part 1: modeling and demonstration," *Journal of Composite Materials*, vol. 29, pp. 1222-1253, 1995.
11. D. Blest, B. Duffy, S. McKee and A. Zulkifle, "Curing simulation of thermoset composites," *Composites Part A: Applied Science and Manufacturing*, vol. 30, no. 11, pp. 1289-1309, 1999.
12. T. Bogetti and J. J. Gillespie, "Two-dimensional cure simulation of thick thermosetting composites," *Journal of Composite Materials*, vol. 25, no. 3, pp. 239-273, 1991.
13. J. H. Oh and D. G. Lee, "Cure cycle for thick glass/epoxy composite laminates," *Journal of Composite Materials*, vol. 36, no. 1, pp. 19-45, 2002.
14. S. Joshi, X. Liu and Y. Lam, "A numerical approach to the modeling of polymer curing in fibre-reinforced composites," *Composites Science and Technology*, vol. 59, no. 7, pp. 1003-1013, 1999.
15. H. Park and S. Lee, "Cure simulation of thick composite structures using the finite element method," *Journal of Composite Materials*, vol. 35, no. 3, pp. 188-201, 2001.
16. H. Park, N. Goo, K. Min and K. Yoon, "Three-dimensional cure simulation of composite structures by the finite element method," *Composite Structures*, vol. 62, no. 1, pp. 51-57, 2003.

17. Z. Guo, S. Du and B. Zhang, "Temperature field of thick thermoset composite laminates during cure process," *Composites Science and Technology*, vol. 65, pp. 517-523, 2005.
18. D. Belov, I. Makarenko, A. Dunaev, A. Babkin, A. Solopchenko, M. Yablokova, A. Kepman, A. Tretyakov, A. Ulyanov and A. Gromashev, "Curing processes simulation of complex shape carbon fiber reinforced composite components produced by vacuum infusion," *Polymer Composites*, vol. 37, no. 7, pp. 2252-2259, 2016.
19. S. Shevtsov, I. Zhilyaev, A. Soloviev, I. Parinov and V. Dubrov, "Optimization of the composite cure process based on the thermo-kinetic model," *Advanced Materials Research*, Vols. 185-192, p. 569, 2012.
20. V. Bheemreddy, Z. Huo, K. Chandrashekhara and R. Brack, "Process modeling of cavity molded composite flex beams," *Finite Elements in Analysis and Design*, vol. 78, pp. 8-15, 2014.
21. M. Chang, C. Chen and W. Young, "Optimal design of the cure cycle for consolidation of thick composite laminates," *Polymer Composites*, vol. 17, no. 5, pp. 743-751, 1996.
22. D. Michaud, A. Beris and P. Dhurjati, "Thick-sectioned RTM composite manufacturing, part 2. robust cure cycle optimization and control," *Journal of Composite Materials*, vol. 36, pp. 1201-1231, 2002.
23. A. Yousefi and P. Lafleur, "Kinetic studies of thermoset cure Reactions-a review," *Polymer Composites*, vol. 18, no. 2, pp. 157-168, 1997.
24. D. Shin and H. Hahn, "A consistent cure kinetic model for AS4/3502 graphite/epoxy," *Composites Part A: Applied Science and Manufacturing*, vol. 31, no. 9, pp. 991-999, 2000.
25. "HexTow® IM7 Carbon Fiber Product Data", www.hexcel.com. [Online].
26. G. Springer and S. Tsai, "Thermal conductivities of unidirectional materials," *Journal of Composite Materials*, vol. 1, pp. 166-173, 1967.

27. N. Kluge, T. Lundstrom, L. Westerberg and T. Nyman, "Modelling heat transfer inside an autoclave: effect of radiation," *Journal of Reinforced Plastics and Composites*, vol. 35, no. 14, pp. 1126-1142, 2016.

IV. INVESTIGATION OF SANDWICH COMPOSITE FAILURE UNDER THREE-POINT BENDING: SIMULATION AND EXPERIMENTAL VALIDATION

Sudharshan Anandan, Gurjot S. Dhaliwal, Shouvik Ganguly and K. Chandrashekhara*

Department of Mechanical and Aerospace Engineering

Missouri University of Science and Technology, Rolla, MO 65409

ABSTRACT

A sandwich structure consists of two thin and strong facesheets, bonded to a thick lightweight core material. The mechanical response of a sandwich structure depends on the properties of its constituents. A numerical model and experimental validation of the three-point bending test of sandwich composites is presented in this study. The core material is aluminum honeycomb. The facesheets are made of IM7/Cycom5320-1, which is a carbon fiber/epoxy prepreg system. A comprehensive model of the failure under flexural loading was developed. Facesheet failure was modeled using Hashin's failure criteria. A detailed meso-scale model of the honeycomb core was included in the model, which enables simulation of core crushing due to local buckling of cells in the honeycomb core. The load-displacement data obtained from the numerical model was compared with the experimental results. In addition, facesheet failure location and damage propagation through core crushing were also validated using experimental results. The effect of elevated temperature on the three-point bending behavior was also studied numerically as well as experimentally. An increase in test temperature to 121 °C resulted in a drop of 9.2% in

flexural strength. Good agreement was found between experimental tests conducted at high temperature and numerical results.

1. INTRODUCTION

1.1. BACKGROUND

Honeycomb sandwich structures consist of a thick honeycomb core material which is “sandwiched” between two relatively thin composite facesheets. The composite facesheet is bonded to the core using a film adhesive. Sandwich composites have better bending stiffness compared to composite laminates, and a high strength to weight ratio, due to which they are used in aerospace structures [1]. The honeycomb core is a cellular material which has reduced density, resistance to out-of-plane loads, high flexural stiffness and energy absorption. The composite facesheets resist in-plane loading while the core provides bending stiffness. Structural response of sandwich composites is dependent on the properties of the constituents. After mechanical characterization of the constituent materials, behavior of sandwich structures can be simulated using numerical models. A completely experimental approach to characterize mechanical behavior of sandwich structures can be time consuming and expensive. A numerical model can be helpful to evaluate the mechanical properties of sandwich structures and help select the desired combination of sandwich structure constituent materials for further testing. Such “virtual testing” methods can be very useful in studying the mechanical behavior of composites and sandwich structures [2]. Aerospace sandwich structures can be exposed to extreme

conditions in service. The sandwich constituents, honeycomb core and facesheet are affected differently when exposed to elevated temperatures. This behavior can also be studied effectively using numerical models.

The mechanical behavior of honeycomb cores has been characterized by Gibson and Ashby [3]. Numerical simulation methods have been used to study the behavior of various cellular core structures and optimize core geometries using dynamic finite element analysis (FEA) [4]. Li et al. studied the mechanical behavior of cellular cores with irregular cell shapes using numerical modeling [5]. Giglio et al. conducted finite element simulations to study the behavior of sandwich structures under flatwise compression and three-point bending [6, 7]. Nomex honeycomb cores with aluminum facesheets were investigated. The effect of friction between the puncher and the facesheet was analyzed using numerical models. A detailed meso-scale model of a Nomex honeycomb core was developed by Seeman and Krause [8]. For core compression, it was observed that a single layer of shell elements was capable of representing the mechanical behavior of the Nomex core.

Zhou et al. studied the damage in sandwich panels subjected to bending and the effect of indenter shape, facesheet thickness and core density [9]. Nomex and aluminum cored sandwich structures were evaluated. It was found that damage mechanisms depend on the shape of the indenter and facesheet thickness. When a hemispherical indenter is used, failure is in the form of core crushing and facesheet delamination. Three-point bending of sandwich specimens has also been modeled using homogenized core parameters [10]. The linear portion of the load-displacement curve was modeled and good agreement

was found between simulation and experiments. Analytical solutions for homogenized core properties have been reported in [11, 12].

1.2. FAILURE IN THREE-POINT BENDING

Failure mode maps for three-point bending tests have been developed, using an analytical approach, based on core and facesheet properties [13]. Under three-point bending, sandwich panel failure can take place due to different modes various modes. Facesheet failure can occur due to in-plane stresses, facesheet wrinkling and intra-cell dimpling.

Facesheet failure occurs when the in-plane stresses, in either of the facesheets, reach the critical value. Under three-point bending, the maximum bending moment is at the mid-span of the beam. For symmetrical sandwich specimens, the stress is the same on tension and compression sides. However, failure in composite facesheets is generally on the compressive side. The facesheet stress at the point of failure of sandwich composites can be calculated using Equation 1 [14].

$$\sigma = \frac{P_{max}S}{2t_f(t_s + t_c)b} \quad (1)$$

Where P_{max} is the load to failure, t_f is facesheet thickness, t_s is the total sandwich thickness, t_c is the core thickness, and b is the breadth of the sandwich structure. The term S stands for the support span during the three-point bending test.

Under axial loads, facesheet wrinkling takes place due to skin buckling with a wavelength greater than the honeycomb cell width [15, 16, 17]. The critical stress for facesheet wrinkling can be calculated for honeycomb sandwich constructions with composite facesheets based on Equation 2 [1, 18].

$$\sigma_w = \sqrt{\frac{2 t_f E_c \sqrt{E_{fx} E_{fy}}}{3 t_c \sqrt{1 - \nu_{xy} \nu_{yx}}}} \quad (2)$$

Where E_c stands for core modulus, E_{fx} is the facesheet modulus in the axial direction, and E_{fy} is the facesheet modulus in the transverse direction. ν_{xy} and ν_{yx} are facesheet Poisson's ratios.

Honeycomb sandwich structures with very thin facesheets can fail due to intra-cell dimpling of the facesheets [13]. This mode of failure occurs due to in-plane stresses in the facesheets, in the region which is unsupported by the walls of the honeycomb. Classical models consider the facesheets to be supported on elastic foundations. Thomsen and Banks developed an improved model for intra-cell buckling in honeycomb sandwich structures with very thin facesheets [19].

Core failure can also occur under three-point bending loads. Common modes of failure are core shear and failure due to local indentation. Shear forces can lead to core shear failure. The core shear failure mode is dependent on geometric parameters of the sandwich, loading span and core density. Since the honeycomb core are orthotropic, the

orientation of the honeycomb cells also affect core failure. According to ASTM C393, core shear failure occurs if:

$$S \leq \frac{2\sigma_{fmax}t}{kF_s} \quad (3)$$

Where S is the support span, σ_{fmax} is the expected facesheet ultimate strength, k is the core shear strength factor to ensure facesheet failure (recommended value is 0.75), and F_s is the core shear strength.

Honeycomb sandwich structures under three-point bending can exhibit failure due to local indentation at the point of loading. Failure is due to core crushing under the puncher. If the area of contact between the puncher and sandwich is known, the critical failure stress of this mode can be calculated. It is also assumed that the load transfer is uniform over this contact area. However, for cylindrical puncher indenting a flat facesheet surface, the contact area is difficult to estimate. This mode of failure is also affected by material irregularities, localized shear stresses, puncher shape and other imperfections in the material. Previous studies on Nomex cores with aluminum facesheets have shown core crushing failure [9]. Local indentation failures can be simulated by using a full three-dimensional finite element model of the honeycomb core.

1.3. CURRENT WORK

Modeling the honeycomb core using homogeneous orthotropic solid geometries can result in low computational times. The mechanical stiffness can be modeled using a set of elastic moduli, which are dependent on cell geometries and honeycomb density [20]. The response of honeycombs to in-plane and out-of-plane loads have been described previously [3, 12]. Numerical homogenization can also be performed using finite element analysis, instead of analytical solutions, to obtain core effective properties [7, 14]. Catapano and Montemurro used a numerical homogenization technique to evaluate effective elastic properties of a honeycomb [21]. A Genetic Algorithm (GA) based optimization scheme was used to determine optimal facesheet and core parameters for a honeycomb structure. While homogenized models can provide accurate representation of the linear load-displacement behavior, they are not capable of predicting local core crushing and meso-scale damage. The current work focuses on developing a meso-scale numerical model of the three-point bending test on sandwich composites. The core mechanical behavior was simulated using a meso-scale model. Composite facesheets were used in the sandwich structure and the failure propagation in the facesheet was included in the model. The effect of elevated temperatures was incorporated and all simulations were validated using experiments. Results show good agreement between experimental results and model predictions at room temperature and elevated temperatures.

2. NUMERICAL MODELING

2.1. FACESHEET FAILURE

Failure in the facesheets can be modeled using Hashin's criteria. The following modes of failure can be simulated using these criteria: (a) fiber rupture due to tensile loads; (b) fiber buckling and kinking due to compressive loads; (c) matrix cracking under transverse tension and shearing; and (d) matrix crushing under transverse compression and shearing [22]. The initial behavior of the undamaged facesheet is linear elastic [23]. Once the failure stress is reached, damage propagation in the facesheet is modeled using a linear softening criterion. The elastic constants are reduced using a damage parameter denoted by d . The constitutive equations for facesheet mechanical behavior are shown in Equations 4-7.

$$\sigma = C_d \varepsilon \quad (4)$$

$$C_d = \frac{1}{D} \begin{bmatrix} (1 - d_f)E_1 & (1 - d_f)(1 - d_m)v_{21}E_1 & 0 \\ (1 - d_f)(1 - d_m)v_{12}E_2 & (1 - d_m)E_2 & 0 \\ 0 & 0 & (1 - d_s)G_{12}D \end{bmatrix} \quad (5)$$

$$D = 1 - (1 - d_f)(1 - d_m)v_{21}v_{12} \quad (6)$$

$$d_s = 1 - (1 - d_f^t)(1 - d_f^c)(1 - d_m^t)(1 - d_m^c)v_{21}v_{12} \quad (7)$$

Initially, the facesheet is undamaged and the parameter, d , is equal to zero. This results in linear elastic behavior. Once failure load is reached, damage initiation in the

facesheets is controlled by Hashin's criteria. Failure initiates when one of the criteria in Equations 8 is satisfied. The quadratic stress failure criteria are used.

$$\begin{aligned}
 &\text{Fiber tension } (\sigma_{11} > 0) && \text{Fiber compression } (\sigma_{11} < 0) : \\
 &\quad \vdots && F_f^c = \left(\frac{\sigma_{11}}{X^c}\right)^2 \\
 &F_f^t = \left(\frac{\sigma_{11}}{X^T}\right)^2 && \\
 &\text{Matrix tension } (\sigma_{22} > 0) : && \text{Matrix compression } (\sigma_{22} < 0) : \\
 &\quad \vdots && F_m^c = \left(\frac{\sigma_{22}}{2S^T}\right)^2 + \left[\left(\frac{Y^c}{2S^T}\right)^2 - 1\right] \left(\frac{\sigma_{22}}{Y^c}\right)^2 \\
 &F_m^t = \left(\frac{\sigma_{22}}{Y^T}\right)^2 + \left(\frac{\tau_{12}}{S^L}\right)^2 && + \left(\frac{\tau_{12}}{S^L}\right)^2
 \end{aligned} \tag{8}$$

Where, F_f^t denotes fiber tensile failure index, F_f^c is fiber compressive failure index, F_m^t is matrix tensile failure index, F_m^c is matrix compressive failure index, σ_{11} and σ_{22} are longitudinal and transverse stresses respectively, and τ_{12} is the shear stress.

Table 1. Temperature dependent properties of the facesheet material [24]

Elastic properties				
Temperature (°C)	Longitudinal modulus (E_1)	Transverse modulus (E_1)	Poisson's ratio (ν_{12})	Shear moduli (G_{12}, G_{13})
24	156 GPa	9.3 GPa	0.30	5.5 GPa
121	158 GPa	8.3 GPa	0.32	4.9 GPa
Strength properties				
Temperature (°C)	X^T	Y^T	X^c	Y^c
24	2503 MPa	75.9 MPa	2078 MPa	165 MPa
121	2477 MPa	62.4 MPa	2016 MPa	135 MPa

X^T, Y^T, X^c, Y^c, S^L and S^T are longitudinal tensile strength, transverse tensile strength, longitudinal compressive strength, transverse compressive strength, longitudinal shear strength and transverse shear strength, respectively (Table 1). Temperature dependence of material properties were incorporated based on data provided in the manufacturer datasheet. Once failure initiates at any integration point in the facesheet, damage evolution takes place according to a linear softening law. For all modes of failure, stiffness degradation takes place according to Equation 9.

$$d = \frac{\delta_{eq}^f (\delta_{eq} - \delta_{eq}^0)}{\delta_{eq} (\delta_{eq}^f - \delta_{eq}^0)} \quad (9)$$

Where, d is the damage variable, δ_{eq} is the current equivalent displacement, δ_{eq}^f is the equivalent displacement at failure and δ_{eq}^0 is the equivalent displacement at failure initiation. The equivalent displacement and stresses are represented schematically in Figure 1. The equivalent displacement for each failure mode is given by Equation 10.

$$\begin{array}{ll}
 \text{Fiber tension } (\sigma_{11} > 0) : & \text{Fiber compression } (\sigma_{11} < 0) : \\
 \delta_{eq}^t = L^c \langle \varepsilon_{11} \rangle & \delta_{eq}^c = L^c \langle -\varepsilon_{11} \rangle \\
 \sigma_{eq}^t = \langle \sigma_{11} \rangle & \sigma_{eq}^c = \langle -\sigma_{11} \rangle \\
 \text{Matrix tension } (\sigma_{22} > 0) : & \text{Matrix compression } (\sigma_{22} < 0) : \\
 \delta_{eq}^t = L^c \sqrt{\langle -\varepsilon_{22} \rangle^2 + \varepsilon_{12}^2} & \delta_{eq}^c = L^c \sqrt{\langle \varepsilon_{22} \rangle^2 + \varepsilon_{12}^2} \\
 \sigma_{eq}^t = \frac{\langle \sigma_{22} \rangle \langle \varepsilon_{22} \rangle + \tau_{12} \varepsilon_{12}}{\left(\frac{\delta_{eq}^t}{L^c} \right)} & \sigma_{eq}^c = \frac{\langle -\sigma_{22} \rangle \langle -\varepsilon_{22} \rangle + \tau_{12} \varepsilon_{12}}{\left(\frac{\delta_{eq}^c}{L^c} \right)}
 \end{array} \quad (10)$$

Where “ $\langle \rangle$ ” stands for the Macaulay operator. After initiation of failure the value of the corresponding damage variable increases. The value of δ_{eq}^f is controlled by G^c , or fracture energy, which denotes the energy dissipated during failure in each mode.

To reduce mesh dependency during material analysis, a characteristic length, L^c , is introduced into the formulation, which is used to calculate the equivalent displacement [23]. The constitutive law for each element can be expressed as a relation between the equivalent displacement and equivalent stress. For a completely degraded facesheet, $d = 1$. In this failure model, the fracture energy G^c must be specified for each mode of failure. The fracture energy is the area described by OAB (Figure 1). G^c for each failure mode of failure, is given in Table 2.

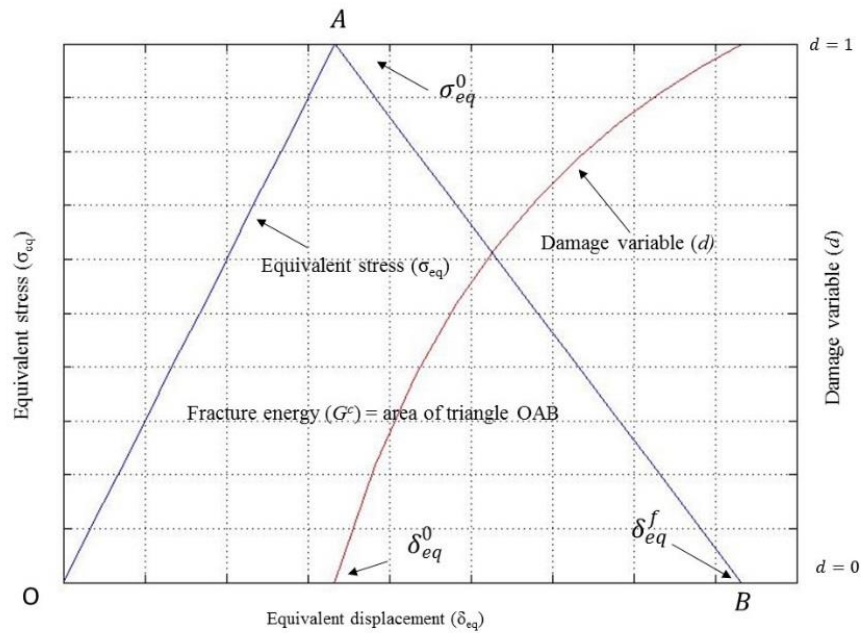


Figure 1. Schematic of linear softening behavior [22]

Table 2. Fracture energies of the facesheet material [22]

Longitudinal tension	Longitudinal compression	Transverse tension	Transverse compression
81.5 kJ/m ²	106.5 kJ/m ²	0.28 kJ/m ²	0.79 kJ/m ²

2.2. HONEYCOMB CORE MODEL

The honeycomb cells have a very large height to thickness ratio and can be modeled using shell elements. A single honeycomb cell of a commercial aluminum honeycomb is shown in Figure 2 (a). In a typical honeycomb core, the cell walls oriented along the ribbon directions have twice the wall thickness. This difference in wall thicknesses was included in the shell section definitions (Figure 2 (b)).

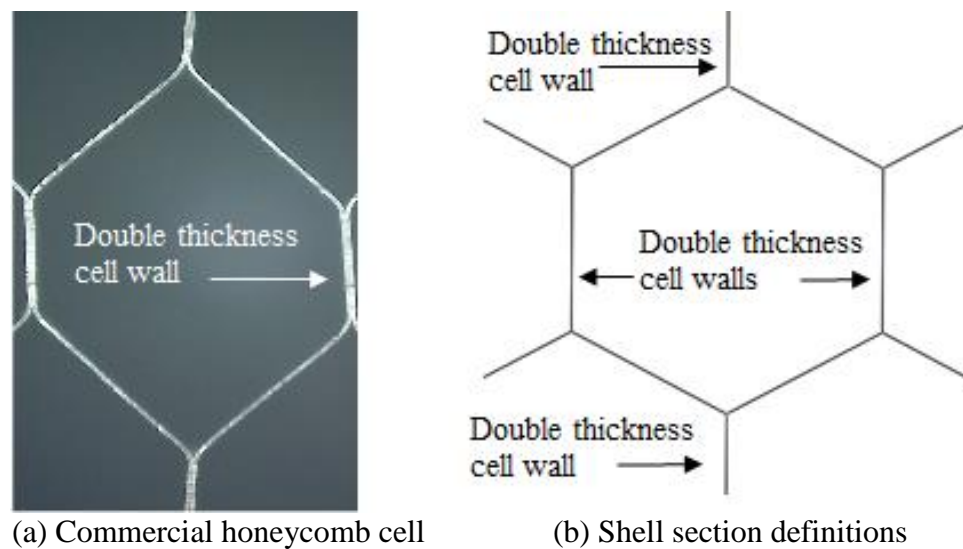


Figure 2. Honeycomb cell modeling.

Failure can take place due to plastic buckling in the cell walls or shear failure in the core. An elastic-plastic model was used to describe the behavior of the aluminum core. The modulus of the honeycomb constitutive material, Aluminum 5052, was 70 GPa and Yield stress was 255 MPa. Poisson's ratio was 0.3.

Each cell wall was modeled using a single layer of shell elements. The failure in the honeycomb core is affected by the mesh size. In order to capture local failure phenomena accurately, a fine mesh region was included in the central area of the core. The meso-scale model of the honeycomb core is shown in Figure 3. The central region of the core had a mesh size of 0.5 mm, which results in four elements along each cell wall of the honeycomb. The outer regions had a mesh size of 1 mm, corresponding to 2 elements along the length of the honeycomb cell wall. Correspondingly, the facesheet was also divided into coarse and fine mesh regions. The central region of the facesheet, above the fine mesh region of the honeycomb core, had a mesh size of 1 mm, while the outer regions had a mesh size of 2 mm.

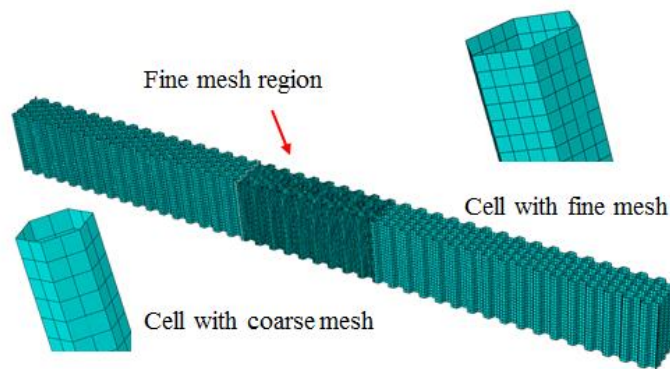


Figure 3. Honeycomb core showing regions of fine and coarse mesh

2.3. MODELING OF THREE-POINT BENDING TEST

The numerical model of the three-point bending test was built corresponding to the experimental setup. The specimen configuration was according to the requirements in ASTM D7250 and ASTM C393 (Figure 4).

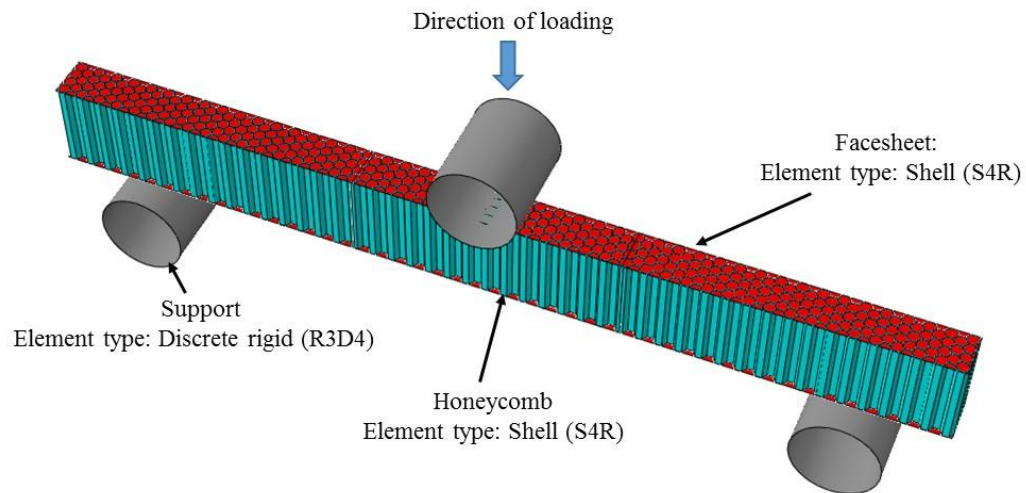


Figure 4. Three-point bending test setup

The facesheets were modeled using a single layer of shell elements (S4R) and had a $[0^\circ/90^\circ]_s$ composite layup. The supports and puncher, which were cylinders of 25 mm diameter, were modeled using discrete rigid elements. The motion of the supports was controlled using a reference point and constrained along all degrees of freedom. The puncher was free to move along the z axis, which is perpendicular to the face of the sandwich composite. Motion along all other degrees of freedom was constrained. A general

contact interaction was incorporated to model the contact between all surfaces of the numerical model. The Coulomb friction model was used at the interface between the puncher/supports and the facesheet. The coefficient of friction between the sandwich faces and surfaces of supports and puncher was set as 0.3. The facesheet and core components were bonded using kinematic tie constraints. The analysis was performed using Abaqus/Explicit software package. The stable time increment was 1E-9 which leads to extremely high computational costs. In order to reduce computational requirements, mass scaling technique was used. In addition, a reduced width of the sample was simulated. The specimen width in the simulation was equal to the width of 4 honeycomb cells. This smaller sample width was used (~12.7 mm), compared to a standard sample (50.8 mm) to reduce computational time. Results were scaled up to correspond to the strength of the test samples used in experiments.

3. EXPERIMENTS

Composite sandwich panels were manufactured using an out-of-autoclave prepreg process. This process is a low-cost alternative to autoclave curing and can result in significant reductions in operating costs [25]. The facesheets were made of IM7/Cycom 5320-1 prepreps. The selected facesheet material is a toughened aerospace epoxy system which can be cured out-of-autoclave. The layer orientation was $[0^{\circ}/90^{\circ}]_s$. The core designation was CRIII-1/8-5052-0.002, manufactured by Hexcel. The term 1/8 in the core designation stands for the core cell size which was 1/8 in. (3.175 mm). Aluminum 5052 is the constituent material of the honeycomb and 0.002 in. (0.0508 mm) is the thickness of

the foil gauge. It corresponds to the thickness of a single cell wall in the honeycomb. The core density was 8.1 pcf (127 kg/m^3). Core and facesheet were bonded using Cytec FM300-2 film adhesive. The layup including composite facesheets, film adhesive and the honeycomb core was co-cured under atmospheric pressure at recommended cure cycle of 250 °F (121 °C) for two hours. Samples were then post cured at 350 °F (177 °C) for two hours. Test specimens measuring 10 in. x 2 in. (254 mm x 50.8 mm) were cut from the manufactured sandwich panel for three-point bending experiments. The edges were polished with sand paper in order to remove imperfections which may affect the test results.

Three-point bending tests were conducted on sandwich specimens according to ASTM D7250 and ASTM C393 [26, 14]. Load was applied using an Instron 5585 testing machine with a 100 kN load cell. The experimental setup is shown in Figure 5. The cylinders used as supports and puncher had a diameter of 25 mm. The support span length was 8 in. (203.2 mm). Tested sandwich panels had the ribbon-direction of the honeycomb, perpendicular to the axis of the puncher. The uppermost layer of the facesheets had fibers oriented perpendicular to the axis of the puncher.

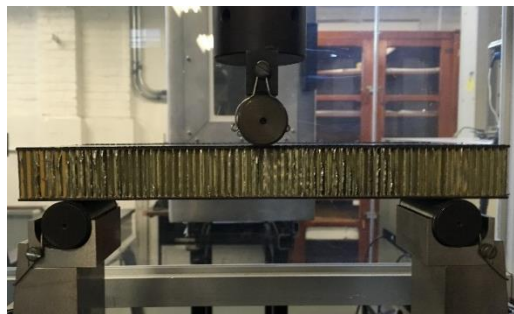


Figure 5. Experimental setup for three-point bending test

For high temperature testing, the entire setup was moved into an environmental chamber, available at Missouri S&T. The elevated temperature chosen for this study is 100 °C. The chamber was heated to the required temperature. Samples and fixture were conditioned inside the chamber for two hours prior to testing. Three-point bending tests were conducted as per ASTM standard C393.

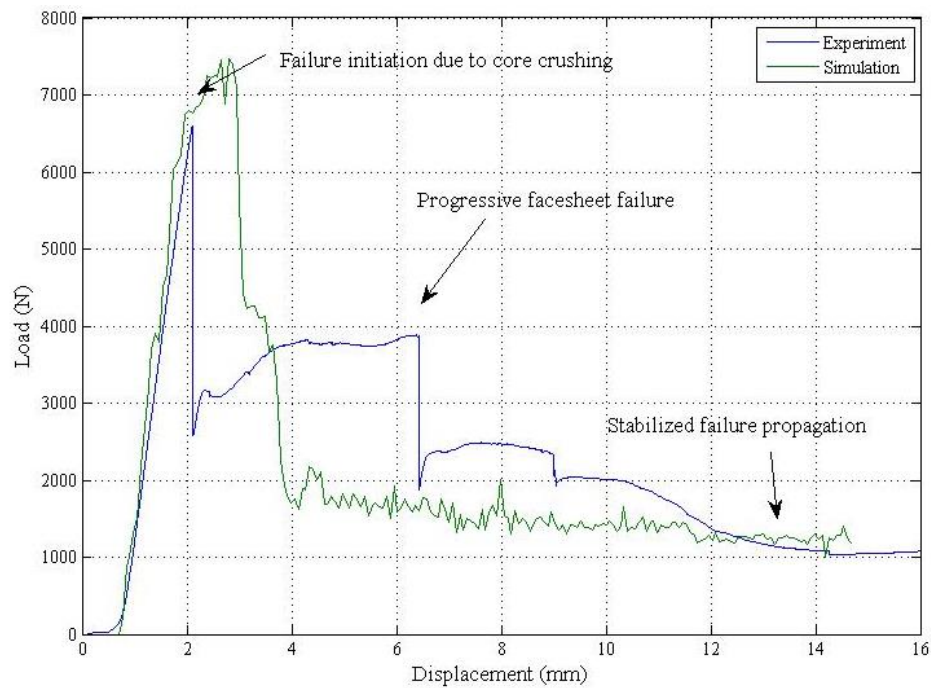


Figure 6. Load-displacement behavior under three-point bending

A loading rate of 3 mm per minute was maintained during the test. The application of load was continued well after failure in order to capture the stabilized failure propagation zone. All tested specimens exhibited a similar general trend in the load-displacement curve.

Three zones can be observed in the experimental curve (Figure 6). The first zone is an initial linear elastic zone where the sandwich is undamaged. The load increases until a peak is observed, and then failure initiates. It is followed by a progressive failure zone. Finally, a stabilized damage propagation region is observed. At this point, the facesheet has already failed and energy is absorbed mainly through the failure of the honeycomb core and damage propagation in the facesheet.

4. RESULTS AND DISCUSSION

The numerical model was used to predict sandwich behavior under three-point bending. The load displacement curve from the numerical model is also shown in Figure 6. The simulation was performed until the puncher displacement reaches 14 mm. There is good agreement, between experiments and simulations, in the elastic region of the curve. The peak load obtained in the simulation is a little higher in comparison to the experimental results. In the numerical simulations, the damage propagation is more catastrophic in nature, while experiments showed a gradual failure propagation zone. The reasons behind this behavior will be explored in this study. The stabilized load carrying capacity of the panel after failure is predicted accurately by the numerical model.

4.1. FAILURE UNDER THREE-POINT BENDING

When subjected to flexural loads, sandwich panel failure can take place various modes such as facesheet failure, facesheet wrinkling, intra-cell facesheet dimpling, core

shear and local failure due to indentation [13]. Based on the characteristics of the sandwich structure, critical failure stresses under various failure modes can be calculated. The in-plane stresses in the facesheets are not high enough to cause facesheet wrinkling according to Equation 2. For the span length and sandwich parameters considered in this study, expected mode of failure can be due to facesheet failure under compression, or core crushing.

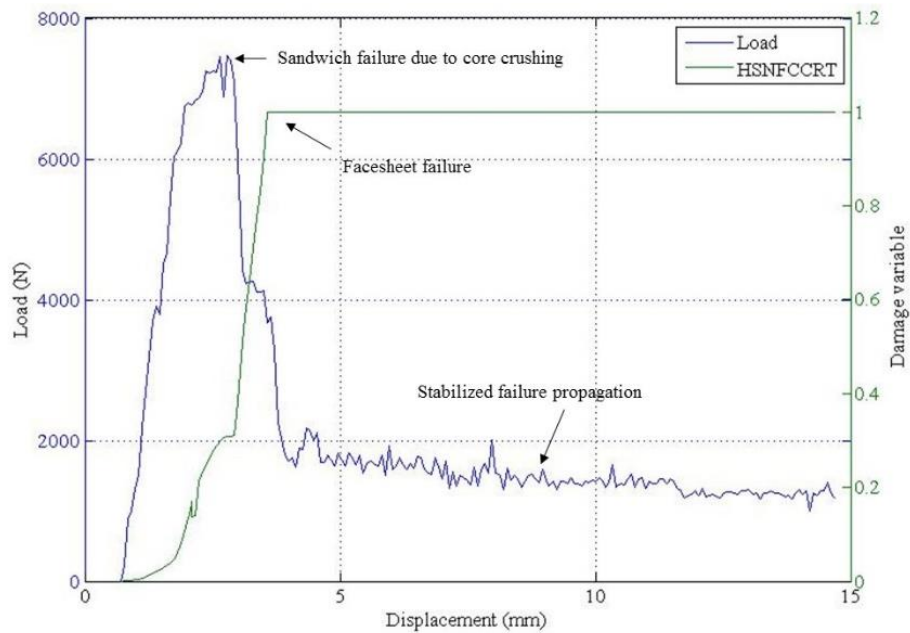


Figure 7. Damage evolution in the facesheet during three-point bending. HSNFCCRT stands for Hashin's Fiber Compression Failure Criterion

The maximum facesheet stress at the failure load of 6598 N can be calculated to be 260 MPa. This corresponds to the stress in the outermost layer of the facesheet, in contact

with the puncher. Figure 7 shows the evolution of the compressive failure criterion in the upper facesheet, which is in contact with the puncher, as predicted by the numerical model. Facesheet failure occurs when the failure criterion reaches the value of 1. Sandwich failure is observed at a displacement prior to the failure of the composite facesheet. This indicates that the failure initiation is due other mechanisms such as core crushing in the honeycomb sandwich which is then followed by progressive facesheet failure.

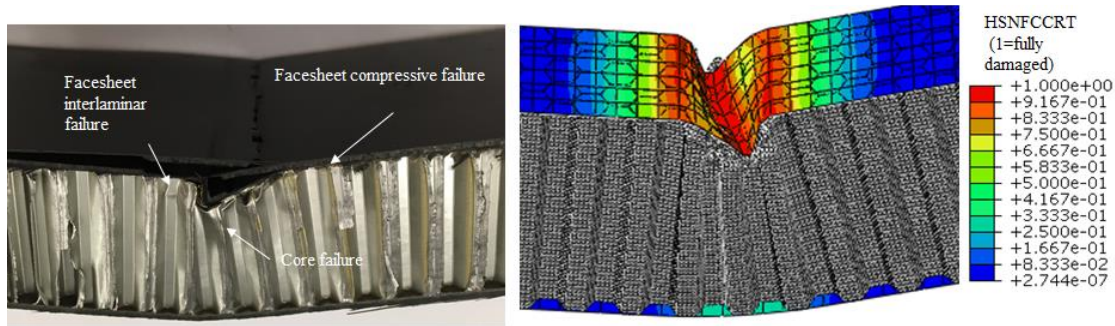


Figure 8. Failure in composite sandwich structures under three-point bending. HSNFCCRT stands for Hashin's Fiber Compression Failure Criterion. Damaged regions are colored red

Figure 8 depicts sandwich failure under three-point bending. Local core compressive failure is observed in the region under the puncher. Significant cell buckling is observed in this region followed by folding of cell walls. Previous studies, have observed a densification phenomenon once the cell walls come in contact with each other [7]. In the current study, the puncher displacement was stopped before such a point was reached. The composite facesheets show a variety of failure modes. Compressive failure is clearly

observed in the region directly under the puncher. In addition to compressive failure, interlaminar failure is also observed in the facesheet. This interlaminar failure propagates down the length of the sandwich composite, away from the region under the puncher. Figure 8 shows the location of failure predicted by the FEA model. Facesheet failure due to compression is observed in the location beneath the puncher. Location of facesheet compressive failure observed in the experiments corresponds well with the predictions by the numerical model. Total facesheet failure is seen in the regions directly under the puncher. From the experiments it was observed that the facesheet failure occurred due to the combination of additional failure modes. A combination of compressive failure and propagation due to interlaminar failure was observed. The interlaminar failure was not observed in the simulations because the facesheets were modeled using a single layer of shell elements. The meso-scale model for the honeycomb allows simulation of localized cellular failure. Initiation of failure in the sandwich composite was due to core compression in the region under the puncher. The core materials in composite sandwich structures are subjected to shear and normal loads, when loaded in a three-point bending configuration. Gdoutos and Daniels reported that in long span beams under three-point bending, a complex biaxial state of stress can exist in the core, which leads to failure [16]. Figure 9 shows the detailed images of progression of failure in the honeycomb core. Failure initiation is observed in Figure 9 (a) and 9 (b) by local buckling of the honeycomb cell walls. On continued loading, crushing of the core is observed as in Figures 9 (b-d). The localized failure leads to stress concentrations which initiates failure in the composite

facesheet. Failure progresses due to plastic buckling in the core. Significant plastic failure is observed, as shown in Figure 10.

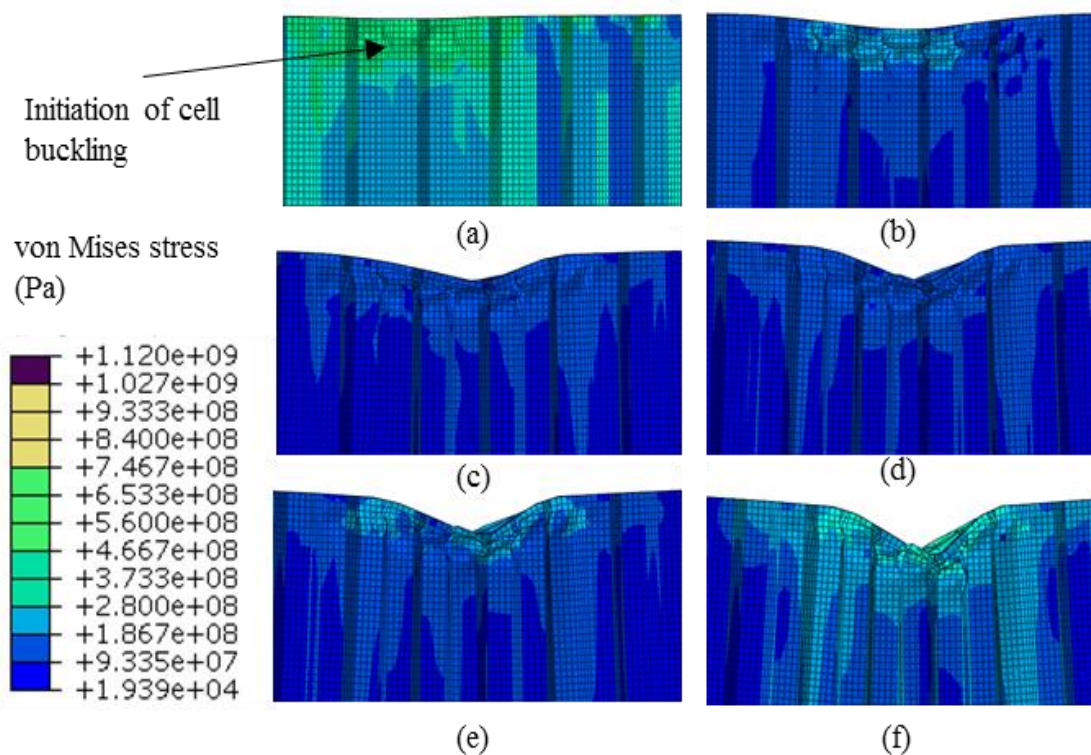


Figure 9. Progression of failure in the honeycomb core

The regions of plastic buckling correspond to plastic buckling failure of aluminum honeycombs under out-of-plane loads as mentioned by Gibson and Ashby [3]. A comparison of experimental and numerical failure due to core crushing is shown in Figure 10. The mode of failure observed in experiments corresponds well with the core failure progression predicted by the numerical model.

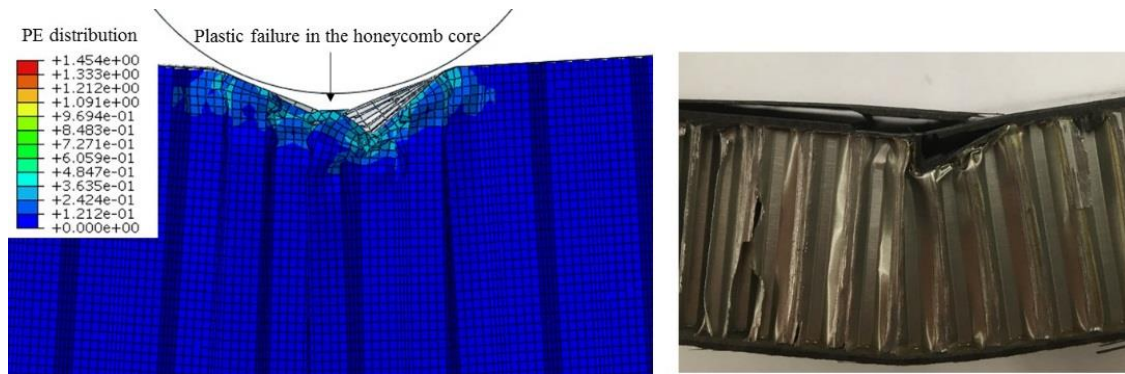


Figure 10. Core failure in three-point bending. Comparison between experimental and simulation results is shown. PE stands for plastic strain.

4.2. EFFECT OF ELEVATED TEMPERATURES

The numerical model was used to predict three-point bending behavior of sandwich structures at elevated temperatures. The adhesive is not included in the numerical model because failure is dominated by facesheet compressive failure and core crushing, rather than core-facesheet debonding. The test temperature chosen in this study was 100 °C. The temperature falls within the service temperature range of the film adhesive used in this study. Figure 11 shows the variation of honeycomb core and facesheet properties with temperature. The core properties were obtained from the Hexcel product datasheet [27]. Around 12% reduction in strength is observed when the ambient temperature is increased to 100°C. Previous studies have reported that the properties of the composite laminates are dependent on the service temperature [28]. The thermoset matrix dominated properties tend to be sensitive to temperature changes. The longitudinal properties are not as sensitive to changes in temperature changes because they are fiber dominated. It is expected that 90°

compression, 90° tension and interlaminar shear strength will reduce when temperature is increased. In this study, facesheet properties at room temperature and 121 °C were obtained from the Cycom 5320-1 datasheet. Intermediate values were obtained using linear interpolation. Figure 11 shows the variation of facesheet compressive strength in the 90° direction with temperature.

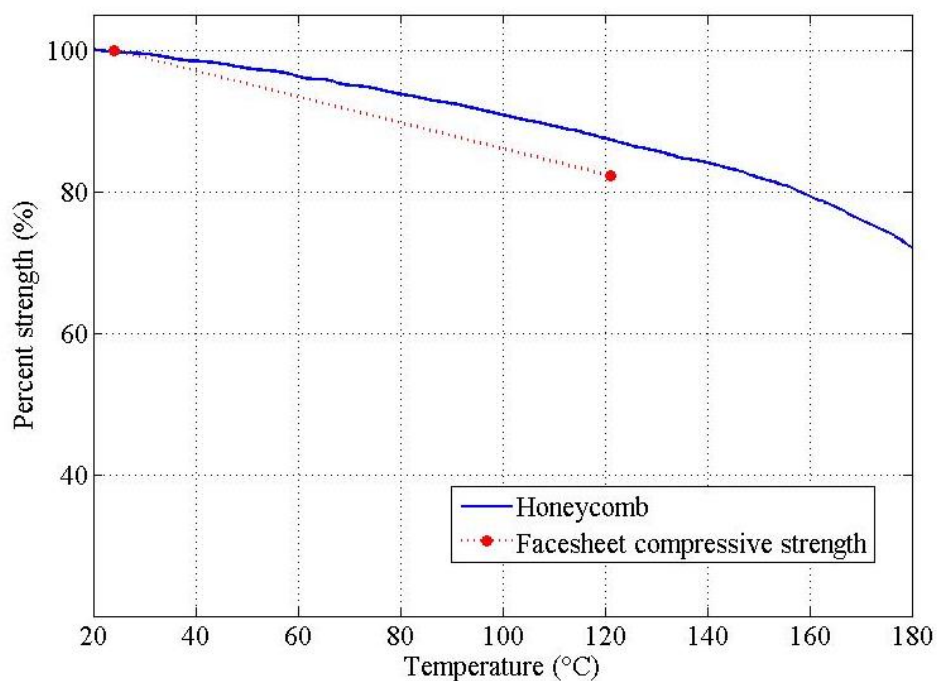


Figure 11. Temperature dependent variation in the properties of honeycomb and facesheet

A reduction of 14% is observed as temperature is increased to 120 °C from room temperature. Temperature dependent properties were incorporated into the numerical

model. The “predefined field” option in Abaqus was used to define the test temperature. Simulations were then utilized to predict the drop in strength of the honeycomb sandwich structure at elevated temperatures.

Representative curves of experiments at room temperature and elevated temperature are shown in Figure 12. The results suggest that the strength of the sandwich structure drops by 9.2% when the temperature is increased from room temperature to 100 °C. However, the slope of the elastic region does not show a significant variation when the temperature is increased. This can be due to the relative temperature insensitivity of the facesheet moduli as shown in Table 1 in section 3.2. In addition, the variation in modulus of aluminum is also minimal in this temperature range. As a result, a change in temperature has a significant effect on the load bearing capacity but a minimal effect on sandwich stiffness.

The progressive damage propagation in the facesheet is more significant at room temperature compared to elevated temperature. One possible reason for this observation can be a reduction in interlaminar shear strength of the facesheet, which reduces the energy absorbed by this failure mode. The loads at stabilized damage propagation are very similar in both cases. Results of simulation and experiments at elevated temperatures are shown in Figure 13. There is good agreement between experimental and numerical results with reference to load carrying capacities of the sandwich. Failure under high temperature tests shows a similar general trend as compared to the room temperature simulations. There is also good agreement between the numerical results and simulation in the progressive failure zone.

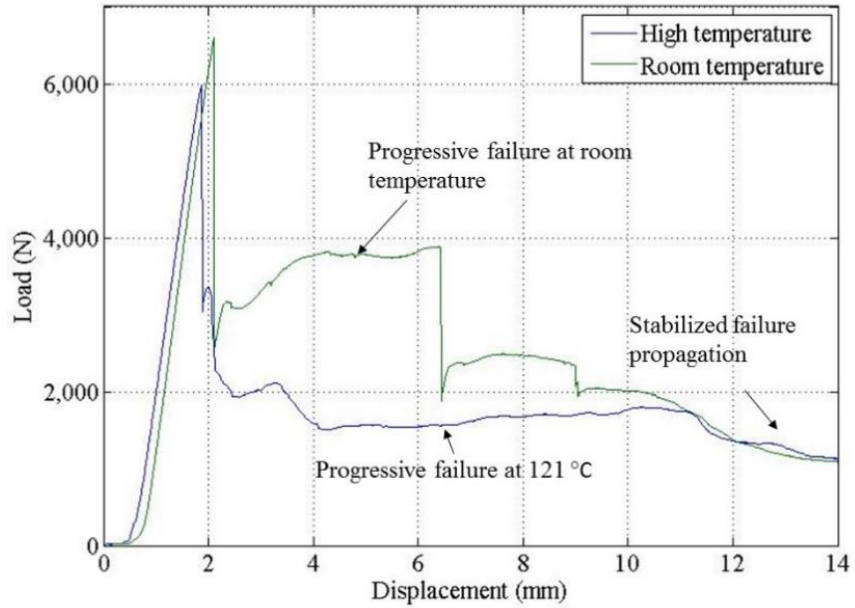


Figure 12. Comparison of load displacement curves at room temperature and high temperature (100 °C). Experimental results are shown in the figure

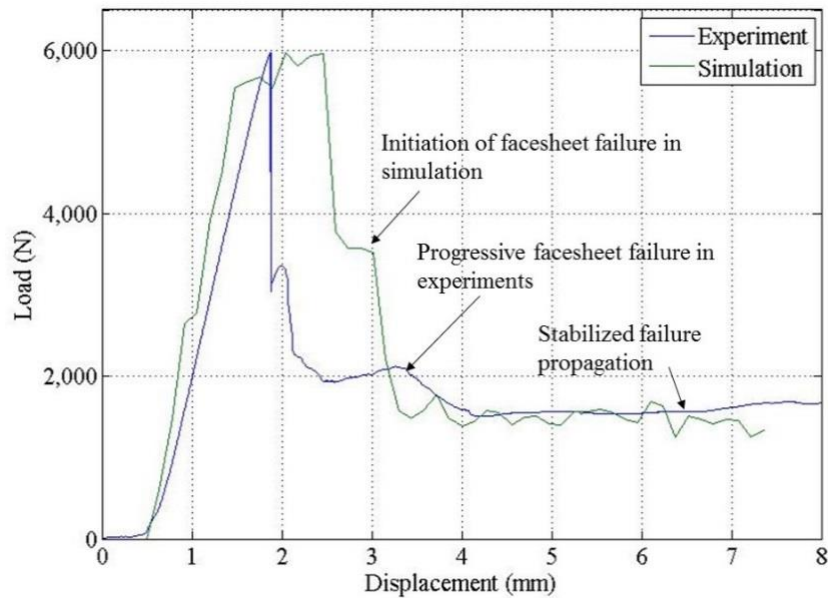


Figure 13. Experimental and numerical load-displacement curves at elevated temperature of 100 °C

4.3. EFFECT OF PUNCHER LOCATION

As mentioned by Giglio et al., the exact position of the puncher with respect to honeycomb cells may affect the results of the numerical model [6]. The force displacement behavior can vary with the position of the central axis of the puncher with respect to the center of a cell. The relative position of the puncher was varied in the numerical model. Three different positions were evaluated as shown in Figure 14 (a). P1 corresponds to the position used in the baseline numerical model, where the axis of the puncher is in line with the center of a honeycomb cell. In P3, the axis is in line with the end of a honeycomb cell. For this study, the span length was kept constant. Figure 14(b) shows the variation in load-displacement behavior. The overall trend shows little change. There is a small variation in the damage propagation region, which is affected by the local failure.

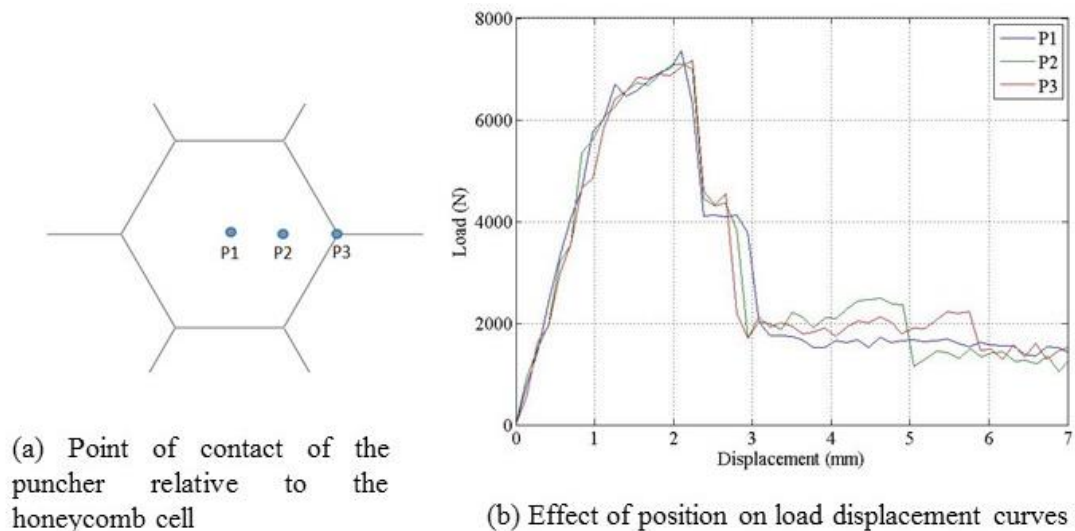


Figure 14. Effect of relative position of the puncher on results of the three-point bending tests

The localized failure is difficult to examine experimentally but can be easily investigated using simulations. Figure 15 shows the variation of localized failure in the core as the puncher is moved to the right. It can be observed that the point of maximum deformation shifts as the puncher is moved.

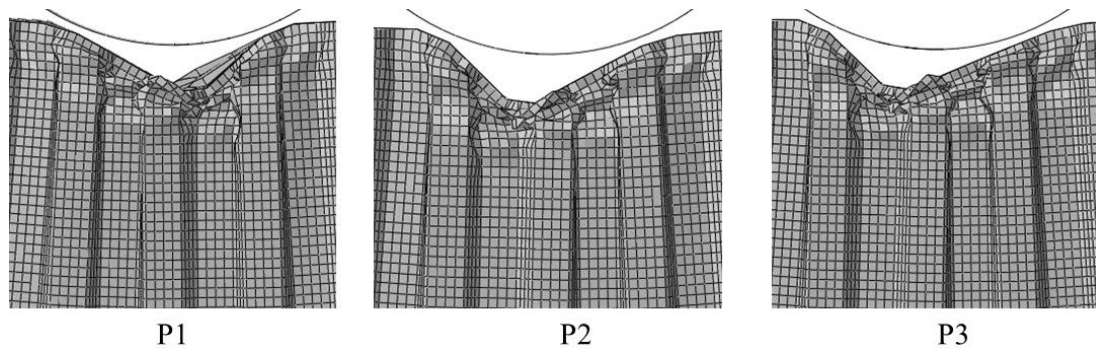


Figure 15. Variation of localized damage with a change in puncher location

However this change in localized failure did not affect load to failure or the linear portion of the load-displacement curve. Therefore, changes in the relative position of the puncher relative to the honeycomb cells do not affect the results of the test in a significant manner.

5. CONCLUSIONS

This paper focused on modeling of a composite sandwich structure under three-point bending. The sandwich structure had facesheets made of carbon/epoxy composites and the core material was aluminum honeycomb. Hashin failure model was used to

simulate damage propagation in the facesheets. Experimental validation was also performed using three-point bending tests on sandwich structures with carbon/epoxy facesheets and aluminum honeycomb core. Simulation results showed good accuracy in predicting the load carrying capacity as well as overall damage behavior in the sandwich composite. Local core crushing was simulated accurately. Failure of cell walls due to local buckling was observed in simulations as well as experiments. When the temperature was increased to 100 °C, the strength of the sandwich structure decreased by 9.2%, while the stiffness did not change. This effect was also captured effectively by the numerical models. The location of the puncher axis relative to cell geometry is a parameter is difficult to determine using experiments, was evaluated using the numerical model. It was observed that the sandwich stiffness was not significantly affected by the relative location of the puncher, while the load to failure decreased slightly. Numerical simulations, after experimental validation, can be used to effectively determine parameters which affect behavior of sandwich composites. The model can also be used to estimate mechanical behavior of composite sandwich structures, prior to experimental testing.

ACKNOWLEDGEMENTS

This research is sponsored by the Industrial Consortium of the Center for Aerospace Manufacturing Technologies (CAMT) at Missouri University of Science and Technology.

REFERENCES

1. J. Vinson, *The behavior of sandwich structures of isotropic and composite materials*, Lancaster: Technomic, 1999.
2. M. Okereke, A. Akpoyamare and M. Bingley, "Virtual testing of advanced composites, cellular materials and biomaterials," *Composites: Part B*, vol. 60, pp. 637-662, 2014.
3. L. Gibson and M. Ashby, *Cellular solids, structure and properties*, Cambridge: Cambridge University Press, 1999.
4. S. Heimbs, "Virtual testing of sandwich core structures using dynamic finite element simulations," *Computational Materials Science*, vol. 45, pp. 205-216, 2009.
5. K. Li, X. Gao and J. Wang, "Dynamic crushing behavior of honeycomb structures with irregular cell shapes and non-uniform cell wall thickness," *International Journal of Solids and Structures*, vol. 44, pp. 5003-5026, 2007.
6. M. Giglio, A. Gilioli and A. Manes, "Numerical investigation of a three point bending test on sandwich panels with aluminum skins and Nomex honeycomb core," *Computational Materials Science*, vol. 56, pp. 69-78, 2012.
7. M. Giglio, A. Manes and A. Gilioli, "Investigations on sandwich core properties through an experimental–numerical approach," *Composites: Part B*, vol. 43, pp. 361-374, 2012.
8. R. Seeman and D. Krause, "Numerical modelling of Nomex honeycomb sandwich cores at meso-scale level," *Composite Structures*, vol. 159, pp. 702-718, 2017.
9. G. Zhou, M. Hill, N. Loughlan and N. Hookham, "Damage characteristics of composite honeycomb sandwich panels in bending under quasi-static loading," *Journal of Sandwich Structures and Materials*, vol. 8, pp. 55-90, 2006.
10. A. Stocchi, L. Colabella, A. Cisilino and V. Alvarez, "Manufacturing and testing of a sandwich panel honeycomb core reinforced with natural-fiber fabrics," *Materials and Design*, vol. 55, pp. 394-403, 2014.

11. I. Masters and K. Evans, "Models for elastic deformation of honeycombs," *Composite Structures*, vol. 35, pp. 403-422, 1997.
12. S. Malek and L. Gibson, "Effective elastic properties of periodic hexagonal honeycombs," *Mechanics of Materials*, vol. 91, pp. 226-240, 2015.
13. A. Petras and M. Sutcliffe, "Failure mode maps for honeycomb sandwich panels," *Composite Structures*, vol. 44, pp. 237-252, 1999.
14. ASTM Standard C393, "Standard test method for core shear properties of sandwich constructions by beam flexure," ASTM International, www.astm.org, 2016.
15. B. Harris and W. Crisman, "Face wrinkling mode of buckling of sandwich panels," *Proceedings of the ASCE Engineering Mechanics Div 91*, fourth ed., pp. 93-111, 1965.
16. E. Gdoutos and I. Daniel, "Failure modes of composite sandwich beams," *Theoretical Applied Mechanics*, vol. 35, no. 1-3, pp. 105-118, 2008.
17. S. Yussuff, "Theory of wrinkling in sandwich construction," *Journal of the Royal Aeronautical Society*, vol. 59, pp. 30-36, 1955.
18. B. Zalewski, W. Dial and B. Bednarczyk, "Methods for assessing honeycomb sandwich panel wrinkling failures," NASA/TM-2012-217697, pp. 1-22, 2012.
19. O. Thomsen and W. Banks, "An improved model for the prediction of intra-cell buckling in CFRP sandwich panels under in-plane compressive loading," *Composite Structures*, vol. 65, pp. 259-268, 2004.
20. H. Soliman and R. Kapania, "Equivalent constitutive behavior of sandwich cellular cores," *Journal of sandwich structures and materials*, vol. 19, pp. 424-455, 2015.
21. A. Catapano and M. Montemurro, "A multi-scale approach for the optimum design of sandwich plates with honeycomb core. Part I: homogenisation of core properties," *Composite Structures*, vol. 118, pp. 664-676, 2014.

22. I. Lapczyk and J. Hurtado, "Progressive damage modeling in fiber-reinforced materials," *Composites Part A: Applied Science and Manufacturing*, vol. 38, pp. 2333-2341, 2007.
23. ABAQUS Online users manual, Version 6.12, 2015.
24. Cytec Solvay, "Cycom 5320-1 Epoxy Resin System," 2015.
25. T. Centea, L. Grunenfelder and S. Nutt, "A review of out-of-autoclave prepregs – Material properties, process phenomena, and manufacturing considerations," *Composites Part A: Applied Science and Manufacturing*, vol. 70, pp. 132-154, 2015.
26. ASTM Standard D7250, "Standard practice for determining sandwich beam flexural and shear stiffness," ASTM International, www.astm.org, 2016.
27. Hexcel Corporation, "Hexweb honeycomb attributes and properties," 2017.
28. Z. Guo, J. Feng, H. Wang, H. Hu and J. Zhang, "A new temperature-dependant modulus model of glass/epoxy composite at elevated temperature," *Journal of Composite Materials*, vol. 47, no. 26, pp. 3303-3310, 2012.

SECTION

4. CONCLUSIONS

The first paper of this work involves the evaluation of OOA cured carbon/BMI composite laminates. Process parameters which result in low void contents were identified. The effect of cure cycle variations on mechanical and thermal properties of the OOA cured BMI composite laminates was evaluated. All samples had glass transition temperatures high enough to replace conventional epoxies. It was found that maximum interlaminar shear strengths were obtained when parts were cured at 375 °F (191 °C) for 6 hours. Post curing up to a temperature of 444.5 °F (229.1 °C) results in an increase in ILSS. At higher temperatures, mechanical properties degrade. Based on the results of experimental testing it was found that maximum ILSS can be obtained in samples post cured at 444.5 °F (229.1 °C) for four hours. Test samples were manufactured using the optimized cure and process parameters. Their properties compared well with those of an autoclave cured composite.

The second paper involved evaluation of OOA sandwich composites. The results of the previous study were used to develop cure and process parameters for high temperature sandwich composites. The effect of vacuum pressure on the properties of the high temperature sandwich composites was investigated. Samples were manufactured under full vacuum (-100 kPa) and partial vacuum (-80 kPa). Adhesive bond strength was evaluated using FWT tests and adhesive bond fracture toughness tests. Edgewise compression tests were conducted on samples with facesheet orientation $[0^{\circ}/90^{\circ}]_s$. Vacuum pressure levels used in this study, did not have a significant effect on edgewise compressive

strength and had a minor effect on adhesive bond strength. Increase in test temperature to 177 °C (350 °F) resulted in a reduction in edgewise compressive strength as well as adhesive bond strength. Measured bond strengths at room temperature were comparable to those mentioned in previous studies involving aerospace grade epoxy adhesives and autoclave cured BMI adhesives.

In the third paper, mathematical cure kinetic models were implemented in a Multiphysics model to simulate the curing process in composites. Thick composite laminates were manufactured at Missouri S&T and the temperature at the center of the parts, during cure, was measured using thermocouples. The magnitude of the thermal peak, predicted by the simulation, was in good agreement with the measured values. Based on a parametric study, it was found that post-curing has a significant effect on the degree of cure in thick laminates. Variation in the autoclave/oven convection coefficient had a significant effect on the location of the thermal spike in the temperature profile. The cure cycle was modified by incorporating a gradual ramp in the curing phase. Using a ramp, in place of an isotherm, can reduce the thermal spike but it also reduces the degree of cure in the laminate. However, the degree of cure after a post-cure phase, for laminates manufactured using a modified cure cycle (with a ramp) and the recommended cure cycle (with an isotherm), is similar. Composite laminates were manufactured using the modified cure cycle and recommended cure cycle. It was observed that the final mechanical properties, after post-curing, of both laminates were similar.

In the fourth paper, numerical models were built to study damage in composite sandwich structures, subjected to three-point bending, under room temperature and

elevated temperatures. Hashin failure model was used to simulate damage propagation in the facesheets. Simulation results showed good accuracy in predicting the load carrying capacity as well as overall damage behavior in the sandwich composite. Local core crushing in the aluminum honeycomb core was simulated accurately. Failure of cell walls due to local buckling was observed in simulations as well as experiments. When the temperature was increased to 100 °C, the strength of the sandwich structure decreased by 9.2%, while the stiffness did not change significantly. This effect was also captured effectively by the numerical models. The location of the puncher axis relative to cell geometry is a parameter is difficult to determine using experiments, was evaluated using the numerical model. It was observed that the sandwich stiffness was not significantly affected by the relative location of the puncher, while the load to failure decreased slightly. It was shown that numerical simulations, after experimental validation, can be used to effectively determine parameters which affect behavior of sandwich composites.

The research presented here can be extended in several ways. The experimental work on OOA composites involved evaluation of lab-scale composite laminates and sandwich structures. There is a lot of scope for scale-up and manufacturing of complex components. In addition, non-metallic cores can be used to manufacture high temperature sandwich structures. Further research can be done regarding the applicability of other non-autoclave processes such as compression molding, using the cure cycles developed in this study. The numerical models can be extended to include the development of residual stresses during cure of composite components. The validated numerical model for sandwich composites can also be extended to include other core and facesheet materials.

In addition, the validated numerical models can be used for designing cure cycles, selecting materials for sandwich structures and design of high temperature complex shaped structures.

BIBLIOGRAPHY

1. H. Stenzenberger, M. Herzog, P. Koenig, W. Roemer and W. Breitigam, "Bismaleimide Resins: Past, Present, Future," in International SAMPE Symposium and Exhibition, Reno, Nv, 1989.
2. C. Ridgard, "Next Generation Out-of-Autoclave Systems," in *International SAMPE Symposium and Exhibition*, Seattle, Wa, 2010.
3. Z. Sakota, H. Thomas Hahn, L. Lackman and G. Bullen, "Out of Autoclave Curing of Composites," in *International SAMPE Symposium and Exhibition*, Long Beach, CA, Apr 30 - May 4, 2006.
4. T. Centea, L. Gunenfelder and S. Nutt, "A Review of Out-of-Autoclave Prepregs – Material Properties, Process Phenomena, and Manufacturing Considerations," *Composites Part A: Applied Science and Manufacturing*, vol. 70, pp. 132-154, 2015.
5. H. Hsiao, S. Lee and R. Buyby, "Core Crush Problem in Manufacturing of Composite Sandwich Structures: Mechanisms and Solutions," *AIAA Journal*, vol. 44, no. 4, pp. 901-907, 2006.
6. L. Grunenfelder and S. Nutt, "Void Formation in Composite Prepregs- Effect of Dissolved Moisture," *Composites Science and Technology*, vol. 70, pp. 2304-2309, 2010.
7. T. Centea and P. Hubert, "Measuring the Impregnation of an Out-of-Autoclave Prepreg by Micro-CT," *Composites Science and Technology*, vol. 71, pp. 593-599, 2011.
8. M. L. Costa, S. F. Almeida and M. C. Rezende, "The Influence of Porosity on the Interlaminar Shear Strength of Carbon/ Epoxy and Carbon/Bismaleimide Fabric Laminates," *Composites Science and Technology*, vol. 61, pp. 2101-2108, 2001.
9. A. Levy, J. Kratz and P. Hubert, "Air Evacuation during Vacuum Bag Only Prepreg Honeycomb Sandwich Structures: In-plane Air Evacuation Prior to Cure," *Composites Applied Science and Manufacturing*, vol. 68, pp. 365-376, 2015.

10. T. Vo, K. Vora and B. Minaie, "Effects of Postcure Temperature Variation on Hygrothermal-Mechanical Properties of an Out-of-Autoclave Polymer Composite," *Journal of Applied Polymer Science*, vol. 130, pp. 3090-3097, 2013.
11. G. Grimes, "The Adhesive-Honeycomb Relationship," *Applied Polymer Symposium*, vol. 3, pp. 157-190, 1996.
12. R. Okada and M. Kortschot, "The Role of Resin Fillet in the Delamination of the Honeycomb Sandwich Structures," *Composite Science and Technology*, vol. 62, pp. 1811-1819, 2002.
13. S. Grove, E. Popham and M. Miles, "An Investigation of the Skin/Core Bond in Honeycomb Sandwich Structures using Statistical Experimentation Techniques," *Composites Part A: Applied Science and Manufacturing*, vol. 37, no. 5, pp. 804-812, 2006.
14. S. Tavares, N. Callet-Bois, V. Michaud and J.-A. Manson, "Vacuum-bag Processing of Sandwich Structures: Role of Honeycomb Pressure," *Composites Science and Technology*, vol. 70, pp. 797-803, 2010.
15. J. Kratz and P. Hubert, "Processing Out-of-Autoclave Honeycomb Structures: Internal Core Pressure Measurements," *Composites Part A: Applied Science and Manufacturing*, vol. 42, no. 8, pp. 1060-1065, 2011.

VITA

Sudharshan Anandan was born in Bengaluru, Karnataka, India in 1987. He received his Bachelor of Engineering degree in Mechanical Engineering in 2009 from National Institute of Technology Karnataka, Surathkal, India. He joined M.S. degree program in Mechanical Engineering at Missouri University of Science and Technology, Rolla, Missouri, USA in August 2011. He held the Graduate Research Assistant position through his masters at Missouri University of Science and Technology. He received his Master's Degree in May 2014.

In August 2013, Sudharshan Anandan enrolled in the Ph.D. program at Missouri University of Science and Technology. He served as a Graduate Research Assistant from August 2013 to May 2018. He was a Graduate Teaching Assistant in the Department of Mechanical Engineering from January 2016 to December 2017. In May 2018, he received his Ph.D. degree in Mechanical Engineering from Missouri University of Science and Technology.